11-2021

IMPACT OF DATE-PIT ACTIVATED CARBON IN DIFFERENT APPLICATIONS: BIOMEDICAL AND ENVIRONMENT

Betty Titus Mathew

United Arab Emirates University

College of Science

IMPACT OF DATE-PIT ACTIVATED CARBON IN DIFFERENT APPLICATIONS: BIOMEDICAL AND ENVIRONMENT

Betty Titus Mathew

This dissertation is submitted in partial fulfilment of the requirements for the degree of Doctor of Philosophy

Under the Supervision of Professor Khaled Abbas El-Tarabily

November 2021

Declaration of Original Work

I, Betty Titus Mathew, the undersigned, a graduate student at the United Arab Emirates University (UAEU), and the author of this dissertation entitled "*Impact of Date-Pit Activated Carbon in Different Applications: Biomedical and Environment"*, hereby, solemnly declare that this dissertation is my own original research work that has been done and prepared by me under the supervision of Professor Khaled Abbas El-Tarabily, in the College of Science at UAEU. This work has not previously formed the basis for the award of any academic degree, diploma or a similar title at this or any other university. Any materials borrowed from other sources (whether published or unpublished) and relied upon or included in my dissertation have been properly cited and acknowledged in accordance with appropriate academic conventions. I further declare that there is no potential conflict of interest with respect to the research, data collection, authorship, presentation and/or publication of this dissertation.

Student's Signature:  Date: _23/12/21___

Advisory Committee

1) Advisor: Khaled Abbas El-Tarabily

Title: Professor

Department of Biology

College of Science

2) Co-advisor: Abdel-Hamid Ismail Mourad

Title: Professor

Department of Mechanical and Aerospace Engineering

College of Engineering

3) Co-advisor: Amr Amin

Title: Professor

Department of Biology

College of Science

Approval of the Doctorate Dissertation

This Doctorate Dissertation is approved by the following Examining Committee Members:

1) Advisor (Committee Chair): Khaled A El-Tarabily
   Title: Professor
   Department of Biology
   College of Science
   Signature ____ Khaled El-Tarabily _____ Date 28-11-2021

2) Member: Dr. Mohammed Akli Ayoub
   Title: Associate Professor
   Department of Biology
   College of Science
   Signature ____ _____ Date 28-11-2021

3) Member: Abdul Jaleel Cheruth
   Title: Associate Professor
   Department of Integrative Agriculture
   College of Agriculture and Veterinary Medicine
   Signature _____ ___ Date 28-11-2021

4) Member (External Examiner): Youssef A. Attia
   Title: Professor
   Department: Arid Land Agriculture
   Institution: King Abdulaziz University, Jeddah, Saudi Arabia
   Signature Youssef A. Attia, November 28, 2021 Date 28-11-2021

This Doctorate Dissertation is accepted by:

Dean of the College of Science: Professor Maamar Benkraouda

Signature Maamar Benkraouda Date Feb. 28, 2022

Dean of the College of Graduate Studies: Professor Ali Al-Marzouqi

Signature Ali Hassan Date Feb. 28, 2022

Copy ____ of ____

Abstract

Activated carbon (AC) or activated charcoal are black carbonaceous porous solid material with prominent physico-chemical properties such as low volume pore size distribution, high specific surface area, and high-degree of surface reactivity for adsorption and other chemicals reactions. AC as strong and reliable adsorbent have been reported to be employed in diverse applications stretching from water/air purification, medical, sewage treatment, energy storage devices, catalyst, supercapacitor electrodes fabrication, and as biosensors component. In this current work, AC was produced from date pits, which is a common biological waste product in UAE, and used for biomedical and environmental applications instead of using commercial AC. Date pits-based AC was produced by physical activation method followed by thorough characterization for physical and chemical properties analysis. The developed activated carbon was employed for evaluation of bilirubin adsorption capacity and plant growth promoting ability for marine plants. Date-pits based AC demonstrated highly selective and most effective capacity for bilirubin adsorption as revealed by isotherm-modeling analysis compared to controls, collagen and matrigel. *In vitro* cell culture studies further indicated cytocompatibility of established date-pit based against liver specific cell lines THLE2 and HepG2 cells with preservation of liver cell integrity. Furthermore, AC coated rhizosphere-competent halotolerant actinobacterial strains were utilized as bioinoculants on seawater-irrigated *Salicornia bigelovii* plants and assessed for plant growth promoting abilities. The three rhizosphere-competent isolates, *Streptomyces chartreusis* (*Sc*), *S. tritolerans* (*St*) and *S. rochei* (*Sr*) capable of producing growth hormones were investigated individually and as consortium (*Sc/St/Sr*) to determine their effects on the performance of *S. bigelovii* growth in the greenhouse. Herein, the synergetic combination of strains indicated greater effects on *S. bigelovii* biomass (62.2% and 77.9% increase in shoot and root dry biomass, respectively) and seed yield (79.7% increase) compared to the individual strains and control treatment. Taken together, developed AC were employed as biomaterial for removal of protein-bound toxins in bioartificial liver devices and as bioinoculant adsorbent for plant growth promotion. Overall, this current study, emphasize the potential role of date pits-based AC in biomedical and

environmental applications, and open doors for applications in diverse domains such as healthcare sector and environmental issues.

Keywords: Activated Carbon, Adsorbent, Biomaterial, Bilirubin Detoxification, Date Pits, Plant Growth Promoter.

Title and Abstract (in Arabic)

تأثير الكربون النشط والمحضر من نوى التمر في تطبيقات مختلفة في الطب الحيوي والبيئة

الملخص

الكربون النشط هو عبارة عن مادة صلبة مسامية كربونية سوداء تتميز بخصائص فيزيائية كيميائية بارزة تشمل حجم المسام المنخفض، مساحة سطح محددة عالية، ودرجة عالية من التفاعل السطحي للامتصاص والتفاعلات الكيميائية الأخرى. تم من قبل استخدام الكربون المنشط كمادة ممتازة وقوية في تطبيقات متنوعة مثل تنقية الماء والهواء، ومعالجة مياه الصرف الصحي، والمجالات الطبية، وأجهزة تخزين الطاقة، وتصنيع الأقطاب الكهربائية الفائقة، وايضا كأجهزة استشعار حيوية. في الدراسة الحالية، تم إنتاج الكربون النشط من نوى التمر، وهو منتج محضر من نفايات بيولوجية شائعة في دولة الإمارات العربية المتحدة، وقد تمت تجربة الكربون النشط والمحضر محلياً وذلك في التطبيقات الطبية الحيوية والبيئية. تم إنتاج الكربون النشط بطريقة التنشيط الفيزيائي متبوعاً بالتوصيف الشامل لتحليل الخواص الفيزيائية والكيميائية. تم استخدام الكربون النشط المطور وذلك لتقييم قدرته على امتصاص البيليروبين وأيضا لاختبار قدرته مدمجاً مع بعض أنواع البكتيريا النافعة على زيادة نمو نبات الساليكورنيا والذي يستخدم حالياً لإنتاج الوقود الحيوي للطائرات. أظهرت الدراسة قدرة الكربون النشط وبانتقائية فعالة على امتصاص البيليروبين. علاوة على ذلك، تم استخدام سلالات من البكتيريا النافعة والمغلفة بالكربون النشط كمخصبات بيولوجية لزيادة نمو نبات الساليكورنيا والتي تروى بمياه البحر وتقييم قدرتها على زيادة نمو هذا النبات الاقتصادي. أظهرت الدراسة أنه عند استخدام خليط من هذه البكتيريا النافعة على بذور النبات حدوث زيادة في النمو الجذري والخضري بنسبة 62.2٪ و77.9٪ على التوالي. وأظهرت البكتيريا أيضاً المحمولة على الكربون النشط قدرة هائلة في زيادة كمية البذور وبنسبة 79.7٪ زيادة مقارنة بالنباتات والتي لم يتم فيها استخدام البكتيريا والكربون النشط. أثبتت الدراسة أنه يمكن استخدام الكربون النشط المطور كمواد حيوية لإزالة السموم المرتبطة بالبروتين في أجهزة الكبد الاصطناعية الحيوية وأيضاً كمخصب حيوي لزيادة نمو نبات الساليكورنيا. وبشكل عام، تؤكد هذه الدراسة على الدور المحتمل للكربون النشط والمصنوع من نوى التمر في التطبيقات الطبية الحيوية والبيئية وأنها قد تفتح الأبواب للتطبيقات في مجالات متنوعة مثل قطاع الرعاية الصحية والقضايا البيئية.

مفاهيم البحث الرئيسية: نوى التمر، الكربون النشط، الممتزات، المواد الحيوية، إزالة السموم من البيليروبين، محفز نمو النبات.

Acknowledgements

Throughout the writing of this dissertation, I have received a great deal of support and assistance. I would first like to thank my supervisor, Professor Khaled Abbas El-Tarabily, for the continuous support and patience. His guidance and motivation helped me during my PhD degree.

Apart from my supervisor, I won't forget the gratitude to rest of the team. Professor Abdel Hamid Ismail Mourad whose endless guidance and support is hard to forget throughout my life. I would like to express my gratitude to Professor Amr Amin, Dr. Ali Hilal Alnaqbi and Professor Synan Abu Qamar who all also played a major role in this journey.

I would like to acknowledge Dr. Essam Saeed and lab mates, who helped me during my research works. I want to thank Department of Biology, College of Medicine and Health Sciences, and Department of Mechanical and Aerospace Engineering, who supported me in accessing their laboratory facilities. I would also like to thank College of Graduate Studies for the financial support. I would like to thank Dr. Bobby Mathew and Dr. Fadi Al Naimat from Mechanical Engineering and Aerospace Department for their support in my Ph.D. tenure.

In addition, I would like to thank my parents, my siblings and my friends for their wise counsel and sympathetic ear.

Dedication

To my beloved parents and family

Table of Contents

List of Tables

List of Figures

List of Abbreviations

AC	Activated Carbon
ACC	1-AminoCyclopropane-1-Carboxylic
ACCD	ACC Deaminase
ALF	Acute Liver Failure
BAL	Bio-Artificial Liver
Car	Carotenoids
Chl	Chlorophyll
DSC	Differential Scanning Calorimetry
DW	Dry Weight
IAA	Indole-3-Acetic Acid
IPYA	Indole-3-Pyruvic Acid
PA	Polyamines
Put	Putrescine
SDW	Seed Dry Weight
SEM	Scanning Electron Microscopy
Spd	Spermidine
Spm	Spermine
TGA	Thermogravimetric Analysis

Chapter 1: Introduction

1.1 Overview

Activated carbon (AC), also termed as activated charcoal or active carbon are black carbonaceous solid material with low volume pore size distribution which increase the surface area, and surface reactivity for adsorption and other chemicals reactions (Brito et al., 2018; Gao et al., 2020). AC functions as one of the most important microporous adsorbents owing to its remarkable adsorptive ability, enhanced affinity for a variety of dissolved organics, and custom-tailoring ability in order to suit its utilization for specific applications (Lakshmi et al., 2018; Xu et al., 2018). The application and performance of AC as adsorbents are determined by their surface chemical properties and textural properties, which ranges from biomedical applications, pharma industry, atmospheric pollution control, gas and energy storage, wastewater treatment, solvent recovery, food industry, catalyst support, etc. (Gao et al., 2020; Ramalingam et al., 2020; Zhang & Shen, 2019; Zhang et al., 2020).

During adsorption process, mesoporous AC produced by chemical or physical process help in adhesion of the ions, atoms, or molecules from surface of the dissolved solid or a liquid or a gas. Moreover, AC can be considered as low cost and chemically stable material with remarkable surface containing millions of pores with well-developed porosity analogous to a molecular sponge for various applications (Ayinla et al., 2019). The surface area of 1 g of AC revealed by gaseous method is approximately 3,000 m^2 (32,000 sq ft) due to presence of high degree of micro porosity. The microporosity and high surface area determine the activation level of AC for various applications. Carbonization and activation represents the two basic procedures employed for activated carbon synthesis (Ayinla et al., 2019). In general,

temperature range of 300–900°C is employed for the carbonization procedure using carbon precursor's pyrolysis and reduction of volatile content of raw materials. This procedure create char with a high content of fixed carbon and associated primary porosity (Oginni et al., 2019). On the other hand, to increase the surface area and pore volume, activation procedure opens new pores and develops existing pores in AC. In addition, activation provides certain unique characteristics to AC by changing or adjusting the surface chemical nature. There is more attention on activation process as this step is more crucial in providing different properties to AC than carbonization. Currently, physical activation, chemical activation, and physiochemical activation represents the three main techniques for the preparation of AC (Oginni et al., 2019).

The principle adsorptive and physical properties of the produced AC solely rely on the type and properties of raw materials utilized for production. Therefore, as starting material for production of AC, any cost-effective material can be used with percentage of carbon content will be higher than inorganic content. The selection of raw materials is mainly decided by several criteria's such as ease of activation, low inorganic content, and low degradation upon storage (Menéndez-Díaz & Martín-Gullón, 2006).

AC is usually derived from charcoal (activated coal) is mainly available in three forms: powder form, granular form, and pellet form (Menéndez-Díaz & Martín-Gullón, 2006). Owing to its simplicity in terms of design and operation, selectivity towards certain substances as well as ability to totally eliminate pollutants even from dilute solutions, AC demonstrated superior adsorption properties and escalated surge in its utilization in different domain such as chemistry, pharma industries, biomedical and environmental area. This has further led to an increasing quest towards development of durable, dependable, and selective alternatives for environmental

protection and conservation. Taken together, AC act as a carbonaceous porous solid material for improvement of the quality of human daily life as well as commercial consumer products (Ahmad et al., 2012).

1.1.1 Date Palm, Date Pits and its Importance in the Middle East and UAE

Date palm scientifically called as *Phoenix dactylifera* L. of *Arecaceae* family represents the most important fruit tree, which are mainly prevalent in temperate, tropical, and sub-tropical regions of the world and more precisely expanded from North Africa to the Middle East particularly in the United Arab Emirates (UAE) (Ahmad et al., 2012). Generally, a fully-grown date palm tree has feather looking leaves around 3–5 meters long along with a trunk or stem around 15–25 meters tall. Currently, available palms trees in the UAE accounts for more than 40 million dates, and still many of the dates sold locally are imported. The importance of date palm fruit stretching from providing sustenance to Bedouin settlers and have been rooted in Arabic culture since long time as its being depicted in local literature and earn a prime place in the Quran (Ghnimi et al., 2017).

Efforts are underway to enhance the number of palm in addition to 44 million up to now, that to spread across the country. The government aims to encourage the farmers to embrace newer and advanced agricultural methods and environment friendly techniques for a better future. With a vast array of date palm varieties (2600) available throughout the world, UAE has the varieties that are native to the local desert and do not require a lot of maintenance (Ghnimi et al., 2017).

The *Phoenix* varieties are the most common ones. Most of the species in this family tolerate high heat, therefore, making them a suitable and popular variety for this region. Normally, they can grow as tall as 20 meters tall with single trunk but

sometimes are clumped as well. Their massive and thick trunks make them graceful and stately (Ghnimi et al., 2017). The trees have leaflets arranged on either side of the stem which are a foot long and can be harmful to eyes and the skin. The rate of growth of these trees is quite slow and may take up to 10 years to transform into a fully grown, mature tree (Ghnimi et al., 2017).

Date seeds or pits represents 6-15% of the total weight of ripe date fruit (Ghnimi et al., 2017; Hussein et al., 2017). Date pits are normally discarded and being utilized as ingredients of animal feed or consumed as non-caffeinated coffee by the Arabs. Owing to its valuable medicinal properties and chemical composition, date seeds has been extensively utilized for various applications (Alyileili, Belal et al., 2020; Alyileili, El-Tarabily et al., 2020).

The medicinal properties of date pits include antiviral properties, prevention of DNA damage, treatment of blood sugar-related issues, prevention of kidney and liver damage and others (Jassim & Naji, 2010; Diab & Aboul-Ela, 2012; Halaby et al., 2014; Abdelaziz et al., 2015). Date pits are composed of various biomolecules such as carbohydrates, dietary fibers, proteins, fats, minerals, and ash. In addition, date seed contains oil (5–13% content) for various purpose. Date pits oil may be used for nutritional purpose and also utilized as edible cooking oil and margarine production based on the fatty acid composition and its high thermal stability, respectively (Mrabet et al., 2020). The thermal resistance properties associated with date seed oil enhances the shelf life and storage ability for a long time. Lauric and oleic acids represent the main saturated and unsaturated fatty acids present in date seeds oil, respectively (Besbes et al., 2005).

In addition, Date Seed Oil (DSO) antioxidant content is similar to olive oil and can be utilized as a good antioxidant source as per consumer’s requirements (Taha et

al., 2019). Furthermore, date palm oil also contains significant amounts of few other components such as phenolic compounds. tocopherols, phytosterols and tocotrienols (Idowu et al., 2020). The presence of these phytochemicals and other medicinal properties confers added value to date seed oil for utilization in various applications, such as formulation of food products, cosmetics, and pharmaceuticals (Mrabet et al., 2020). The health benefits of date pits oils include skin protection from ultraviolet (UV) rays, fights against free radicals, proper nourishment to the scalp for hair growth due to presence of omega fatty acids (Alharbi et al., 2021).

1.1.2 AC from Biologically Derived Materials

AC is carbon-based powerful adsorption material along with presence of wide spectrum oxygenated functional groups (Togibasa et al., 2021). Another significant importance of AC includes its usage as carbon precursors owing to its physico-chemical characteristics, carbon adsorption properties, micro-nano structural and textural features for varied applications. AC are conventionally produced employing various lignocellulosic materials such as palm kernel shell, olive bagasse, oil palm trunk, date palm pits, olive cake, coconut shells, wood, oil palm empty fruit bunch, rice husk, etc (Zhou & Wang, 2020).

A wide range of biomass precursors having high carbon content can be used to produce AC. AC production from lignocellulosic biomass offers several advantages such as the diversity and abundance of precursors and its renewable nature, which helps in relatively simple production steps due to the high reactivity of the biomass. This further contributes towards cost cutting of waste disposal and decreases the negative impact to the environment (Foo & Hameed, 2009; González-García, 2018). The common raw materials include coal, peat, woody biomass (both soft and

hard), date palm seeds, coconut shells, nutshells, olive stones, palm kernels and others (Foo & Hameed, 2009). Currently, almost all organic materials with relatively high carbon content can be utilized as raw materials for AC production. AC properties such as pore-size and purity of final product is predominantly determined by the type of raw materials being utilized (Foo & Hameed, 2009). Therefore, in the last one decade, the usage of waste biomass and lignocellulosic resources have gained tremendous impetus as far as AC production is concerned. In the recent years, great deal of research interest being focused in exploring inexpensive and effective raw materials alternative to the existing commercially available AC for AC production with high yield and in a non-hazardous way (Bernardo et al., 2016).

Due to rising environmental concerns in recent years, exploration of farm wastes, woody biomass, agricultural by-products, aquatic biomass, industrial biomass wastes and everyday waste materials as precursors for AC have largely shifted the attention towards usage of biologically safe materials (Zhou & Wang, 2020). As far as environmental sustainability is concerned, more focus is mainly on biomaterials derived activated carbon. The development of low-cost activated carbons using different precursors depends on several factors such as free availability, cost-effectiveness, and its non-hazardous nature (Bernardo et al., 2016).

In addition, surface, textural, structural characteristics, with low amount of ash and high contents of fixed carbon are desirable criteria for production of AC (Maulina et al., 2020). Nonetheless, utilizing renewable lignocellulosic wastes, agro-industrial waste materials and municipal residuals provides significant advantages in terms of ability in harnessing the potential of obtained AC in diverse applications such as adsorbents (Gautam et al., 2014), électrodes (Sha et al., 2015), catalyst (Petkovic et

al., 2009), fertilizer (Mui et al., 2010), liming and neutralizing agents (Htwe et al., 2016).

Date pits represent one of the best candidates for AC production among all the agricultural wastes owing to its increased carbon content, low cost, and its abundance especially in Mediterranean countries (Ben Amor & Ismail, 2015). Date seeds are suitable raw material for producing AC due to its excellent natural structure, ligno-cellulosic composition, enhanced physico-chemical properties, and low ash content (Al-Alawi et al., 2017).

Currently there are approximately 100 million date palm trees available worldwide, and around 62 million are present only in Middle East countries particularly UAE and North Africa. As per statistics, around 15000 tons of date palm leaves are discarded as waste materials in Saudi Arabia only (Al-Alawi et al., 2017; Jonoobi et al., 2019). Out of all parts of the date tree alongside leaves, trunk and seeds, date palm seeds or date pits obtained from palm trees represents one of the most important sources for manufacturing activated carbon (Hussein et al., 2015; Nasser et al., 2016).

In addition, date palm seed having very high carbon content is a potential raw material for AC production among fruit stones. The date seed is usually oblong in shape, ventrally grooved, hard-coated seed with a small embryo with 0.5 g to 4 g weight. Depending on the date palm fruit maturity, variety and grade, date pits constitute approximately 6 to 20% of the fruit weight (Thomas & George, 2015).

The composition of date seed essentially contains following constituents in percentage (Hu et al., 2017):

i. Cellulose (23.9±0.1).

ii. Hemicellulose (26.8±0.1).

iii. Lignin (21.6±0.1).

iv. Ash (1.0±0.1).

The traditional use of date seeds includes oil source with high antioxidant properties (important in cosmetic products), as animal feed, coffee substitute, as an adsorbent for dye-containing waters, and as a raw material for production of AC (Belhachemi et al., 2009). The properties and performance of AC largely depends upon the raw material source. Date seeds- or date pits-based AC has been extensively utilized for absorption of heavy and toxic metals.

Therefore, much focused research and exploration in different applications such as in absorption of heavy and toxic metals, making paper, energy production and soil fertilizers using date pits based AC are required (Foo & Hameed, 2011; Reddy et al., 2015; Ogungbenro et al., 2017).

1.1.3 Properties and Types of AC

AC are amorphous, non-graphite carbonaceous material with excellent adsorptive property owing to presence of low volume pores and large surface area (Mayyas & Sahajwalla, 2019). AC represents a complex structure mainly comprises of carbon atoms with a highly porous adsorptive medium stacked unevenly in such a way that it makes every nook, cracks, crannies, and crevices between the layers highly porous (Mahmoudi et al., 2014).

AC having intrinsic network of pores that makes it suitable for adsorption process by removing impurities from gaseous and liquid medium. The adsorption ability of AC related to its very strong physical adsorption forces and highest adsorbing porosity (Mahmoudi et al., 2014).

1.1.3.1 Fundamental Properties of AC

There are various fundamental properties of activated carbon which are being utilized for its usage in various applications.

Surface Area: internal surface area dictates the effectiveness of the activated carbon. AC has a surface area greater than 1000 m^2/g and 3 g of AC can have the surface area equal to a football ground. Larger surface area of AC makes this extremely suitable as adsorption agents (Yahya et al., 2015).

Pore radius: AC has a diverse and unique distribution of pore sizes. The mean pore radius of activated carbon is often measured in angstrom (Yahya et al., 2015).

Total Pore Volume (TPV): void spaces inside AC particle represents total pore volume. TPV is generally expressed in milliliters per gram (mL/g), which indicates volume in relation to weight of the particle. The effectiveness of AC relies on TPV, which in turn depends upon the raw material used and activation process type utilized for AC production (Yahya et al., 2015).

1.1.3.2 Different Classes of AC

Granular AC (GAC): Granular AC is basically irregular shaped carbon particles produced by milling and sieving of size ranging from 1-5 mm (Menéndez-Díaz & Martín-Gullón, 2006). They are more durable and have better lifetime than other forms of AC and can be used for both gaseous and liquid applications. It finds wide application in refineries wherein the AC is packed in columns, through which the liquid flows (Bayer et al., 2005). Also, they are advantageous for applications in gases due to their acceptable pressure drop. Besides GAC can also be reactivated at an average interval of 2-17 months and

can be reused with a minimal loss of material ranging from 5-15% (Bayer et al., 2005; Menéndez-Díaz & Martín-Gullón, 2006).

Powdered AC (PAC): the powdered form of AC is mainly used for liquid phase applications have a size less than 100 nm. In batch application processes, PAC are advantageous as it offers the flexibility of varying its amount to be added based on the requirement. Other advantages of PAC include its lower processing cost and flexibility in operation that means the dosage of PAC can be increased or decreased based on the process conditions and applications.

Extruded AC (EAC): the AC is in an extruded form and cylindrical shape with diameters ranging from 0.8 to 5 mm. EAC have low dust content and very high mechanical strength, which are suitable for heavy duty applications like gas phase applications. As there is low pressure drop in extruded activated carbon, it is widely used for automotive emission control, gas purification, solvent recovery, etc (Sichula et al., 2011).

1.1.4 Methods for Production of AC

Carbonization (pyrolysis) and activation of carbonaceous raw materials represents two basic steps in AC production. Carbonization process employs an inert environment and elevated temperature for generation of solid product called char through pyrolysis of precursors materials (Balahmar et al., 2017). Carbonization step employs thermal decomposition process for generation of enriched carbon mass with a rudimentary porosity by eliminating the non-carbon species from precursors (Balahmar et al., 2017).

In addition, volatile matter and hydrogen are eliminated from the raw material. In this process, temperature plays very prominent role followed by rate of heating,

nitrogen flow rate and residence time (Heidarinejad et al., 2020). Generally, high temperature such as ~ 600-700°C produces less char and increased ash content. Therefore, optimization of temperature is very much important for production of high yield of AC along with very less ash content (Balahmar et al., 2017).

Carbonization process is further followed by development of pores within generated AC through activation process as obtained char through carbonization process possesses little adsorption ability (Heidarinejad et al., 2020). Activation step is more crucial considered than carbonization process in terms of generation of properties of AC. Thus, attention is more focused towards activation process.

Activation process enhances pore diameter, pore volume, porosity, and surface area of activated carbon (Heidarinejad et al., 2020). Activation process is performed in different phases for removing unorganized carbon, exposing biomass for activation by different kinds of activating agents for generation of large sized pores with high microporosity (Temdrara et al., 2015).

Currently, there are three main methods being employed for activation of carbon: physical, chemical and physio chemical (Temdrara et al., 2015). A list of representative steps being employed in physical and chemical activation methods are illustrated in Figure 1.1.

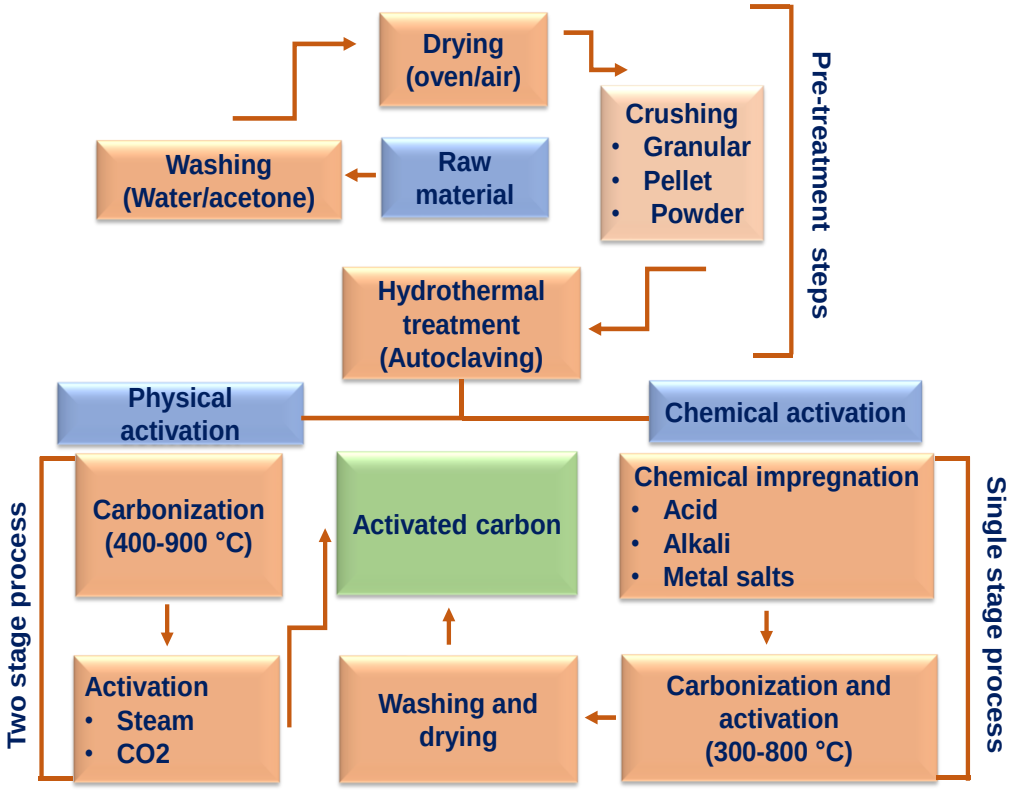

Figure 1.1: Flowchart showing different steps involved in physical and chemical activation methods for production of AC

1.1.4.1 Physical Activation

Physical activation is a dual stage inexpensive and environmentally friendly process and does not employ any harsh chemicals. In addition, AC produced by physical activation processes is preferable as far as environmental and biomedical applications are concerned (Balahmar et al., 2017). Herein, the carbonization procedure is carried out in the presence of an inert gas (N_2 or Ar) environment at a temperature range of 800–1200°C followed by the activation stage using various oxidizing gases (O_2, CO_2, H_2O steam) (Balahmar et al., 2017; Danish & Ahmad, 2018).

This activation process generally uses CO_2 or steam at temperature range greater than 700°C. The diffusion rates of steam are 2-3 times faster than CO_2 even

with the same degree of conversion. The smaller molecular size of water facilitates diffusion are responsible for effective porous structure in within the char. The physical activation process is affected by various factors such as nature of carbon precursors being used, particle size, carbonization time, gas flow rate, heating rate, and temperature (Danish & Ahmad, 2018).

The advantages of physical activation process include cleanliness, green production of AC without any need to remove secondary wastes unlike chemical activation. Despite of the advantages, relatively low carbon yield, high activation temperature requirement, relatively long processing time, and AC with poor specific surface area represents few of the disadvantages associated with the physical activation method (El-Naas et al., 2010; Rodríguez-Reinoso & Molina-Sabio, 1992).

1.1.4.2 Chemical Activation

Chemical activation, also known as "wet oxidation," is a solitary process, employs chemical activators and carbonization and activation stage takes place simultaneously. Herein, activation method involves impregnation with chemical activators in the temperature range of 450–850°C using acids (HNO_3, H_2SO_4, and H_3PO_4), alkali (NaOH and KOH) or salts ($ZnCl_2$, $MgCl_2$, $FeCl_3$, $AlCl_3$, and K_2S) (Ahmed & Theydan, 2012; González-García, 2018).

The porous structure and porosity are generated in AC by dehydration and degradation process. The chemical agents used in this method are dehydrating agents which inhibits the formation of bitumen and influences the pyrolytic decomposition and thereby increasing the carbon content with formation of porous structure AC (Heidarinejad et al., 2020).

Various factors which affects the chemical activation process comprise with the type of activating agent, mass ratio of activating agent to carbon precursor, mixing method, and temperature given (Sevilla & Mokaya, 2014). The advantages of chemical activation method include utilization of low heating temperature, high carbon yield, short processing time, production of AC with large surface area and well-controlled porosity (Zhang & Shen, 2019). However, this method suffers from few shortcomings too such as its inevitable washing process due to utilization of chemicals and its drastic corrosivity (Dai et al., 2018).

The comparative differences between both physical and chemical activation method in terms of activation process and parameters for production of activated carbon with desired properties is represented in Table 1.1.

1.1.4.3 Physico-Chemical Activation

The assortment of both physical and chemical activation process leads to physico-chemical activation. In the method, after carbonization step both physical and chemical activations are simultaneous performed unlike only physical or chemical activation method individually applied (Gao et al., 2020).

Herein, chemical impregnation of carbon precursors is performed utilizing an oxidizing gas atmosphere using chemical activating agents resulted by a physical activation step (Gao et al., 2020). Therefore, it's also a two-step activation process like physical activation process and activation occurs at high temperature range from 600 to 850°C in the presence of various dehydrating agents (KOH, $ZnCl_2$ or H_3PO_4) and oxidizing agents (CO_2 or steam) (Hazzaa & Hussein, 2015; Hameed et al., 2009).

Table 1.1: Comparative properties of physical and chemical activation methods for production of Activated Carbon (AC)

S. No.	Physical Activation	Chemical Activation
1.	Commercial point of view: Physical activation process is utilized for production of ACs with high micro porosity and desirable physical characteristics.	Commercial point of view: Chemical activation utilizes lower activation temperature and indicate lower contact time which can save money and time.
2.	Steps: two-step activation method.	Step: one step activation method.
3.	Time: more processing time required.	Time: less processing time required.
4.	Activating agents: steam, CO_2, O_2.	Activating agents: Chemicals (KOH, H_3PO_4 or $ZnCl_2$ etc.
5.	Surface area: provides more surface area than chemical activation methods.	Surface area: provides relatively less surface area.
6.	Temperature: generally, needs higher temperature for activation (activation temperature – (700°C).	Temperature: lower temperature required for activation.
7.	Disadvantages: less yield of AC, high temperature requirement for activation, low packing density of AC resulting due to presence of empty spaces.	Disadvantages: corrosive nature of some activating agents, high cost of the activating agents, additional washing steps required to remove activation agents.

The combined activation methods impinge pore cavity and ultimately lead to porous structure and improvement of mass transfer within the AC matrices. The advantages associated with physio-chemical activation include controllable surface modification and textural property (Hazzaa & Hussein, 2015). The downsides of physio-chemical activation include complex and excessive energy consumption steps, high cost, long preparation time, which further limits its usage in large-scale industry applications. Despite of its longer preparation time and high-cost requirement, this activation method can produce AC with favorable properties in terms of mesoporosity and specific surface properties prerequisite for particular applications (Hazzaa & Hussein, 2015).

In earlier studies, either physical or the chemical activation is used to prepare AC with high microporosity (Kumar & Jena, 2015). In recent years, physio-chemical

activation methods are employed for activation purpose for specific applications. Moreover, agents play pivotal roles in the development of pores or other surface chemical groups throughout the activation process irrespective of what activation method was utilized for activation (Hazourli et al., 2009).

A representative comparative list of all three activation methods in terms of yield of AC and textural properties generated is shown in Table 1.2. Among all the activation methods, chemical activation method confirms to be the finest method for AC production with high yield.

Table 1.2: Representative list of different activation methods showing comparison in terms of yield and textural properties of produced Activated Carbon (AC)

Activation method	**Activation conditions**	**Surface area S_{BET} (m^2/g)**	**Yield (%)**	**Reference**
Physical Activation				
CO_2	900°C, 4 h	490	----	(El-Naas et al., 2010)
Steam	800°C, 1 h	702	17	(Awwad et al., 2013)
Chemical Activation				
KOH	800°C, 1 h, 0.5%	1032	----	(Merzougui & Addoun, 2008)
$ZnCl_2$	600°C, 3 h, 0.5%	999	46	(Alhamed & Bamufleh, 2009)
H_3PO_4	450°C, 1.2 h, 3%	952	41	(Reddy et al., 2012)
NaOH	600°C, 1 h, 3%	1282	----	(Islam et al., 2015)
$FeCl_3$	700°C, 1 h, 1.5%	780	47	(Theydan & Ahmed, 2012)
Physio-Chemical Activation				
HNO_3/steam	600°C, 3 h, 10%	950	----	(Hazourli et al., 2009)
KOH/CO_2	850°C, 2 h, 9 Litre/h	763	20	(Hameed et al., 2009)
H_3PO_4/steam	600°C, 3 h, 1%	1100	----	(Hazourli et al., 2009)

1.1.5 *Salicornia*

Salicornia (glasswort) is a fast-growing halophytic plant, which can grow in different climates ranging from temperate to tropical particularly in coastal salt marshes and in salty habitats of many countries including Kuwait, the United States, and United Arab Emirates (UAE) (Shepherd et al., 2005; Al-Yamani et al., 2013; Shahid et al., 2013). The general characterization of this plant genus is it has apparently leafless shoots and extreme reduced morphology (Davy et al., 2001). Apart from human consumption and animal feed, *Salicornia* species derived oilseeds are potential source of oil for production of biofuels and biodiesel (Abideen et al., 2015; Doncato & Costa, 2018).

Saline soils in arid and semi-arid regions exhibit prominence of diverse types of halophytes species (English & Colmer, 2011). Thus, salinity of soil salinity represents serious environmental stress, which can affect the global agricultural productivity of halophytes (Mayak et al., 2004).

Currently, among halophyte cultivation *Salicornia* cultivation represents one of most successful examples. *Salicornia* crops are extreme tolerant to salts and require saline irrigation water with high salt concentration for growth (Ventura & Sagi, 2013). In order to become commercial halophyte crop, *Salicornia* growth should be economically viable with high yield production under saline conditions (Abideen et al., 2015). At present, small-scale production *Salicornia* plant with irrigation with saline water is being practiced, however; development of halophyte crops at large agricultural scale is still in its infancy (Doncato & Costa, 2018).

Currently, lots of strategies are being employed for promoting growth of *Salicornia* using bacterial inoculants such as rhizospheric bacteria and endophytic

Plant Growth Promoting Bacteria (PGPB) serves considerable interest in promoting the growth of *Salicornia* species (Mesa-Marín et al., 2019). The endophytic bacteria-plant interactions provide various beneficial effects to the host-plant which includes Nitrogen (N) fixation, Plant Growth Promotion (PGP), systemic resistance to plant pathogens, biological control against pathogens, phytoremediation improvement, and adaptation of crop to environment challenges (Khare et al., 2018; El-Tarabily et al., 2019).

1.2 Literature Review about AC and its Application

AC are carbonaceous materials also known as activated char exhibits numerous fingerprints without having any specific chemical formulae (Mayyas & Sahajwalla, 2019). The varying fingerprints of AC include large surface area, well developed and tunable pores and porosity, highly reactive surface properties, excellent adsorptive ability, and reliable physio-chemical stability (Sharma et al., 2016; Gao et al., 2020).

In addition, AC are inexpensive, have abundantly available raw material for its production, good blood compatibility, high mechanical and thermal properties stretch its applications from adsorption to biomedical and even environmental domain. Overall, the difference or variation in constituent fingerprints/features relies mainly on the raw material/precursors, type of activation method used, and the adopted processing conditions for production of AC (Gao et al., 2020).

The conventional precursors being utilized for production of activated carbon include animal wastes, feeds, pitches, and others, which represents non-renewable and depleting source material. The choice of raw materials ultimately affects the economic availability of the final product (Ayinla et al., 2019). Therefore, in order to overcome these problems, inexpensive, abundantly available, and renewable source material are

being explored for maintaining the environmental sustenance. In this context, more focus is on the development of low-cost AC with properties comparable with the commercially available expensive AC using renewable sources in recent years (González-García, 2018). A wide range of precursors such as, lignocellulosic wastes, industrial and agricultural wastes have been utilized and extensively explored worldwide for the production of AC for application in different domains as adsorbent (González-García, 2018). AC are produced with different properties and efficiencies depending on the nature of the bio-wastes utilized and therefore, the chemical composition of the precursors is accountable for the production of activated chars. Regardless of the source, AC is produced in two steps namely carbonization (pyrolysis) and activation (Heidarinejad et al., 2020).

AC have demonstrated diverse applications in various domains stretching from water purification, air purification, as catalyst, in metal extraction, gas storage, medicine sewage treatment, decaffeination, supercapacitor electrodes fabrication, and energy storage devices active materials (Nayak et al., 2017; Xu et al., 2018; Lakshmi et al., 2018; Meng et al., 2018; Phiri et al., 2019; Gao et al., 2020; Ramalingam et al., 2020; Zhang & Shen, 2019; Zhang et al., 2019).

The importance of AC in the application of various domains makes extensive research studies by researchers throughout the world. In earlier studies, Guo and Lua (2003) studied the adsorptive properties of AC produced from palm wastes by chemical activation by H_3PO_4 and KOH. They further found that the surface functional groups and subsequent occurrence of chemisorption provided significant influence on the adsorptive capacity of produced AC (Guo & Lua, 2003). Sevilla and Mokaya (2014) reported a method to tailor biomass-based AC properties such as porosity and morphology for application in hydrogen storage and supercapacitors electrodes

(Sevilla & Mokaya, 2014). Yahya et al. (2015) studied fabrication of AC from diverse agricultural wastes and discussed effect of different activation processes on textural (surface area, pore volume) and physio-chemical properties of produced AC (Yahya et al., 2015). Furthermore, Jain et al. (2016) reported enhancement of AC porosity via hydrothermal treatment of biomass wastes before activation process (Jain et al., 2016). Rashidi and Yusup (2017) provided a comprehensive detailed information about technological advancement of palm waste produced AC and effect of different heating methods on textural properties (Rashidi & Yusup, 2017).

In another study, González-García (2018) discussed in detail about ACs produced from lignocellulosic precursors, its physio-chemical characterization techniques, and various properties such as adsorption capacity, micro/nano structural features, surface chemistry (González-García, 2018).

Recently, Gao et al. (2020) have extensively reviewed the production of AC using different chemical activators such as acidic, alkaline, neutral, and self-activating chemical agents. In addition, influence of activation approaches on physical and chemical properties of resultant AC was also evaluated and discussed in details (Gao et al., 2020). A list of activated carbon in different fields are shown in Figure 1.2.

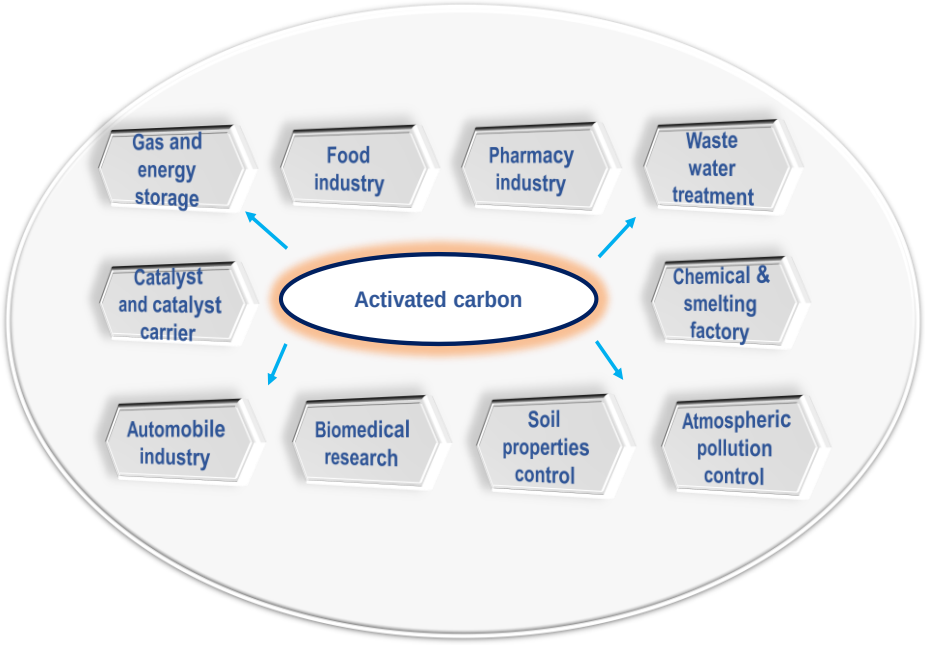

Figure 1.2: Schematic showing application of biomass wastes derived Activated Carbon (AC) in different domains

1.2.1 Application of AC as an Adsorbent

AC with internal porous architecture, mesoporous nature and high surface area makes it suitable candidate for adsorption applications. AC as an adsorbent have shown effectiveness in removal of various organic and inorganic pollutants owing to presence of mesoporous structure, high surface area, and adsorption ability (Ayinla et al., 2019).

Researchers have commonly employed two-and three-parameter isotherm equations for evaluation of the adsorption behavior of AC and compared the maximum range of uptake of several pollutants on AC. Various researchers have demonstrated the adsorption efficiency of date palm wastes derived AC for adsorption of synthetic dyes that plays pivotal role in research and development (Ahmed & Dhedan, 2012; Alqaragully, 2014). Foo and Hameed (2011) reported the adsorption capacity of methylene blue dye on AC using different models such as Freundlich, Langmuir and

Temkin isotherm models for fitting the adsorption isotherm data (Foo & Hameed, 2011). They observed that adsorption efficiency was strongly related to the pH and indicated enhanced adsorption ability of AC (38 to 276 mg/g) with the increase in pH from 2 to 12.

Theydan and Ahmed (2012) further studied adsorption of phenol on AC generated by $ZnCl_2$ (ZAC) and $FeCl_3$ (FAC) chemical activations. The results indicated endothermic adsorption nature and showed enhanced adsorption of phenol with the increase of temperature with maximum capacities of adsorption around 169.55 and 181.03 mg on ZAC and FAC, respectively. El Bakouri et al. (2009) demonstrated the possible applicability of date stones derived AC on removal of drin pesticides such as aldrin, dieldrin and endrin from aqueous solutions. The uptake of pesticides was more when there was increase in the initial pesticide concentration and decrease in adsorbent particle size. The decrease in particle size indicated maximum capacities of adsorption 373.728, 295.305, and 228.047 mg/g for aldrin, dieldrin, and endrin, respectively due to significant increase in the surface area (El Bakouri et al., 2009).

In another study, researchers reported adsorption behavior of pesticides like 2,4-dichlorophenoxy acetic acid (2,4-D), bentazon, and carbofuran on date seeds derived AC generated via physio chemical activation using KOH/CO_2 (Salman & Hussein, 2014). Furthermore, adsorbent ability of activated carbon in removal of heavy metals has been extensively investigated. Ameh (2013) reported the adsorption behavior of Copper (Cu) and Cadmium (Cd) on chemical activation generated activated carbon (Ameh, 2013). The variables such as carbon dose, initial metal concentration and the solution pH combined effect affected the uptake ability and maximum adsorption capacity of Cu and Cd was 118.06 and 88.42 mg/g, respectively.

A list of different adsorptions behavior of different adsorbates (heavy metals, dyes, pesticides, and phenolic compounds) onto date pits derived AC generated through different activation methods is presented in Table 1.3.

Table 1.3: Representative list showing comparative adsorption capacities of Activated Carbon (AC) derived from date pits for removal of dyes, phenolic compounds, pesticides, and heavy metals

Activation method	**Adsorbate**	**Adsorption conditions**	**Maximum absorbance capacity (mg/g)**	**Reference**
NaOH	Methylene blue	1 gm/l, 30°C, 24 h, pH 7	612.1	(Islam et al., 2015)
$ZnCl_2$	Methyl orange	0.5 gm/l, 30°C, 6 h, pH 3.5	434.8	(Mahmoudi et al., 2014)
CO_2	4-Chlorophenol	4 g/l, 72 h, 25°C, pH 6.7	390	(Sekirifa, Pallier et al., 2013)
KOH	p-Cresol	1 g/l, 5 days, 25°C	322.5	(Merzougui & Addoun, 2008)
KOH/CO_2	2,4-D	1 g/l, 9 h, 30°C, pH 3.6	238.1	(Hameed et al., 2009)
KOH/CO_2	Carbofuran	1 g/l, 30 h, 30°C	135.1	(Salman & Hussein, 2014)
Steam	Lead	0.2 g/l, 25°C, pH 5.5	1260	(Awwad et al., 2013)
Steam	Cobalt	0.2 g/l, 25°C, pH 5.5	1310	(Awwad et al., 2013)
Steam	Zinc	0.2 g/l, 25°C, pH 5.5	1594	(Awwad et al., 2013)
KOH	Cadmium	1 g/l, 24 h, 25°C, pH 5.9	124	(El-Hendawy, 2009)

1.2.2 Applications of AC in Biomedical Engineering

AC owing to its excellent adsorbent property finds wide applications in various fields including biomedical field. The AC being utilized in medicine and pharmaceutical industries are new type of AC called as ‘medicinal AC’ due to its medicinal usage. In order to utilize AC in biomedical industry, AC must be capable of

absorbing a vast range of biomolecules from complex carrier fluids such as blood, plasma, or stomach contents and therefore it must be biocompatible (Mansurov et al., 2020). In this context, AC should not damage the blood cells, promotes minimal changes in plasma proteins or enzymes, should not provide immunological and carcinogenic effect, and specific to target tissues without affecting or deteriorating the adjacent tissues (Mikhalovsky et al., 2012).

1.2.2.1 AC in Pharmaceutical Industry

AC plays an important role among the multitude of medicines and has been used in healthcare industry since very long. It has been utilized as oral antidote against a wide range of toxic substances and poisons. In addition, it has been utilized for extracorporeal purification of bodily fluids, particularly, blood, and in wounds and burns treatment (Mikhalovsky et al., 2012). Recently, new generation AC with improved mechanical properties, porous structure with ability to bind high molecular-weight and protein-bound biological toxins for range of treatment strategies were developed. This new generation of AC demonstrated great potential in improved treatment of acute and chronic diseases with reduction in healthcare cost burden (Mikhalovsky et al., 2012). Activated charcoal prevents its absorption from the gastrointestinal tract due to its ability to adsorb various noxious substances on its surface. The noxious substances include medical drugs, phytotoxins and poisonous chemicals. In a recent study, AC reported as mediator for secondary decontamination mechanism which otherwise may interrupt the potential enterohepatic and/or enter enteric circulation (Zellner et al., 2019).

1.2.2.2 AC for Oral Use and Other Open Wounds

Oral AC is primarily used for treatment of drug overdose and acute poisoning. The major function of an oral adsorbent is to remove toxic substances such as exogenous toxins, secondary toxic metabolites and others which are diffused into the intestine from blood and gastrointestinal tract. The functional groups present on activated carbon surface are responsible for the removal of these toxins (Zellner et al., 2019).

1.2.2.3 AC as Adsorbent Dressings

AC is also utilized as absorbent dressings to stop the spread of infections and fasten the healing process for superficial and profound lesions, as well as for restoration of post-operative trauma. In a study, the microbiological properties of microwave AC made from walnut shells impregnated with Ag, Se and Enoxil preparations were studied. The results demonstrated suitability of AC in various medical fields as bactericidal dressings for protection of the penetrative infections within the body (Petkovic et al., 2009; Petuhov et al., 2019).

1.2.2.4 AC in Hemoperfusion and Bilirubin Removal

Hemoperfusion is an extracorporeal form of medical treatment, which removes toxic elements from patient's blood through the adsorption process in the perfusion tank using adsorbent. This method removes the toxin content which are either lipid soluble or bound with proteins (Rozga et al., 2006). In this method, blood is taken out of an artery/vein followed by pumping through the adsorbent material integrated within a medical device located outside the patient's body. After passing through the adsorbent the cleansed blood returns to the patient's body. Presently, hemoperfusion

is used for treatment of theophylline poisoning (Ramanujan et al., 2007). Hemoperfusion is used in several treatments such as in dialysis for patients with kidney failure and for treatment of acute drug or chemical intoxication, etc (Iguchi et al., 2017).

AC has strong adsorption capacity for non-polar and hydrophobic molecules and have been utilized in clinically in hemoperfusion for removal of bilirubin. AC with polymeric coatings enhances its bio-tolerability making it feasible for use in hemoperfusion devices. The drug elimination is dependent on the affinity of the AC to adsorb the toxin rather than diffusion. Current hemoperfusion devices are biocompatible as it minimizes the direct contact between the adsorbent and the blood constituents by encapsulating the adsorbent material with a thin, porous semipermeable membrane (Iguchi et al., 2017).

In a case study, coated activated-charcoal column hemoperfusion demonstrated dramatic effectiveness for a teenage girl with life-threatening disopyramide poisoning (Iguchi et al., 2017). In another study, the interaction of human serum albumin with the high porosity AC and unconjugated bilirubin was investigated. Researchers reported promising effect of combination of albumin coated HemoSorbent Granulated Deliganding (HSGD) carbon with ligand free solution of Human Serum Albumin (HSA). Thus, the results open new prospective of AC based extra corporeal biochemical correction in patients with hepatic insufficiency (Sarnatskaya et al., 2002).

1.2.2.5 AC in Drug Delivery

Magnetically targeted drug delivery represses an area of research wherein the potential of AC in adsorption and desorption of drugs like theophylline delivery and

retention in target area for prolonged therapy can be provided (Ramanujan et al., 2007). AC is being administered either a single dose or multiple doses in treating cases of acute poisoning due to its well-recognized adsorption capacity (Pfab et al., 2017).

1.2.2.6 AC in Bio-Artificial Liver Devices

AC is used as a main component in dialysis devices such as artificial and Bio-Artificial Liver (BAL) devices owing to its high porosity, large surface area and adsorption capacity towards different compounds, high chemical and thermal stability, easy availability, abundance, cost effectiveness, and advantageous blood compatibility (Iguchi et al., 2017).

AC has been utilized as an adsorbent to remove bilirubin in most hemoperfusion systems. To enhance the efficiency of bilirubin adsorption in liver support devices numerous carbon-based materials have been reported in recent years (Jalan et al., 2004). The placement of cell housing devices by patient's bed side throughout the treatment and maintenance of cell viability and its functionality represent major current challenges. Among all the cell-housing devices, extracorporeal liver assist devices are most important for extracorporeal blood treatments that help maintain different functions of the liver, minimize failure of organs which is a major concern in liver failure, and prolongs existence of patients (Chen et al., 2017).

Extracorporeal liver assist represents an attractive alternative device for improvement of patients' prognosis by allowing time for liver regeneration and/or helps to extent their lives with this support until they receive a matching liver for transplantation (Lee et al., 2016). In order to reach this goal, hepatocytes are introduced in these devices to accomplish liver functions and externally deal with the circulated plasma/blood of patient's associated with liver failure (Teotia et al., 2015).

Hepatocytes are cultured and housed in a cell housing bioreactor, which represents principal biological component of BAL devices. Since last decade, substantial developments have been made in BAL devices for enhancement of hepatocytes *in vitro* culture, however; matrix synthesis and assembly of bioreactor in BAL devices still remains a challenge. Other shortcomings associated with BAL devices technology include poor growth of the hepatocytes, inadequate conventional transport, inefficient immobilization, nutritional elements across the reactor, and non-uniform cell seeding (Damania et al., 2018). Thus, cell culture-based device designs are pertinent requirement for improvement of cellular component competence (Kumar et al., 2011). In addition, instead of porcine hepatocytes or from tumor cell lines which are sensitive towards infection and malignancy transmission, primary hepatocytes or hepatic cell lines are adapted in these devices. Among all the cell lines being utilized in BAL devices, human hepatocytes would present the best cell source candidate for extracorporeal liver assist device in future studies (Van De Kerkhove et al., 2004; Chamuleau et al., 2005).

1.2.2.7 AC as Component in Biosensor Devices

AC is utilized in fabrication of electrodes, one of the component of biosensors devices where its high surface area allows effective immobilization of enzymes required for sensing compound. Herein, it promotes the electron transfer between the electrode and substrate for biosensing (Pinyou et al., 2019). Biosensor's electrodes derived from reduced graphene oxide based activated carbon exhibited good response to glucose with high sensitivity in a short response time (4 seconds) and a lower detection limit of 2 μM. These results suggest the suitability of AC based electrodes in biosensors for urine glucose sensing applications (Hossain & Park, 2016).

Furthermore, another biosensor device fabricated with AC for sensing of dopamine have demonstrated very good results while minimizing the interference by ascorbic acid and outperformed previous dopamine biosensors sensitivity (Rahman et al., 2016).

1.2.2.8 AC-based Nanoparticles as Antimicrobial Agents

Carbon nanotechnology is an upcoming technology with the production of carbon nanoparticles to be used in various applications. Among various carbon-based nanomaterials, emerging AC-based Nano Particles (ACNPs) with unique physico-chemical properties and biocidal properties acts as effective antimicrobial agents (Lakshmi et al., 2018). AC nanoparticles provides antimicrobial action against microorganisms by establishing electrostatic repulsion between carbon surface and Gram-negative microorganisms. AC-based nanoparticles can be modified with positive charges in order to kill Gram-positive bacteria. AC-based nanoparticles derived from biowastes such as coconut husk, sugarcane bagasse, rape seed oil cake and others have been employed as antimicrobial agents (Zhao et al., 2013; Das Purkayastha et al., 2014; Gonçalves et al., 2015).

1.2.3 Application of AC in Environment

Owing to its super adsorption ability, AC specifically in powdered and granular form have demonstrated broad spectrum applications such as in treatment of industry generated liquid and gaseous emissions, in purification and remediation of polluted aquatic environments, gas storage and delivery, metal recovery, catalysis, and as bioinoculant for plant growth promoters to name a few (Cukierman, 2013). AC has been widely utilized for water and air purification and its usage in removal of toxins

from soil has been explored very recently. Boyd et al. (2017) have demonstrated for the first time the role of AC in removing dioxin from the contaminated soil. Dioxins are a group of highly toxic chemical compounds, which are present in soil, sediments and in foods in higher concentration leads to serious health issues ranging from reproduction, development, to immune system. In a study, researchers have mixed the AC with most toxic form of dioxin (tetrachlorodibenzo para dioxin), silica, bentonite (a clay used to line landfills) and exposed to mice to determine the effective role of AC in the removal of dioxins and reducing its entry into the food chain. The capacity of AC in removing dioxins were superior as compared to other components due to presence of unique physio-chemical properties (Boyd et al., 2017).

In another study, researchers demonstrated that the harmful effect of dioxin-contaminated soil or sediment would be alleviated adding AC or not. Herein, the researchers reported accelerated detoxification of DCA, TNT and PCB in soil via amending soil with AC as DCA and TNT were strongly absorbed by AC present is soil. These results indicated favorable conditions for degrading microorganisms and plant growth. Furthermore, decrease of TNT in soil and promotion of bioremediation of highly toxic soil was reported using AC (Kołtowski & Oleszczuk, 2016). Thus, AC amendment in soil demonstrated good potential to remove toxicities from the soil. However, the effectiveness of AC in mitigating the soil toxicities depends upon several factors such as soil, type of amendment, dose and microorganisms present in soil (Kołtowski & Oleszczuk, 2016). In addition, AC are used in various environmental applications.

1.2.3.1 AC in Water Treatment

Due to its high surface area AC is found to be useful in removing many contaminants from both potable water and wastewater (industrial wastewater, landfill leachate, pond, etc.) (Foo & Hameed, 2009).

1.2.3.2 Environmental Air Treatment

Utilized for treatment of industrial air, flue gas, organic odors, etc (Foo & Hameed, 2009).

1.2.3.3 Industrial Processes

AC is utilized for industrial processes such as liquid natural gas processing, gas processing, liquid chemicals processing, water processing, etc (Ghnimi et al., 2017).

1.2.3.4 Food and Beverage

In food and beverage industry, AC is employed in brewing and bottling, edible oil, sweeteners, decaffeination, chemical purification, glycerin, etc (Ghnimi et al., 2017).

1.3 Statement of the Problem

Once used AC cannot be recovered for reuse, especially while being used as adsorbent. For continuous use of the adsorbents, trials were conducted to find the low-cost adsorbents of good value. Date pits are the major biomass in UAE and other Middle Eastern countries where date palm is the local flora. *Phoenix dactylifera* is the scientific name of date palm which plays a major role in the economy of the UAE. AC is mostly used in industries for the removal of toxic contents. AC has a lot of

biomedical applications such as oral medicine, wound healing and hemoperfusion devices beyond its traditional usage. It can also be used in agriculture to control insecticide residues, removal of microorganisms from wastewater and also disinfection of microorganisms in soil and water.

The primary focus of this work is to prepare AC from date pits which is abundantly available in UAE. Date-pits is the natural by-product obtained from dates. The prepared AC can be used in extracorporeal liver devices in future and also as bioinoculants for plant growth promotors.

1.4 Hypothesis and Objectives

Herein, I hypothesize that AC generated from cheaper biomass by-product, date pits, could be utilized for a plethora of applications in biomedical research, filtration, and amelioration of environmental problems. The overall objective of this current research is to explore biomedical and environmental applications of AC generated from date pits. The specific objectives of this research are:

1.4.1 To Evaluate the Adsorbent Capability of Biowaste-Derived AC for Bioartificial Liver Devices for Bilirubin Detoxification

In this objective, AC produced by physical activation from available phytomaterials in UAE like date seeds, jojoba seeds and microalgae will be utilized. The chemical structure and morphology of the final product will be characterized and analyzed for its suitability for highly selective bilirubin adsorption. In addition, cytotoxicity of generated AC will be evaluated using different liver cell lines. This work would demonstrate the potential of date pits-derived AC as a novel alternative for removal of protein bound toxins in bio-artificial liver devices.

1.4.2 To Evaluate the Growth Promotion of *Salicornia bigelovii* Using AC-Coated Halophilic Marine Actinobacteria Used Seawater Irrigation

Herein, rhizosphere-competent isolates from rhizospheric soils of *S. bigelovii* would be isolated and evaluated for the Plant Growth Promoting (PGP) capabilities as AC-coated biological inoculants on seawater-irrigated *S. bigelovii* plants. The findings of this work would provide insights about applicability of AC-coated bioinoculants in promoting *Salicornia* plant growth and enhance seed yield.

Chapter 2: Date Pits-Based AC as A Novel Alternative Biomaterial for Bilirubin Detoxification in Bioartificial Liver Devices

2.1 Introduction

Acute Liver Failure (ALF) is a life-threatening and devastating illness that occurs most often in patients who do not have a pre-existing liver disease. The disease leads to a cascade of other diseases /complications that may lead to mortality (Bernal & Wendon, 2013). ALF is associated with hepatic dysfunction, abnormal liver biochemical values, coagulopathy and encephalopathy that is often followed by multi-organ failure and death. Rates of survival have been improved in recent years by blood purification systems such as Molecular Adsorbent Recirculating System (MARS) which removes both albumin-bound (middle chain fatty acids, tryptophan and its metabolites, toxic bile acids, and bilirubin) and water-soluble (ammonia, phenylalanine, tyrosine) toxins or is used in emergency liver transplantation (Kjaergard et al., 2003). However, liver transplantation in most cases is not readily accessible due to the lack of matching donors and the complications that usually follows the transplantation.

Several biological and non-biological methods have been used to develop an artificial liver device (Jalan et al., 2004). AC is one of the adsorbents used in artificial and Bio-Artificial Liver (BAL) devices. Thanks to its ready abundance and reasonable cost, high porosity, advantageous blood compatibility, high chemical and thermal stability, large surface area and adsorption capacity towards different compounds, most hemoperfusion systems employ AC as an adsorbent to remove bilirubin (Stange et al., 1999; Rozga et al., 2006). With nanopores smaller than 1 nm, the adsorption capacities of AC materials are relatively low towards bilirubin (Müller, 2010).

Recently, several carbon-based materials have been reported as new potential bilirubin adsorbents sought to improve the adsorption efficiency of liver support devices (Ding et al., 2014; Chen et al., 2017). Maintenance of cell viability and functionality throughout treatment and implementing cell-housing devices at the patient's bedside continue to be a major unresolved challenge (Teotia et al., 2015). Among cell-housing devices, extracorporeal liver assist devices are those that describe all measures of extracorporeal blood treatments that help different functions of the liver an attempt to minimize the number of failing organs as a consequence of liver failure, thus, prolonging patients' survival time. Extracorporeal liver assist devices do not eliminate the cause of the disease but instead allows time for liver regeneration and/or providing a bridge to patients waiting for a liver transplant, thus, represent an attractive alternative that may improve the patients' prognoses (Aron et al., 2016).

This goal can be reached via inducing hepatocytes to perform liver functions and process externally circulated plasma/blood of liver failure patients. Hepatocytes are often cultured in a cell housing bioreactor that makes up an essential biological component of BAL devices. Significant developments have been made to enhance *in vitro* culturing hepatocytes. Yet, matrix synthesis and reactor assembly in BAL devices are still lagging. Limited conventional transport, nutritional gradients across the reactor, non-uniform seeding, inefficient immobilization, and poor growth of the hepatocytes are only a few limitations that BAL devices technology is currently facing. Thus, new cell culture device designs are required to bring improvement in cellular component efficiency (Jain et al., 2015).

Primary hepatocytes or hepatic cell lines are used in these devices. The hepatic cell lines derived from porcine hepatocytes or from tumor cell lines may sometimes create infection and malignancy transmission (Arumugaswami & Svendsen, 2016).

Human hepatocytes may then be the best source of the cell for future studies of extracorporeal liver assist device (Damania et al., 2018). Cytotoxicity assay of cells grown in culture is a widely-used method to predict the potential toxic effects of various compounds on the cells (Hamid et al., 2004). There are several commonly used cytotoxicity assays that are currently being used like ATP measurement, MTT, neutral red, membrane integrity/LDH release, macromolecular synthesis and glutathione depletion (Slater et al., 1963; Zakrzewska et al., 2015).

Using raw materials such as date pits, jojoba seeds and microalgae are considered inexpensive biomass sources. They contain large carbohydrates contents, accounting for over 50% of the composition, and have low ash content (Tawalbeh et al., 2005; Mahmoudi et al., 2014; Chen et al., 2015). The preparation of AC from date pit, jojoba, and microalgae raw materials has, however, been scarcely reported. AC prepared from date pits by chemical activation was utilized for methyl orange adsorption (Mahmoudi et al., 2014). AC was prepared from jojoba seed residue by chemical activation and the effects of process variables like activated carbon, particle size, chemical reagent was studied (Tawalbeh et al., 2005). AC was prepared from microalgae by the combination of hydrothermal carbonization and KOH activation processes (Chen et al., 2015).

3D-culture systems are now widely used instead of the 2D- (or static) culture as the former represents the microenvironment where cells actually reside in tissues. Studies have shown that the behavior of 3D-cultured cells recapitulates the *in vivo* cellular responses much better (Guo et al., 2011; Edmondson et al., 2014; Almutary & Sanderson, 2016; Luckert et al., 2017). 3D-culture systems are employed in drug discovery, cancer cell biology, stem cell research, tissue engineering and in other cell-

based analyses (Artym & Matsumoto, 2010; Thurnherr et al., 2011; Damania et al., 2017).

The 3D-culture of various cell lines have been used for drug screening, cytotoxicity assays and cell-biomaterial interaction where the used biomaterials were collagen, collagen-chitosan, Matrigel, fibrinogen matrices, alginate, Pura matrix scaffolds, and polyethylene glycol matrices (Edmondson et al., 2014; Luckert et al., 2017). To examine the perspective of the AC of date pits, jojoba seeds and microalgae as cell carriers in BAL bioreactor HepG2 human cancer cells were assessed in addition to THLE2 normal liver cells. The rationale was that primary hepatocytes are normally functionally viable for a short period (Guo et al., 2011). Moreover, culturing primary hepatocytes in a bioreactor at high cell density (as required for BAL bioreactor) may lead to oxygen deprivation that could reduce cell viability by shear stress due to continuous flow (Ortega et al., 2014). Cell lines in 2D-culture cannot be studied more than 72 hours since the cells need media to be changed or in a stationary state. To overcome this limitation, 3D-cultured cells in bioreactors are often grown on scaffolds, matrices or microcarriers which are dependent on the growth characteristics of those cells (adherent or suspension) (Hilal-Alnaqbi et al., 2011; Hilal-Alnaqbi et al., 2013; Ortega et al., 2014; Nicolas et al., 2017).

In the present study, the AC prepared from date pits has been evaluated for the adsorption of bilirubin from both albumin-containing and albumin-free solutions. Additionally, ACs from two phytomaterials, jojoba and microalgae has also been tested for comparative studies. To my knowledge, this study is the first to assess the effects of AC prepared from date pits, jojoba, and microalgae on the bilirubin-adsorption. The capacity and effectiveness of AC is often dependent on the precursor used and, on the activation, technique adopted. Therefore, in this work, ACs were

prepared using raw materials of date pits, jojoba, and microalgae, as carbon precursors and the selective adsorption of the AC towards bilirubin was evaluated. Finally, the cytotoxicity of the ACs synthesized here was assessed both in THLE2 and HepG2 cells cultured in 2D and in 3D settings.

2.2 Materials and Methods

2.2.1 Preparation of Activated Carbon (AC)

Raw materials of date pit, locally collected, jojoba seeds (*Simmondsia chinensis,* obtained from Egyptian Natural Oil Co., Cairo, Egypt) and dried microalgae cells (*Scenedesmus* sp., obtained from Algal Oil Limited, Philippines) were collected washed with deionized water, dried and grinded using an electric agitated mortar (JK-G-250B2, Shanghai Jingke Scientific Instrument).

Physical activation of the raw materials was carried out in a tube furnace (GSL-1500X, U.S.A.) with carbonization followed by activation. Samples were placed in crucibles and kept inside the furnace. N_2 gas was passed for 10 minutes, then the temperature was gradually increased, under a constant flow of N_2, at a rate of 5°C min^{-1} up to 600°C and maintained at this temperature for 4 hours. The carbonaceous material was then activated at 900°C in the same furnace under the flow of CO_2 gas instead of N_2 gas (Hilal-Alnaqbi et al., 2011).

The as-prepared AC was then sieved using U.S.A. standard testing sieve (according to ASTME–II specification for the mesh size of 200-300 µm) where it was used in the adsorbent experiments. For the preparation of AC nanomaterials (Nano-AC), the AC was wet grinded in Retsch RM 100 grinder and then dried in the freeze dryer (Telstar, Terrassa, Spain) at -55°C and 0.02 mbar for 6 hours. The material is

then filtered using a 0.45 µm Ptfe filter (Thomas Scientific, USA) prior using in the cytotoxicity experiments.

2.2.2 Characterization Techniques

The surface morphology and the Energy Dispersive Spectroscopy (EDS) of the AC samples were conducted using Scanning Electron Microscopy (SEM) at 3 kV accelerating voltage (JSM-5600, Jeol Ltd, Japan). AC samples were dried overnight in a hot air oven at 105°C. The samples were mounted on an adhesive carbon tape attached to an aluminum-stub and subsequently sputter coated with a gold layer (Mahmoudi et al., 2014).

Chemical structure was carried out by Fourier Transform Infrared (FTIR) spectroscopy (Nexus 470 FTIR Spectrophotometer). For this analysis, the AC samples were oven dried at 110°C overnight, stored in capped flasks and kept in a desiccator prior to analysis. Testing samples were prepared by mixing the particles with KBr powder and then compressed into pellets. The pellets were then placed in a sample holder and the spectrum was recorded for wavenumber range from 4000 to 400 cm^{-1}. The size distribution measurements of Nano-AC were conducted by Dynamic Light Scattering (DLS) technique using Zeta Sizer Nano ZS (Malvern, Model ZEN360, England) at 25°C. The zeta potential was measured in a clear disposable zeta cell (DTS 1060C) with the same machine. Herein, the Nano-AC powder was suspended in deionized water (H_2O) using sonication technique (Zakrzewska et al., 2015).

The carbon samples were examined by Differential Scanning Calorimetry (DSC) using (TA-PL analyzer, Q-200, England). A sample was heated from 25°C to 600°C, at a heating rate of 10°C min^{-1}, with a nitrogen flow rate of 50 mL min^{-1}. Thermogravimetric Analysis (TGA) was carried out using a (TGA-PL analyzer, Q-50,

England**)** (Matos et al., 2011; Mourad et al., 2013; Babaghayou et al., 2016). Samples of activated carbon was heated from 25°C to 800°C at a heating rate of 10°C min^{-1} with nitrogen flow rate of 40 mL min^{-1}.

2.2.3 Adsorption Experiments

Albumin (MW = 66000 g mol^{-1}), bilirubin (MW = 584.7 g mol^{-1}) and all other chemicals were purchased from Sigma-Aldrich. All experiments were conducted in a dark room and using brown flasks, to avoid photo degradation of toxins. The stability of the prepared solutions was tested by running control experiments without adsorbents for one week. Bilirubin stock solution of 80 µM was prepared by dissolving 30.4 g of solid bilirubin in 650 mL of 0.1 M NaOH solution. To that, 26 mL of 2% (w/v) albumin solution was added. The volume was completed to 1 L by adding Phosphate Buffered Saline solution (PBS), bringing the final pH to 7.4. From the stock solution two dilutions of 60 µM and 30 µM were prepared (Matos et al., 2011; Ding et al., 2014).

Batch adsorption experiments were performed using AC prepared from date pit, jojoba and microalgae, by mixing 40 mL of bilirubin–albumin solutions with specific amounts of AC, namely, 0.0 g (control), 0.1 g, 0.5 g and 0.8 g for each of the three types of AC. The bottles were then kept in a water bath shaker (Scichemtech, Japan) at a temperature of 37°C to mimic the human body temperature (Müller, 2010). The shaking speed was kept constant at 100 rpm for all the runs, which was high enough to uniformly disperse the AC sample in the solution. Readings were recorded in UV-visible spectrophotometer (Shimadzu UV 1800, Japan), at a wavelength of 416 nm and 279 nm to evaluate bilirubin and albumin concentrations, respectively. At these wave-lengths the bilirubin extinction coefficient is independent of

albumin/bilirubin molar ratio (Annesini et al., 2010; Chen et al., 2017). The calibration was obtained by measuring the optical density of known concentrations of bilirubin and albumin at their respective wavelengths.

2.2.4 Cell Culture and Propagation

Two human cell lines were purchased from the American Type Culture Collection (ATCC; Rockville, MD, USA); normal liver cell line THLE-2 and tumor cell line HepG2. THLE2 cells were maintained in the Bronchial Epithelial Cell Growth Medium (BEGM, Lonza) supplemented with heat-inactivated Fetal Bovine Serum (FBS) at a final concentration of 10% and 1% penicillin and streptomycin (Penstrep, Gibco) and 0.1% gentamycin solution under humidified air with 5% CO_2 at 37°C. HepG2 cells were cultured in Dulbecco's modified eagle medium (DMEM, Hyclone) supplemented with heat-inactivated FBS to a final concentration of 10% and 1% penicillin and streptomycin solution under humidified air with 5% CO_2 at 37°C. Cells were cultured in flasks pre-coated with collagen I (2.9 mg/mL), fibronectin (1 mg/mL) and bovine serum albumin (1 mg/mL) in BEGM according to ATCC guidelines. THLE2 and HepG2 cells frozen in liquid nitrogen were thawed in a 37°C water bath for 2 minutes. Frozen medium was removed by suspending the contents of one vial in 20 ml of propagation medium in a 50 ml falcon tube. The thawed cells were centrifuged at 1000 rpm for 5 minutes at 4°C.

The cell pellets were re-suspended in propagation medium (20% DMEM for HepG2 and 20% BEBM for THLE2) and seeded in pre-coated T-25 flask. Flasks were incubated at 37°C and 5% CO_2 for 2-3 days. The cells were cultured until they attained 40-60% confluence. The cells were then dissociated using trypsin-EDTA solution, re-suspended in their respective medium and counted using a hemocytometer. Cell

viability was assessed using the trypan blue exclusion assay method (Edmondson et al., 2014; Almutary & Sanderson, 2016). 50 µL of the trypan blue was mixed with 50 µL of the cell suspension. Five to ten microliters of this suspension was then pipetted into the cell counting chamber of the hemocytometer.

Trypan blue penetrates only the dead cells and appear dark blue in color. Viable and dead cells were detected under light microscope**.** Cell viability was determined to be over 90% prior to the seeding of cells. Three D culturing methods were implemented along with 2D culture method, the former is presently used for studies in BAL devices (van Wenum et al., 2016). Cells at density of $3x10^5$ cells/cm^2 and in a volume of 250 µl cell medium per cm^2 culture plates were used. Matrigel matrix (Corning EHS, Ref No. 354248), which is a thick gel, was used for culturing the cells. Preparation of Matrigel carried out as per the manufacturer protocol with a final concentration of 5 mg/ml and 150 µl Matrigel per cm^2 culture vessel surface (Edmondson et al., 2014; Luckert et al., 2017). The medium was changed every two days.

2.2.5 Cytotoxicity Assays

The MTT (3-(4,5-dimethylthiazol-2-yl)-2,5-diphenyltetrazolium bromide) (Sigma-Aldrich, USA) assay is used for the quantification of mitochondrial activity by measuring the formation of a dark blue formazan product formed by the reduction of the tetrazolium ring of MTT (Slater et al., 1963; Hamid et al., 2004). The accumulated formazan was dissolved in a detergent and analyzed spectrophotometrically at 570 nm. The amount of formazan is proportional to the number of the viable cells. THLE2 and HepG2 cells were seeded as 5×10^3 cells/mL by adding 100 µL of the cell suspension

to each well of a 96-well tissue culture plate (Slater et al., 1963; Almutary & Sanderson, 2016).

The plate was incubated for a sufficient time to assure attachment and 40% to 60% confluency. A total of 250 µg/ml of Nano-AC is considered as the stock solution from which concentrations of activated carbon ranging from 12.5 µg/ml to 62.5 µg/ml will be added to each well. The last row was left untreated with Nano-AC (control). Another row was treated as blank (i.e., media alone). The Nano-AC produced from date pits, microalgae and jojoba were investigated. The plates were incubated at 37°C, 5% CO_2, for periods of one hour, two hours and three hours.

After incubation with the Nano-AC, the media was aspirated off and replaced with fresh media. Then, MTT solution (10 µL) for a total volume of 100 µL was added in every well and incubated for 3 hours at 37°C with 5% CO_2. Subsequently, MTT-containing medium was removed gently and replaced with DMSO (100 µL per well) to mix the formazan crystals until dissolved. After 20 minutes, absorbance was measured at 570 nm for each well using a microtiter plate reader (BioTek, XL800, USA). The cells viability was calculated as percentage of untreated control values (i.e. optical density of the treated cells/ optical density of the control) (Almutary & Sanderson, 2016).

2.2.6 Characterization of Cells Morphology

Hematoxylin and Eosin **(**H&E) is the standard histologic staining used to evaluate cell structure. Cultured cells were treated with 62.5 µg/ml of Nano-AC, for 24 hours, fixed with ice cold methanol: ethanol (1:1 ratio) for 15 minutes and air dried. The coverslips were washed quickly 6 times in distilled water. The cells were stained with hematoxylin solution for 2 minutes and then rinsed in H_2O. Then the cells were

counter stained with eosin for 10 seconds. The coverslips were rinsed in ethanol series (70%, 96%, and 100%) and air dried, coverslips were mounted with DPX and visualized under bright field microscope (OLYMPUS, IX83 research inverted microscope 2DECK, Japan) equipped with a camera (Olympus, DP 73) (Atale et al., 2014).

For fluorescent microscopy investigation, THLE2 and HepG2 cells were harvested by Trypsinization and 3×10^5 cells/ml were plated on sterile coverslips placed in 10 mm petri-plates. The cells (on coverslips) were contained initially in their respective media (1 ml/coverslip) for 24 hours at 37°C in 5% CO_2 incubator. Cell cultures were then treated with 62.5 µg/ml of Nano-AC and incubated for 24 hours.

The cells were washed twice with Dulbecco's Phosphate-Buffered Saline (DPBS), then, fixed in 4% paraformaldehyde (Sigma-Aldrich) for 10 minutes at room temperature (Atale et al., 2014; Ortega et al., 2014). The cells were washed and permeabilized with 0.1% Triton X100 for 5 minutes, Phalloidin-FITC (Sigma-Aldrich) added and kept for incubation for 40 minutes (Frickmann et al., 2013; Yan et al., 2016; Peñaloza et al., 2017). Cells were washed with DPBS and 0.1% Triton X100 for 4 minutes. The samples were mounted with DAPI-Fluroshield (Sigma-Aldrich) for 10 minutes then washed to remove the excess DAPI (Peñaloza et al., 2017).

Finally, the coverslips were fixed on frosted slides with DPX mountant (Sigma-Aldrich). Similarly, the 3D-cultured cells were allowed to grow in matrigel and collagen for 10 days (Yan et al., 2016; Luckert et al., 2017). The Matrigel acts as a framework for the cells to grow and mimic the conditions inside the human body. The rate of growth in the 3D culture is much slower compared to the normal culture especially in the case of the normal cells. The cells attached themselves to the matrigel and were stained with Phalloidin-FITC and DAPI-Fluroshield' fluorescent dyes, using

the same procedure for the 2D cultured cells.

2.3 Results and Discussion

2.3.1 Phytomaterials and AC Characterization

Figure 2.1 illustrates the SEM images of the raw date pits powder and the AC produced from date pits, jojoba seeds and microalgae. There were significant differences between the surface morphology of each of them. SEM images of date pits powder before activation showed absence of pores Figure 2.1a. Pores with a diameter of around 5 μm are formed after activation for 1 hour Figure 2.1b and c. Date pits-AC exhibited an even, homogeneous, highly porous, and well- pronounced array of honey-combed structures, indicating the possibility for the toxins to be trapped and adsorbed.

The zoomed-in image of Figure 2.1c showed arrays of thread-like structures that form the walls of the pores and thus highly increase the surface area. Figure 2.1d-f shows jojoba-AC images that demonstrated almost uniform pore structure with channels and large holes in the shape of both macropores and mesopores. Each channel contains a large number of mesopores as indicated in the zoomed-in image of Figure 2.1f. Figures 2.1g-i show microalgae-AC images that demonstrate fiber-like structures. The fibers were connected, with cavities between each other. Pores created on the external surface of the carbon during the activation process are mainly due to the release of volatile matter. It could be attributed to the presence of metallic atoms then intercalates the carbon matrix resulting in the widening of spaces between carbon atomic layers.

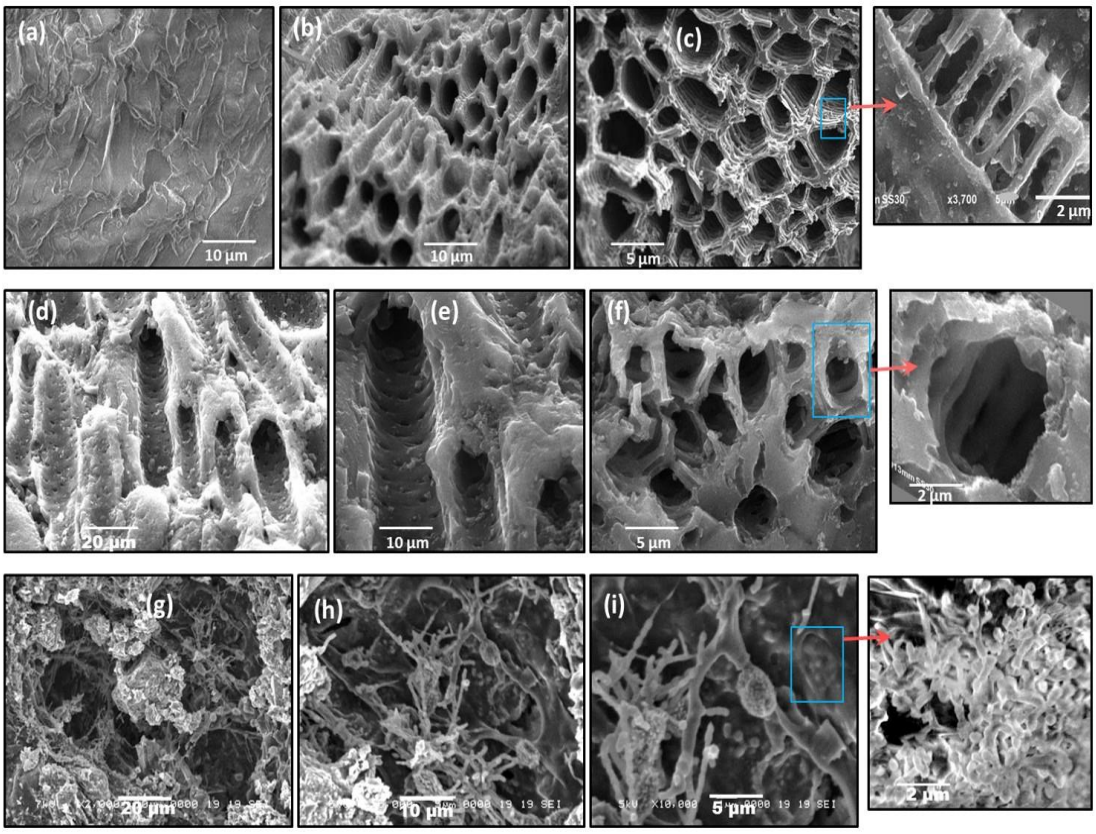

Figure 2.1: SEM images of raw date pits, date pits-activated carbon, jojoba seeds-activated carbon, and microalgae-activated carbon. (a) raw date pits, (b and c) date pits-activated carbon, (d-f) jojoba seeds-activated carbon, (g-i) microalgae-activated carbon

The results of the elemental analysis of AC obtained from the three different precursors, namely, date pits, jojoba seeds and microalgae, at 900°C activation temperature are shown in Table 2.1. Table 2.1 shows mass percentage of carbon, hydrogen, nitrogen, and oxygen. Insignificant amounts of other elements were found but not shown in the table, such as sodium, potassium, calcium, magnesium, phosphorous and iron. The carbon and nitrogen content of jojoba seeds-AC were the maximum. However, the oxygen content was the least. Furthermore, the carbon and nitrogen content of microalgae-AC was the least. Date pits-AC showed carbon, hydrogen, nitrogen, and oxygen content values of 49.82, 4.12, 4.02 and 28.18%, respectively. This is due to the release of volatiles during carbonization that results in

the elimination of non-carbon species and enrichment of carbon (Arena & Nadra, 2001; Mahmoudi et al., 2014).

Table 2.1: Elemental analyses of activated carbons produced from different phytomaterials

Adsorbents	Mass %			
	Carbon	Hydrogen	Nitrogen	Oxygen
Date pit-AC	59.82	4.12	4.02	28.18
Jojoba-AC	65.65	7.72	10.39	13.10
Microalgae-AC	53.58	4.91	3.30	25.71

Figure 2.2 shows FTIR spectra of the three samples of AC that synthesized from date pits, jojoba seeds and microalgae in the wavenumber range 4000-400 cm^{-1}. The three samples of AC showed almost similar functional groups with intensity variation. As a result of physical activation method, carbonization and activation of the raw materials causes the decomposition of O_2 and H groups (Rodríguez-Reinoso & Molina-Sabio., 1992; Arena & Nadra, 2001; Zhou et al., 2017). Oxygen bonded to peripheral carbon atom, from which different functional groups arise (Mahmoudi et al., 2014). The bands around 3400 cm^{-1} are attributed to the asymmetric and symmetric stretching vibrations of O-H bond and indicate the presence carboxylic acid on the surface of the AC. Other peaks observed at 2300-2350 cm^{-1} are assigned to aliphatic bands. The peaks at 1400-1700 cm^{-1} are attributed to conjugated stretching of C-O, C=C, C=O of carbonyl groups. Date pits-AC showed a broad band around 1030 cm^{-1} that is attributed to C-O stretching. This indicates the presence of acids, alcohols and phenols. The band is at 650 cm^{-1} is due to plane ring deformation.

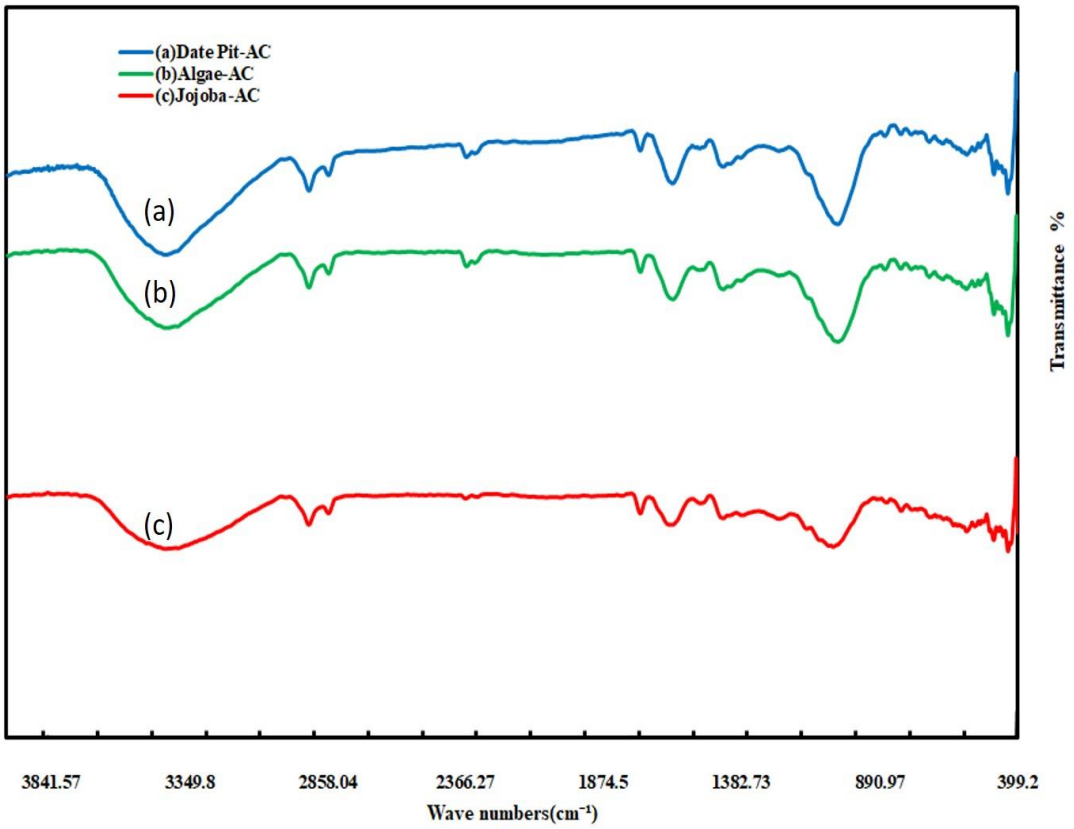

Figure 2.2: FTIR spectra. (a) date pits-activated carbon, (b) jojoba seeds activated carbon, (c) microalgae-activated carbon

Figure 2.3a shows the size distribution of Nano-AC produced from date pits, deionized water (H_2O) dispersion. It has a large size distribution in the range from 65 to 350 nm, and most of the particle's size was less than 200 nm with an average size of 135 nm. Figure 2.3b shows the size distribution of Nano-AC produced from jojoba seeds, H_2O dispersion. It has a narrow size distribution with an average size of 284 nm. Figure 2.3c shows the size distribution of Nano-AC produced from microalgae, H_2O dispersion. It has a large size distribution in the range from 170 to 700 nm, with average size of 344 nm (Mahmoudi et al., 2014; Peñaloza et al., 2017).

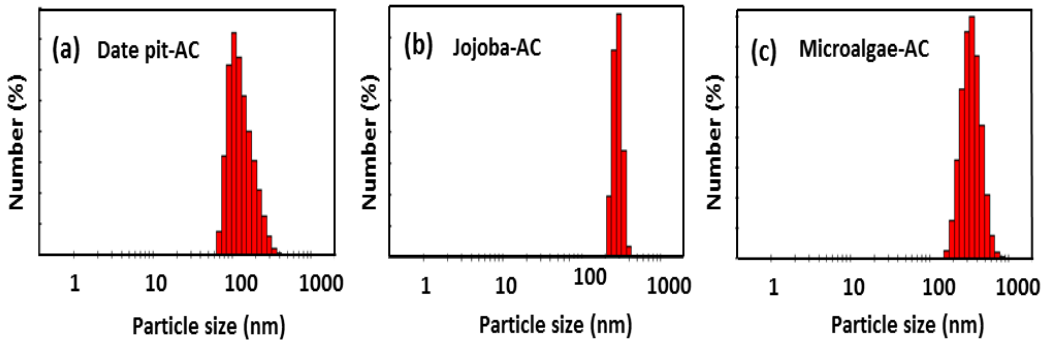

Figure 2.3: Size distribution histograms of the nanomaterial. (a) date pit-activated carbon, (b) jojoba-activated carbon, (c) microalgae-activated carbon, dispersed in H_2O

Figure 2.4a-c shows zeta potential value of -10.1 mV for date pits Nano-AC, -26.3 mV for jojoba seeds Nano-AC and -42.7 mV for microalgae Nano-AC in H_2O suspension. Date pits Nano-AC has small negative charge on the surface which indicate less stability and affinity to agglomerate with the time into clusters, whereas, the produced microalgae Nano-AC has high stability and homogeneity due to the repulsive force among particles. This indicated by the huge negative surface charge of the particles. By increasing the stability of Nano-AC in suspension, adsorption and removals of various toxin molecules will be enhanced (Mandal et al., 2013; Zakrzewska et al., 2015; Chen et al., 2017).

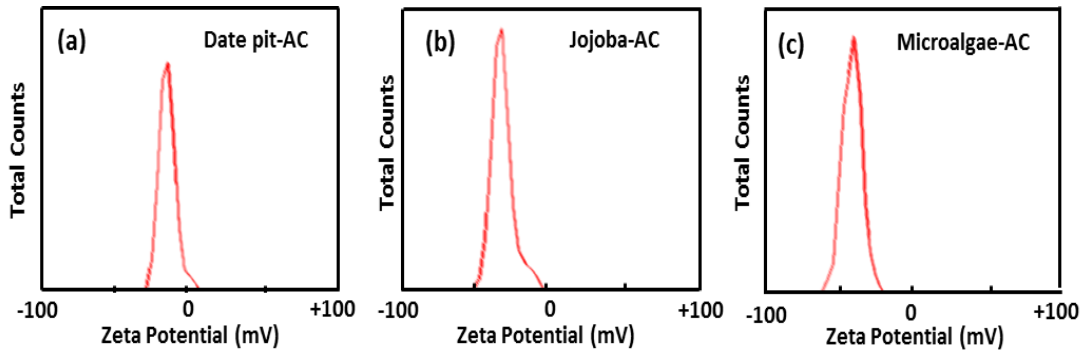

Figure 2.4: Zeta potential of the nanomaterial. (a) date pits-activated carbon, (b) jojoba seeds-activated carbon, (c) microalgae-activated carbon, dispersed in H_2O

In order to determine general decomposition characteristics of the raw phytomaterials during the activation, the sample was subjected to Thermo Gravimetric Analysis (TGA). Figure 2.5a shows the TGA curves of date pits, jojoba seeds and microalgae, in N_2 atmosphere and at 10°C min^{-1} heating rate. The thermal decomposition of the three samples takes place in three stages. At the first stage of the date pit, a sharp weight loss of the raw material was about 12% at 35-100°C. The first stage presents a significant weight loss, due to much volatile released mainly due to the evaporation of water.

The second stage was obtained at 100-450°C was about 10%, in which carbonization process begins and mainly hemicellulose and cellulose fractions decompose. At higher temperatures (450-800°C), the weight loss was due to lignin decomposition. The TGA curve of jojoba seeds showed about 8% weight loss up to 250°C due to dehydration of the sample. During the next stage, a progressive and significant weight loss was observed up to 450°C thanks to the decomposition of cellulose and hemi-cellulose of the sample to condensable gas (acetic acid, methanol, and tar) and incondensable gas (CO, CO_2, CH_4, H_2, H_2O).

At the third stage, lignin begins to decompose and contribute to the weight loss. Also, the residual volatiles from the first stage are further released but carbon was left. The TGA curve of microalgae showed a little decrease at the first stage as the examined microalgae cells were already dried (Mourad et al., 2013; Babaghayou et al., 2016). Thereafter, a progressive and significant weight loss was observed from 140 to 600°C where most of the organic materials are decomposed. Since microalgae is not lignocellulosic in composition but instead comprised of lipids, proteins, nucleic acids and carbohydrates (Mahmoudi et al., 2014).

The third stage above 600°C (at third stage); where the carbonaceous matters in the solid residuals started to decompose. From TGA results it can be stated that the temperatures above 800°C is more appropriate for pyrolysis and activation of the raw materials.

Figure 2.5b shows Differential Scanning Calorimetry (DSC) curves. The DSC curves showed a little drop at a temperature in the first stage, because the sample needs heat to evaporate the remaining water (Mourad et al., 2013). DSC of date pits and jojoba seeds arrived at valley at about 200°C and 212°C, respectively where hemi-cellulose and cellulose decomposed and produced plentiful organic compounds, such as tar, ketone and methanol which would vaporize by adsorbing large amount of heat. Microalgae, however, arrived at valley at about 180°C as lipids, proteins, nucleic acids and non-cellulosic carbohydrates decompose at lower temperature (Mahmoudi et al., 2014).

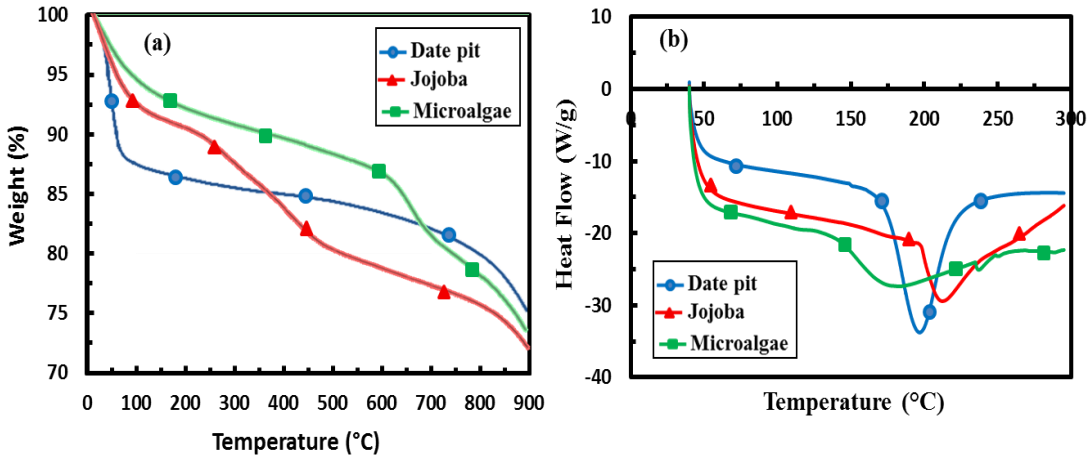

Figure 2.5: Analysis of raw materials with TGA and DSC. (a) Thermogravimetric Analysis Curves (TGA), (b) Differential Scanning Calorimetry curve (DSC), for the raw phytomaterials of date pit, jojoba and microalgae

2.3.2 Adsorption Properties

Figures 2.6a, c and e show bilirubin adsorption via date pit-AC, jojoba-AC and microalgae-AC, respectively, using 0.1 g, 0.5 g and 0.8 g of each, at an initial bilirubin concentration of 30 µM, in the bilirubin–albumin solution. The insignificant drop in the bilirubin concentration in the control experiments ($P< 0.05$), without adsorbent, proves that the drop was mainly due to the adsorption. The amount of bilirubin increased with increase in the AC amount and it was observed that the highest adsorption rate of bilirubin occurred within the first 4 hours (Müller, 2010; Ding et al., 2014). The adsorption typically exhibits two stages. In the initial stage, external surface adsorption dominates, where bilirubin diffuses from the solution to the external surface of the adsorbent. This step is mainly controlled by the surface adsorption kinetics rate. Once the external surface is saturated with the bilirubin molecules, the second stage starts where internal diffusion becomes more important and often lead to a steady decrease in the adsorption rate (Annesini et al., 2010; Ding et al., 2014).

Figures 2.6b, d and f show the albumin concentration in the same solutions with date pits-AC, jojoba seeds-AC and microalgae-AC, respectively, using 0.1 g, 0.5 g and 0.8 g of each. It was clearly demonstrated that in presence of AC, the drop in the albumin concentration was insignificant. This suggests that the as-synthesized AC samples were able to strip off the bilirubin molecules from the bilirubin-albumin complex, rather than adsorbing the complex altogether. For successful removal of bilirubin, the AC should be capable of competing with at least the weak binding sites on albumin for the unconjugated bilirubin. Specifically, electrostatic, hydrophobic interaction and hydrogen bond can be formed between oxygen-containing groups (i.e.,

on the AC) and bilirubin molecules. Owing to AC's high surface area resulted from the macropores, the adsorption efficiency was enhanced.

The selective adsorption of bilirubin in mixed solutions of bilirubin and albumin is based on a difference in the physical sizes of those molecules. Thus, the bilirubin molecules with size about 2 nm can get into the AC through the macropores and immobilize on their inner surfaces leaving albumin behind. As albumin molecules are much larger than the pore size (Annesini et al., 2013; Harm et al., 2014). The binding of the bilirubin molecules to the inner surfaces of the AC is stronger than that to their outer surfaces due to the confinement effects, and a high density of bilirubin molecules. This is a vital feature of the as-synthesized AC that proves its significance for removal of bilirubin from the blood without removal of useful molecules and materials.

To compare the performance of the three adsorbents, a slight difference was observed, where date pits-AC showed the highest adsorption of bilirubin with time Figure 2.6a. However, jojoba seeds AC and microalgae-AC showed almost similar trend with time Figure 6c and e. This variation can be attributed to the deference in the surface morphology as indicated from Figure 2.1. Figure 2.7 shows the initial concentration C0 (mg/l) of bilirubin versus the final concentration Ceq (mg/l). Initially, three different concentrations (80, 60, and 30 μM) of bilirubin were tested and the results of all samples demonstrated reduction in bilirubin. However, date pits-AC has more adsorption capacity than jojoba seeds-AC and microalgae-AC. Jojoba seeds-AC showed the least bilirubin removal and microalgae-AC showed a moderate rate of adsorption.

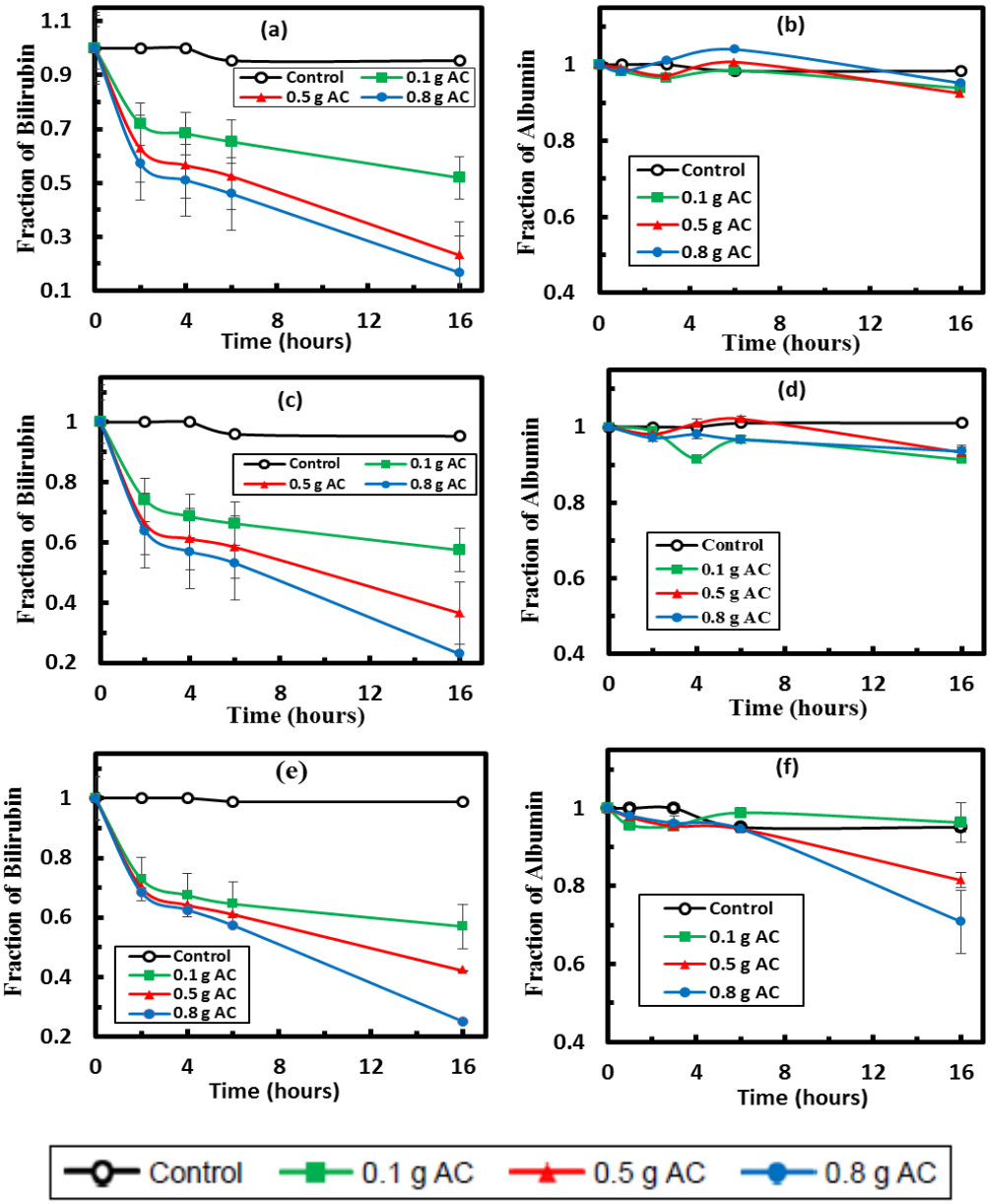

Figure 2.6: Time dependence of remaining bilirubin and albumin in the solution using different concentrations. (a and b) date pits-AC, (c and d) jojoba seeds-AC, (e and f) microalgae-AC. Ct/Co and Ct,A/Co,A are the remaining fraction of bilirubin and albumin concentrations over initial concentrations without the adsorbent, respectively

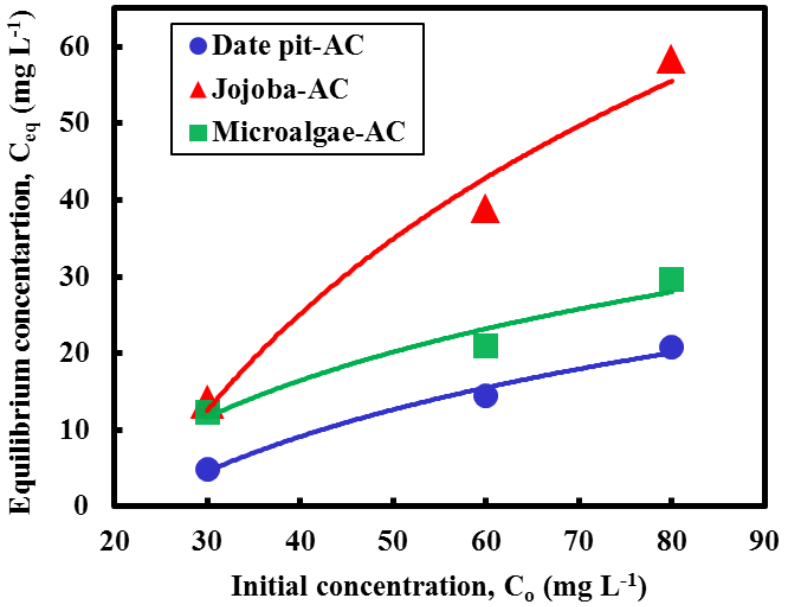

Figure 2.7: Effect of initial bilirubin concentration on the final equilibrium concentration. Initial vs final equilibrium concentration plotted using 0.8 g of date pits-AC, jojoba seeds-AC, microalgae-AC at 37 °C and pH 7.4

Figure 2.8 shows the Langmuir and Freundlich linear isotherm plot for date pits-AC, jojoba seeds-AC and microalgae-AC. Langmuir and Freundlich isotherms are the commonly used isotherms to identify the most suitable adsorption mechanism. The amounts of bilirubin adsorbed on activated carbon at equilibrium q_{eq} (mg/g) were calculated using Equation 1.

$$q_{eq} = (C_o - C_{eq})V_{sample}/m \quad (1)$$

Where, q_{eq} (mg g^{-1}) is the amount of solute adsorbed at equilibrium, C_o in the initial bilirubin concentration (mg L^{-1}), C_{eq} (mg L^{-1}) is the equilibrium concentration of the solute in the bulk solution after 16 hours, V_{sample} (L) is the volume of the sample and m (g) is the mass of the adsorbent used. The Langmuir isotherm, described by Equation 2 assumes that, forces of attraction between the adsorbed molecules are negligible and when a molecule occupies one site, no further adsorption takes place at that site.

$$q_{eq} = q_o b C_{eq} / (1 + b C_{eq}) \quad (2)$$

Where, q_o (mg g^{-1}) is the maximum adsorption capacity and b (L mg^{-1}) is constant related to free energy of adsorption. By plotting the graph $1/q_e$ vs $1/C_{eq}$, Langmuir constants can be determined and the values of q_o and b could be determined from the intercept and slope, respectively. The results shown in Figure 2.8 were used to determine q_{eq} and C_{eq}, which were then used to determine the isotherm parameters q_o and b (Table 2.2).

On the other hand, the Freundlich isotherm, shown in Equation 3 describes the non-ideal and reversible adsorption, applied to multilayer adsorption with non-uniform distribution of adsorption heat and affinity over the heterogeneous surface (Tan et al., 2008).

$$q_{eq} = k_f C_{eq}^{1/n} \quad (3)$$

Where, k_f and n are Freundlich parameters, which can be determined from the slope and intercept of the straight line of log (q_{eq}) versus log C_{eq}, respectively (Tan et al., 2008). The determined parameters of the two isotherms are presented in Table 2.2. The coefficient of determination, R^2, which measures the level of accuracy of the fitting of the Langmuir and Freundlich models, was close to unity. This suggests that both models can well describe the adsorption process, Langmuir model was however, more appropriate. The results show that, the maximum adsorption capacity for the date pits-AC is 2.72 mg g^{-1} which is higher than adsorption capacity of jojoba seeds-AC and microalgae-AC, 0.719 mg g^{-1} and 1.74 mg g^{-1}, respectively.

Table 2.2: Isotherm parameters of the adsorption of bilirubin. Isotherm analysis of date pit-AC, jojoba-AC and microalgae-AC at 37°C and pH 7.4

Isotherm model	Parameter	Date pit-AC	Jojoba-AC	Microalgae-AC
Langmuir	b (L mg^{-1})	0.1249	0.2456	0.0815
	q_o (mg g^{-1})	2.72	0.719	1.741
	R^2	0.9931	0.9917	0.9533
Freundlich	k_f	0.5797	0.5026	0.5573
	1/n	0.5821	0.219	1.9312
	R^2	0.9960	0.9547	0.9465

Abbreviations: b, constant; q_o maximum adsorption capacity; R2, co-efficient of determination; kf &n, Freundlich parameter

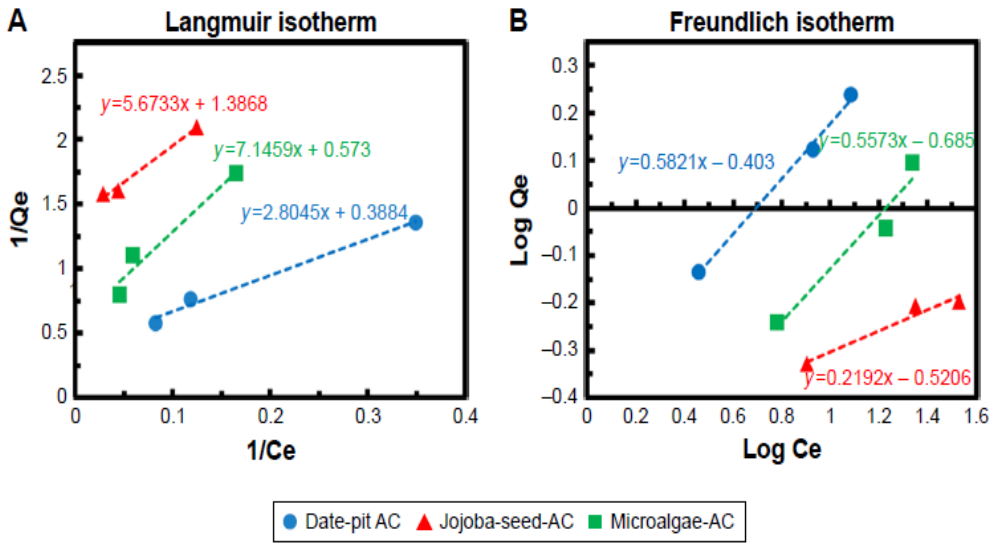

Figure 2.8: Linear isotherm plot of the AC. Plot for date pits- AC, jojoba seeds-AC and microalgae-AC using (a) Langmuir model and (b) Freundlich model

2.3.3 *In vitro* Cytotoxicity of the AC

Normal hepatocytes (THLE2) and human hepatocellular carcinoma cell line (HepG2) were used to evaluate the *in vitro* cytotoxic activity of the as-synthesized AC.

THLE2 and HepG2 cells were incubated with 12.5 µg/ml to 62.5 µg/ml of either date pits- AC, jojoba seeds-AC or microalgae-AC for 3 hours. Cell viability was determined by MTT assay. The reduction of MTT mainly occurs in the mitochondria due to the action of succinate dehydrogenase. Thus, providing a measure of mitochondrial function, only cells that are viable were capable of metabolizing the dye efficiently, and produce the purple formazan, which is proportional to the amount of viable (Mahmoudi et al., 2014; Peñaloza et al., 2017).

Figure 2.9a shows cell viability results of THLE2 cells incubated with date pits, jojoba seeds and microalgae- Nano-AC, using MTT assay. Data analysis was carried out by T-Test two tailed distribution ($P< 0.05$). Readings were collected at three time points post Nano-AC administrations. A minimal decrease in cell viability compared to the untreated control was observed and did appear proportional to incubation time. For example, THLE2 cells that were treated with date pits Nano-AC showed 75% viability in the third hour, whereas jojoba seeds and microalgae Nano-AC showed 45%, 25% viability, respectively, at the same exposure time. The growth inhibition% shows 25% for date-nano and 70% for both algae and jojoba.

Figure 2.9b shows that cell viability of HepG2 cells Nano-AC-treated was decreased, compared to control cells. For example, date pits Nano-AC demonstrated about 60% viability in the third hour, whereas jojoba seeds and microalgae Nano-AC showed about 40% viability. There are slight differences between the two cell lines concerning their sensitivity to Nano-AC samples. The difference between the proliferation rate of the THLE2 and HepG2 cells may be attributed to different uptake mechanisms of Nano-AC by the two cell lines (Peñaloza et al., 2017).

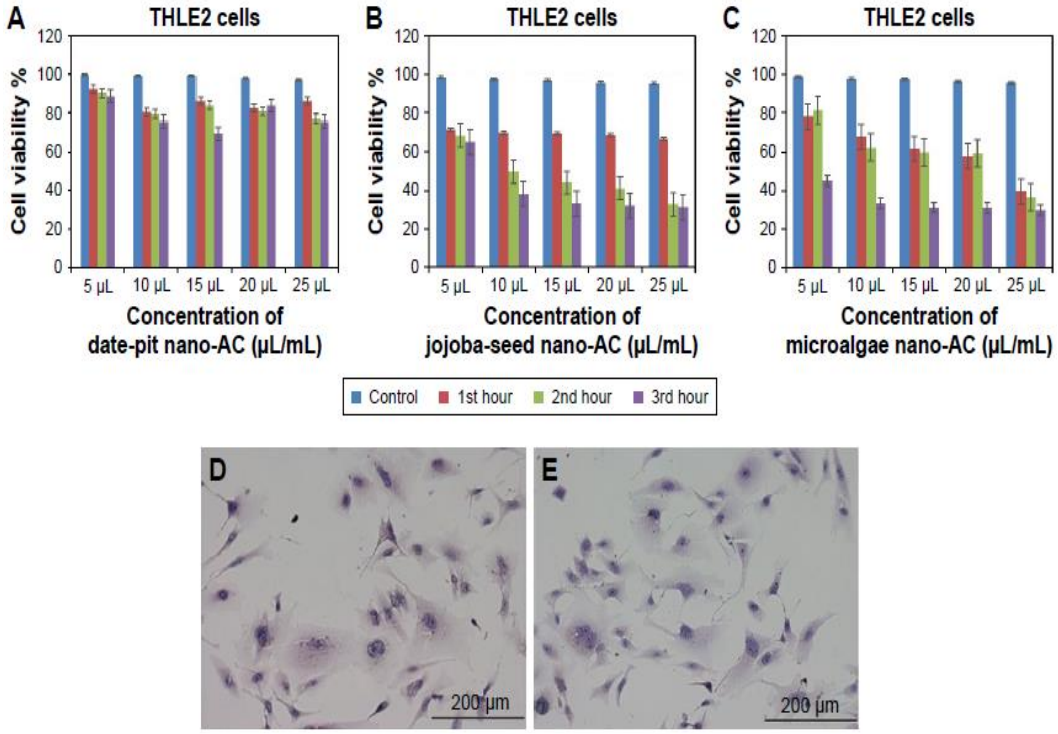

Figure 2.9: MTT assay of THLE2 cells. Viability of (a-c) THLE2 cells by MTT assay; after exposure to Nano-AC for 1 hour, 2 hours and 3 hours. Mean values of three independent experiments are presented (n= 3) P< 0.05. Morphological analyses of viable cells stained with Hematoxylin and Eosin. (d) Control none treated THLE2 cells. (e) THLE2 cells treated with date pits Nano-AC

The results variation in conjunction with the different Nano-AC products applied could be attributed to the difference in the particles size and surface charge (Figure 2.3 and Figure 2.4) (Chen et al., 2017). Furthermore, MTT assay appears to be more sensitive and that can be attributed to either that MTT assay is mainly based on the enzymatic conversion of MTT in the mitochondria and/or the reactive oxygen species generated within the mitochondria may also damage mitochondrial components (Peñaloza et al., 2017).

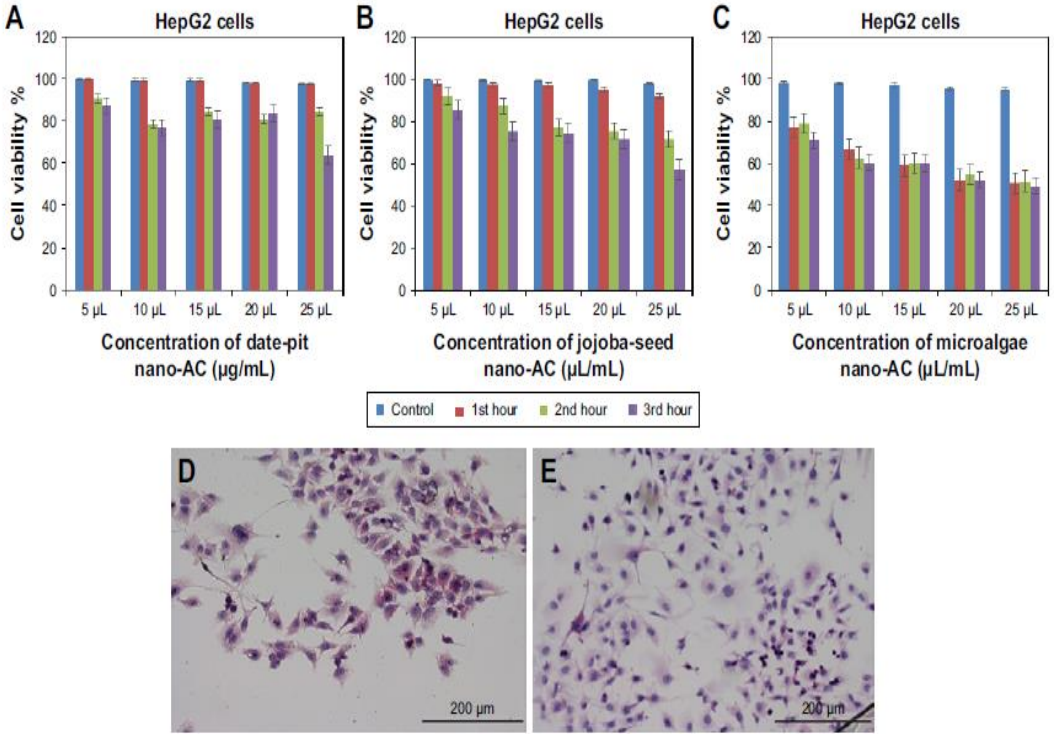

Figure 2.10: MTT assay of HepG2 cells. Viability of (a-c) HepG2 cells by MTT assay; after exposure to Nano-AC for 1 hour, 2 hours and 3 hours. Mean values of three independent experiments are presented (n= 3) P< 0.05. Morphological analyses of viable cells stained with Hematoxylin and Eosin. (d) Control non-treated HepG2. (e) HepG2 cells treated with date pits Nano-AC

2.3.4 Effect of AC on Morphology of THLE2 and HepG2 Cells

Figure 2.9d-e and Figure 2.10d-e show THLE2 and HepG2 cells were stained with Hematoxylin and Eosin where the nuclei appear purple whereas the cytoplasm is pink. Cells are mostly clustered and individual cells are polygonal in shape. The nuclei of HepG2 cells are smaller than that of THLE2 Figure 2.9d, e. After 24 hours of exposure to 62.5 µg/ml of date pit Nano-AC, THLE2 cells did not reveal any apoptotic activity. HepG2 cells showed apoptotic activity which is a characteristic stress signal of cancerous cells (Archana et al., 2013). THLE2 and HepG2 cells were stained with DAPI-Fluroshield and Phalloidin-FITC' fluorescent dyes Figure 2.11a-p. DAPI is a fluorescent tag that binds strongly to A-T rich regions in DNA in the cell nucleus, as

it can pass through an intact nuclear membrane, and exhibits blue fluorescence. Phalloidin-FITC, on the other hands, binds to the cytoskeleton components; namely the actin filaments, that is located directly underneath the plasma membrane and exhibits green fluorescence (Frickmann et al., 2013; Yan et al., 2016; Peñaloza et al., 2017).

Figure 2.11 shows microscopic fluorescent images of 2D and 3D-cultured THLE2 and HepG2 cells treated with date pits, jojoba seeds and microalgae Nano-AC. The integrity and distribution of actin cytoskeletal filaments were marginally affected by the applied Nano-AC treatments (Peñaloza et al., 2017). The morphology changes were also more evident in HepG2 cells compared to normal THLE2 cells.

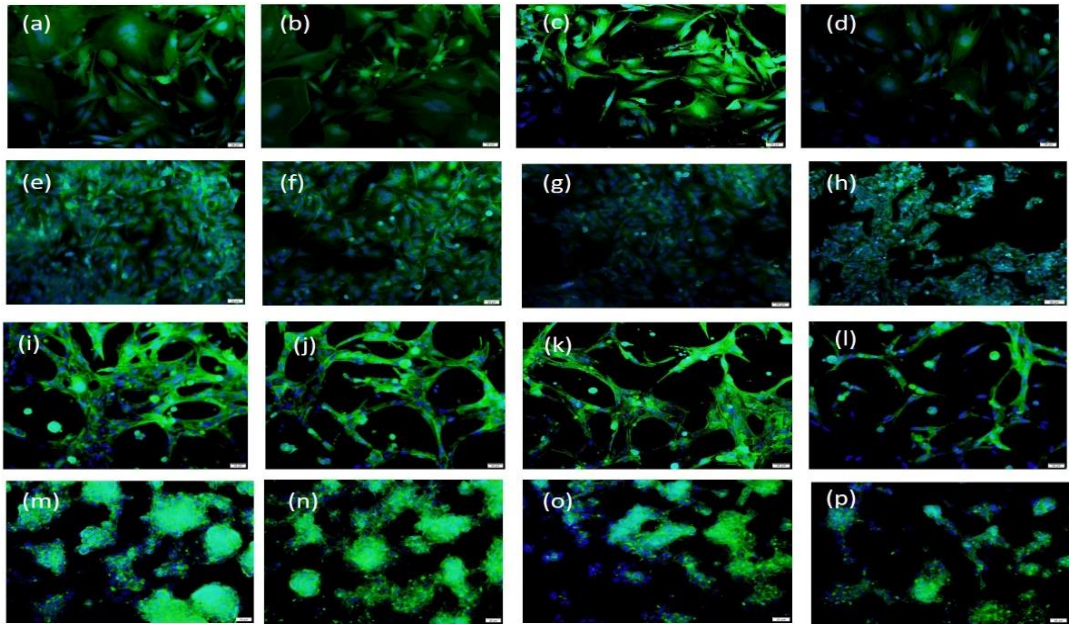

Figure 2.11: Fluorescence microscopic images. (a-d) 2D-cultured THEL2 cells; (e-h) 2D-cultured HepG2 cells; (i-l) 3D-cultured THEL2 cells; (m-p) 3D-cultured HepG2 cells. (a, e, i, and m) controls, (b, f, j, and n) treated with date pit Nano-AC, (c, g, k, and o) treated with jojoba seeds Nano-AC, (d, h, l, p) treated with microalgae Nano-AC, for 24 hours. Actin cytoskeleton (green), cell nucleus (blue), and scale bar = 20 mm

Chapter 3: Evaluation Growth Promotion of *Salicornia bigelovi*i Using Activated Carbon Coated Marine Actinobacteria Used Sea Water Irrigation

3.1 Introduction

Saline water dominates the earth, but the supply of fresh water has always been limited especially in the arid regions of the world. At present, “clean” fresh water scarcity is a major problem in many arid and semi-arid regions in the world, including the United Arab Emirates (UAE) (Odhiambo, 2016). This can be considered a major constraint for sustainable development in agriculture and food production. There is an urgent need to meet the ever-increasing demand for food and agriculture products in such countries with crops that could be irrigated with saline or seawater.

Salicornia bigelovii, known as dwarf glasswort, is a succulent halophytic (salt tolerant) plant proves to be a potential candidate to grow in salt marshes and intertidal areas on coasts of many countries (Loconsole et al., 2019) and can be irrigated with seawater (Glenn et al., 1998; Ventura & Sagi, 2013). There is an increasing concern about the use of *S. bigelovii* in human and animal diet as well as in biofuel production worldwide (Bañuelos et al., 2018; Doncato & Costa, 2018). In the UAE, the cultivation of *S. bigelovii* has become profitable. In addition to human consumption and animal feed, oilseeds of *S. bigelovii* can potentially be a source for sustainable production of biodiesel and aviation biofuel (Al-Yamani et al., 2013; Shahid et al., 2013). Consequently, *S. bigelovii* is a main component of biofuel feedstock cultivated with aquaculture and mangrove silviculture in the Seawater Energy and Agriculture (Ray & Anumakonda, 2011; Ríos, 2014; Sharma et al., 2016).

The impact of microorganisms on plant growth, health, and productivity in extreme environments has been tested under different environmental (Verma et al.,

2017) conditions. Microorganisms are capable of colonizing soils adjacent to the roots of plants (rhizosphere), above-soil portions of plants (phyllo sphere) or living within the tissues of plants (endophytes). Plant Growth-Promoting Rhizobacteria (PGPR) are a group of free-living soil bacteria that exert beneficial effects on plants (Hassan et al., 2019).

These PGPR have the ability to regulate growth, increase nutrients uptake, enhance tolerance to environmental stress, control pathogenic agents and boost yields in plants (Glick et al., 2007; Kumar et al., 2019). Production of metabolites, such as antibiotics, cell wall degrading enzymes, siderophores or hydrogen cyanide, is among the indirect effects of PGPR to increase plant growth (Bashan et al., 2013; Kumar et al., 2019). PGPR can also promote growth directly through Nitrogen (N) fixation, enhancement of plant nutrient uptake, stimulation of transport systems in plants and production of Plant Growth Regulators (PGRs) (Backer et al., 2018). The phytohormones, auxins, cytokinins, gibberellins and Ethylene (ET), are examples of PGRs. Other PGRs can be non-naturally occurring synthetic compounds with phytohormone-like activities such as signaling molecules (e.g., reactive oxygen species and nitric oxide), simple ions (e.g., Ca^{2+}) and Poly Amines (PA) (Bashan et al., 2004, Bashan et al., 2013; Kumar et al., 2019).

The hydrolysis of 1-AminoCyclopropane-1- Carboxylic acid (ACC) by the enzyme ACC Deaminase (ACCD) is a major mechanism utilized by PGPR to lower the levels of ET and to reduce environmental stresses in planta (Glick et al., 2007; El-Tarabily et al., 2019). In general, PGPR strains may contribute to PGP by one or more of direct or indirect mechanisms (Backer et al., 2018).

It is well documented that PGPR colonizing rhizosphere have enhanced the growth and relieved environmental stresses in many agricultural crops (Beneduzi et

al., 2012). However, research of PGPR in marine ecosystems seems to improve health of halophytes (Bashan et al., 2000; Bashan & Holguin, 2002; El-Tarabily et al., 2020). Few studies have demonstrated the effects of PGPR isolated from the rhizosphere or roots of *Salicornia* on its growth and performance (Ozawa et al., 2007; Jha et al., 2012; Mapelli et al., 2013; Hrynkiewicz et al., 2019).

These reports have focused on the direct effect of PGPR on growth promotion of *Salicornia* through enhancing N-fixation. Inoculations of sweater irrigated-*S. bigelovii* with N-fixing and/or phosphorus (P)-solubilizing bacteria have resulted in significant growth promotion (Bashan et al., 2000). When inoculated with *Klebsiella pneumoniae* and *Azospirillum halopraeferens*, *S. bigelovii* showed enhanced agronomic traits (e.g., height and biomass) and biochemical properties (e.g., total contents of proteins and lipids) compared to non-inoculated plants (Rueda-Puente et al., 2004). Interestingly, the halotolerant PGPR isolated from roots of Salicornia can perform different PGP activities such as N-fixation, P-solubilization, and production of Indole-3-Acetic Acid (IAA) and ACCD. In addition, these bacteria improved seed germination *in vitro* only (Jha et al., 2012; Mapelli et al., 2013).

Under greenhouse conditions, the ACCD-producing endophytic actinobacterium *Micromonospora chalcea* enhanced growth and seed yield of *S. bigelovii* (El-Tarabily et al., 2019). Up to date, there is little information about the role of actinobacteria as potential PGP to enhance growth of *Salicornia* under saline conditions in greenhouse/field trials. In general, root colonization and rhizosphere competency are critical prerequisites for selecting successful PGPR candidate (Rilling et al., 2019; El-Tarabily et al., 2020). Mapelli et al. (2013) have reported that the marine bacteria are capable of colonizing *Salicornia* roots *in vitro*. Many reports have focused on isolating bacterial strains from *Salicornia* rhizosphere (Rueda-Puente et al.,

2004; Ozawa et al., 2007; Jha et al., 2012; Figueira et al., 2019). Yet, rhizosphere competence of salt tolerant marine PGPR to competitively colonize *Salicornia* roots with other microbes is still meager. Recently, the PA-producing actinobacteria, *Actinoplanes deccanensis* and *Streptomyces euryhalinus,* isolated from marine environments promote growth and seed yields of *S. bigelovii* stimulating the endogenous levels of PAs and other PGRs (El-Tarabily et al., 2020). There is a great interest in utilizing PGPR as bio-inoculants to enhance the growth of halophytic plants (El-Tarabily et al., 2019; Mesa-Marín et al., 2019).

In the UAE, the cultivation of *S. bigelovii* for livestock feed, aviation biofuel (jet fuel) and renewable energy purposes has become a top priority for the diversification in the UAE's economy. The investigation of the halotolerant marine actinobacteria exhibiting PGP features and associated with *S. bigelovii* rhizosphere naturally adapted to cope with extreme saline conditions could most likely promote growth of *S. bigelovii*.

Therefore, the objectives of this work were to: (i) isolate halotolerant actinobacteria from *S. bigelovii* rhizosphere soils collected from intertidal zone in the UAE; (ii) determine their tolerance to high salinity and their PGP potential under rhizosphere-competent conditions in naturally competitive saline environment; and (iii) examine the ability of the potent isolates to enhance growth of *S. bigelovii* under greenhouse conditions. In this study, plant growth, photosynthetic pigments and levels of endogenous auxins, PA and ACC were evaluated in shoots and roots, in addition to seed yields. Results obtained from the Principal Component Analysis (PCA) support the accuracy of the experiment and the equivalent reliability in screening for plant growth promotion using rhizosphere-competent PGP actinobacteria. The best performing isolates selected were applied individually and in combination to

determine whether growth promotion could be enhanced by mixing actinobacterial species showing different mechanisms of action *in vivo.*

3.2 Materials and Methods

3.2.1 Plant Material and Soil Characteristics

In all experiments, wild-type seeds of *S. bigelovii* Torr. (Scrops, Ninove, Belgium) were surface sterilized by 70% ethyl alcohol (EtOH; Sigma-Aldrich Chemie GmbH, Germany) and 1.05% Clorox (20% household bleach). Two drops of Tween 20 (Sigma-Aldrich) were used in all surface-sterilization steps. Surface sterilized seeds were then washed with 0.22 µm membrane filter-sterilized (Millipore Corporation, MA, United States) full strength seawater (salinity of 4.0%) and were air-dried before use. Pale greyish-yellow sandy soil was collected from Al Rams coast, Ras Al Khaimah, UAE (25° 52' 44″ N, 56° 1' 25″ E), where *S. bigelovii* is naturally growing. Soil was passed through a 1 cm mesh sieve for all greenhouse experiments.

The following soil chemical characteristics were detected: electrical conductivity 9.31 dSm^{-1}; pH 8.18 (in 0.01 M $CaCl_2$), organic C 1.15%, and the nutrients (mg kg $soil^{-1}$) [N (5.3 as $NH4^+$; 2.9 as $NO3^-$), oxalate extractable amorphous Fe (382), sulfate (311), bicarbonate extractable K (265), total P and available P (44, 8.3, respectively)].

3.2.2 Collection of Rhizosphere Soils

Rhizosphere soils of six young *S. bigelovii* seedlings were collected from the above-mentioned study site. Excavated soil (maximum depth of 15 cm) from around the root balls was placed into sterile plastic bags and brought to the laboratory. Samples were passed through 5 mm sieve of which each sample consisted of

rhizosphere soils from two seedlings, randomly pooled as one replicate. The three collected rhizosphere soil samples were airdried at 25°C for 4 days to reduce the viable vegetative bacterial cells (Williams et al., 1972).

3.2.3 Isolation of Actinobacteria from Salicornia Rhizosphere Soils

The aerobic culturable actinobacterial populations of the freshly sampled rhizosphere soils were determined using the soil dilution plate count method. Three replicates of 10 g rhizosphere soil samples were dispensed into 100 mL of membrane filter-sterilized full-strength seawater, and the soil suspension was placed in an ultra-sonic cleaner at a frequency of 55,000 cycles s^{-1} for 20 seconds. The soil suspension was then shaken at 250 rpm at 28°C for 30 minutes on a rotary shaker, Model G76 (New Brunswick Scientific, NJ, United States).

Dilutions of 10^{-2}–10^{-5} were made in membrane filter sterilized full strength seawater and 0.2 mL aliquots were spread onto Inorganic Salt Starch Agar (ISSA) (Küster, 1959) made with membrane filter-sterilized full-strength seawater in sterile petri dishes. Cooled (45°C) sterile ISSA medium was amended with 50 µg mL^{-1} cycloheximide (Sigma-Aldrich) and 50 µg mL^{-1} nystatin (Sigma-Aldrich). Five plates per dilution were used and air-dried in a laminar flow. Plates were incubated for 7 days at 28°C in dark and colonies were counted (log_{10} colony forming units (cfu) g^{-1} dry soil). Unless otherwise indicated, actinobacteria were purified and maintained on ISP3 medium (oatmeal agar) plates made with membrane filter-sterilized full-strength sweater and supplied with 0.1% yeast extract (OMYEA) (Shirling & Gottlieb, 1966).

Streptomycete Actinobacteria (SA) and Non-Streptomycete Actinobacteria (NSA) were tentatively identified to the genus level according to Cross (1989). Colonies of SA and NSA were identified based on morphological characteristics,

ability to form sporangia, distribution of aerial and/or substrate mycelia, presence or absence of aerial mycelia, the stability and fragmentation of substrate mycelia (Cross,1989). Isolates were stored as mycelia and spores in 20% glycerol at −20°C (Wellington & Williams, 1977).

3.2.4 Tolerance of Actinobacterial Isolates to Different Concentrations of NaCl

Tolerance to salt stress was evaluated by growing the selected isolates on ISSA medium made with deionized water and supplemented with the following NaCl concentrations: 0, 10, 20, 40, 60, and 80 g L^{-1} medium. The isolates were streaked in triplicates on the plates and incubated for 7 days at 28°C in dark (Williams et al., 1972).

Actinobacterial growth and heavy sporulation on ISSA supplemented with 80 g NaCl L^{1} (8%) indicated the efficiency of the selected isolates to tolerate high NaCl concentration and to be true halotolerant isolates. Only these isolates were chosen for subsequent experiments.

3.2.5 *In Vitro* Indicator Root Colonization Plate Assay

The ability of the obtained halotolerant actinobacterial isolates to colonize *S. bigelovii* was carried *in vitro* using the primary qualitative root colonization plate assay (Kortemaa et al., 1994) to determine if *S. bigelovii* root exudates can act as the only carbon source to support the growth of each isolate. Surface sterilized *S. bigelovii* seeds were pre-germinated on membrane filter-sterilized full strength seawater agar plates for 2 days before being transferred onto new plates (one seed/plate). Eight replicates were inoculated with each isolate grown on OMYEA (one isolate/plate). Seeded plates without treatment were used as controls. Actinobacterial suspension (approximately 10^8 cfu mL^{-1}) was prepared for each isolate from OMYEA plates made

with membrane filter-sterilized full-strength seawater. An inoculum (0.2 mL) was placed 1–2 mm alongside the emerging radicle (Kortemaa et al., 1994).

The seawater agar plates were vertically incubated at 28°C in dark and the root colonization by the isolates was detected after 8 days. Colonization was calculated as a percentage of the total root length (Kortemaa et al., 1994) .

3.2.6 Scanning Electron Microscopy (SEM)

According to the indicator root colonization plate assay, roots were initially fixed with Karowskys fixative (2.5% glutaraldehyde and 2% paraformaldehyde) for 4 hours at 25°C. Samples were treated with 0.2 M phosphate buffer, pH 7.2 at 4°C for 2 hours and post-fixed in 1% osmium tetroxide for 1–2 hours. After washing with deionized water, samples were dehydrated with a series of EtOH dilutions ranging from 30 to 100% at 4°C.

Once in 100% EtOH, roots were dried in a critical-point dryer (Polaron CPD Bell Brook Business Park, Bolton Close England) and mounted on carbon tabbed Aluminum (Al) stubs. Stubs were fixed in the Polaron sputter coater vacuum chamber and sputtered with gold Au/Pd target for 5 minutes at 20 mA. Phillips XL-30 SEM (Eindhoven, The Netherlands) was used to examine the colonized root samples.

3.2.7 Production of IAA, PA, and ACCD by Actinobacteria

All microbiological media in the experiments described in sections. Production of IAA, PA, and ACCD by Actinobacteria and other PGP activities of the three promising isolates were prepared using membrane filter-sterilized full-strength seawater. The selected root colonizing isolates were *in vitro* tested for their capability to produce IAA, PA, and ACCD. To detect IAA, Erlenmeyer flasks (100 mL)

containing 50 mL of sterile Inorganic Salt Starch Broth (ISSB) (Küster, 1959) were supplied with 5 mL of 5% filter-sterilized L-tryptophan (Khalid et al., 2004).

The flasks were inoculated with 2 mL of each isolate prepared from 5 days old shaken ISSB culture of about 1×10^8 cfu mL−1, covered with Al-foil and incubated on a rotary shaker (Model G76) at 250 rpm at 28°C in dark for 7 days.

Non-inoculated flasks were used as a control. After incubation, suspensions from each flask were centrifuged at 12,000 × g for 30 minutes. The supernatant was filtered through Millipore membranes and collected in sterile tubes. Six milliliters of culture supernatants were pipetted into test tubes and 4 mL of Salkowski reagent (2 mL of 0.5 M $FeCl_3$ + 98 mL 35% $HClO_4$) were applied (Gordon & Weber, 1951). Tubes were left for 30 minutes to develop red color; and the intensity of the color was determined by optical density at 530 nm using a scanning spectrophotometer (UV-2101/3101 PC; Shimadzu Corporation, Analytical Instruments Division, Kyoto, Japan). A standard curve was established according to the color of the standard solutions of IAA, and auxin compounds were expressed as IAA-equivalents (Gordon & Weber, 1951).

Eight replicate samples were analyzed. The obtained actinobacterial isolates were tested for the production of Putrescine (Put) as a polyamine using Moeller's Decarboxylase Agar Medium (MDAM) amended with 2 g L^{-1}L-arginine-monohydrochloride (Sigma-Aldrich) and 0.02 g L^{-1} phenol red (Sigma-Aldrich) (Arena & Nadra, 2001). Isolates growing on OMYEA were streaked in triplicate on MDAM plates with or without Arginine (control). Plates were incubated at 28°C for 3 days in dark. Production of Put by the decarboxylating isolates was determined by the existence of a dark red halo beneath and around the colonies.

All isolates showing large red halo color on MDAM were further tested for production of Put, Spermidine (Spd), and Spermine (Spm) in Moeller's Decarboxylase Broth Medium (MDBM) amended with 2 g L^{-1} of L-arginine mono hydrochloride by reverse-phase High-Performance Liquid Chromatography (HPLC; Spectra Lab Scientific Inc., ON, Canada). Erlenmeyer flasks containing 50 mL of MDBM were inoculated with 3 mL of 20% glycerol suspension of each isolate (10^8 cfu mL^{-1}) and incubated on a rotary shaker at 250 rpm at 28°C. After incubation for 10 days in dark, the suspension from each flask was centrifuged at 12,000 × g for 30 minutes. The membrane filter-sterilized cell-free culture broth was collected in sterilized McCartney tubes. The derivatization of the filter-sterilized cell-free filtrates and the internal polyamine standards were carried out as follows: 0.5 mL of filtrate was added to a 0.5 mL of saturated solution of sodium bicarbonate (Sigma-Aldrich) and 2 mL of dansyl chloride (Sigma-Aldrich) solution (10 mg mL^{-1} in acetone).

The reaction vessel was incubated at 60°C for 20 minutes and 50 µL of 28% ammonium hydroxide were added. After 30 minutes, the reaction mixture was filtered again through 0.22 µm Millipore membranes and used for the HPLC. The HPLC chromatograms (eight replicates of each isolate) were produced by injecting 10 µL aliquot of the sample onto a 10 µm Bondapak C18 column (4 mm × 30 cm) in liquid chromatograph (Waters Associates) equipped with a 254 nm UV detector (Smith & Davies, 1985). The selected isolates were also screened for the production of ACCD. Five-day-old isolates grown on rich OMYEA were streaked in triplicates on N-free Dworkin and Foster's salts minimal agar medium (DF) plates (Dworkin & Foster, 1958) amended with either 3 mM ACC (Sigma-Aldrich) or 2 g $(NH_4)_2SO_4$ (control).

The heat-labile ACC was filter-sterilized, and the filtrate was added to the salt medium. Plates were incubated at 28°C in dark for 7 days. Isolates growing on

DF+ACC plates indicated the efficiency of the isolate to utilize ACC and produce ACCD. To determine the activity of ACCD, isolates were grown in ISSB at 28°C for 5 days in dark. Cells were centrifuged, washed with 0.1 M Tris HCl (pH 8.5) and inoculated onto DF+ACC broth on a rotary shaker at 250 rpm for another 5 days. Cells were resuspended in 0.1 M Tris-HCl and ruptured by freezing/thawing cycles thrice (Shah et al., 1998).

The lysate was centrifuged at 80,000 × g for 1 hour. The enzymatic activity of ACCD was assayed by monitoring the amount of α-ketobutyrate liberated (Honma & Shimomura, 2014). Protein concentrations were determined as described (Bradford, 1976). Eight replicate samples were analyzed.

3.2.8 Rhizosphere Competence Assay Under Naturally Competitive Environment

To investigate whether particular members of actinobacteria producing high levels of IAA, PA, or ACCD are avid colonizers of the rhizosphere (rhizosphere-competent), the non-sterilized soil tube assay was used (Ahmad & Baker, 1987) using rifampicin resistant mutants (Misaghi & Donndelinger, 1990). The surface-sterilized *S. bigelovii* seeds were coated with each isolate as described below. Non-treated seeds served as controls. In each tube containing non-sterilized field soil (collected from the same site described above), one seed was planted 5 mm deep. Tubes were vertically placed into boxes containing the same soil and watered with full strength seawater to container capacity.

Boxes were covered and held upright with no more added seawater to the tubes after sowing (Ahmad & Baker, 1987). Boxes were kept in a greenhouse (photosynthetic photon flux density of 700 µmol $m^{-2}s^{-1}$) at 25 ± 2 and Relative Humidity (RH) of 60 ± 5%. After 4 weeks, *S. bigelovii* were harvested from the soil

tube assay. The length of the harvested roots was measured, and only the top 12 cm of roots were retained, and were aseptically cut into 2 cm segments (Ahmad & Baker, 1987). Loose particles of the rhizosphere soil on root segments were removed and air-dried. Rhizosphere soil particles were numbered based on the root segments from which they were recovered (Ahmad & Baker, 1987).

Roots and soil particles were separately studied to determine the root-colonization frequencies (R%) and Population Densities (PD; log10 cfu g^{-1} dry soil) of each isolate in the rhizosphere soil, respectively (Ahmad & Baker, 1987) on ISSA plates made with membrane filter-sterilized full-strength sweater and supplemented with 100 µg mL^{-1} rifampicin (Sigma-Aldrich). To be considered as colonized-rhizosphere or -root segment, colonies of the isolated strains were obtained on ISSA plates amended with rifampicin either in the corresponding rhizosphere soil sample, on the root segment or both (Ahmad & Baker, 1987) after 7 days of incubation at 28°C in dark. Percentage of root segments colonized was calculated as the proportion of the total number of segments colonized to the total segments sampled at each distance. Experiments were repeated twice with eight replicates in each; and only the strongest three rhizosphere-competent isolates producing either IAA, PA, or ACCD were chosen for the greenhouse experiments.

3.2.9 Identification and Construction of Phylogenetic Tree of Selected Actinobacteria

Amplification of 16S rRNA gene using Polymerase Chain Reaction (PCR) of the three isolates (#7, #1, and #21) and their sequencing were carried out by Deutsche Sammlung von Mikroorganismen und Zellkulturen GmbH (DSMZ, Braunschweig, Germany). According to Rainey et al. (1996), the PCR primers used were: 900R (5'-CCGTCAATTCATTTGAGTTT-3'); 357F (5'-TACGGGAGGCAGCAG-3') and

800F (5'-ATTAGATACCCTGGTAG-3'). Nucleotide sequences were submitted to GenBank and assigned accession numbers MN795132, MN795133, and MN795131 for isolates #7, #11, and #21, respectively. Pairwise sequence similarity using 16S rRNA gene sequence was determined.

For the phylogenetic analyses, reference strains were selected from the top hits of the determination using GenBank BLAST1. An amplification of 1,516, 1,519, and 1,519 bp from isolates #7, #11, and #21 was obtained and aligned with closely-related strain sequences of *Streptomyces* using CLUSTAL-X (Thompson et al., 1997) in Molecular Evolutionary Genetics Analysis 7.0 (MEGA7) software (Kumar et al., 2016). Phylogenetic trees were constructed using the Maximum Likelihood (ML) method of which bootstrap values were calculated based on 1000 re-samplings. The morphology of the spore chains and surface was carried out for the three isolates using Phillips XL-30 SEM.

3.2.10 Other PGP Activities of The Three Promising Isolates

To detect auxins as IAA and IPYA (Indole-3-Pyruvic Acid), the three isolates (#7, #11, and #21) were cultivated in 50 mL ISSB supplemented with 5 mL of a 5% of L-tryptophan (Sigma-Aldrich). Gibberellic Acid (GA3) and cytokinins [isopentenyl adenine (iPa), isopentenyl adenoside (iPA) and Zeatin (Z)], were detected on Strzelczyk and Pokojska-Burdziej (1984) medium. After 10 days, the extraction of these PGRs from the concentrated filter-sterilized cell-free broth and the HPLC parameters used to determine the concentrations of IAA, IPYA, GA3, iPa, iPA, and Z were carried out as described by Tien et al. (1979). The production of siderophores was determined using chrome azurol S agar plates (Schwyn & Neilands, 1987).

Yellow-orange halo zone developed around the colony was considered positive for siderophores production. The N-fixing activities of isolates were examined by the acetylene reduction assay (Holguin et al., 1992) using Varian 6000 gas chromatogram (Varian Instrument Group, United States). Production of NH3 was determined using Nessler's reagent (Dye, 1962). Solubilization of insoluble rock phosphate (Tianjin Crown Champion International Co., Ltd., Tianjin, China) was estimated using Pikovskaya's agar medium (Pikovskaya, 1948) with bromophenol blue in which tricalcium phosphate was replaced with rock phosphate. Production of clear zone was an indicator of P-solubilization.

All rock phosphate-solubilizing actinobacterial isolates showing large zones of clearing on Pikovskaya's agar were further tested quantitatively for their abilities to solubilize rock phosphate in modified National Botanical Research Institute's phosphate broth (Nautiyal, 1997) containing 5 g L^{-1} rock phosphate. Water-soluble P was analyzed by the colorimetric procedure of Murphy and Riley (1962) using molybdophosphoric acid blue complex. The drop in pH and the released soluble P amount were taken as an indicator of the efficiency of isolates. In all the above-mentioned tests, eight independent replicates were used for each isolate.

3.2.11 Assessment of Inhibitory Activity Among Actinobacterial Isolates

The spot-inoculated plate technique described by de Boer et al. (1999) was used to determine the isolate's sensitivity to the diffusible metabolites of the other isolates. Suspensions of actinobacterial spores were cultured on OMYEA in 10 mM $MgSO_4$. For each isolate, approximately 10^8 cfu mL^{-1} was used as an inoculum. Actinobacterial isolates were spot inoculated on OMYEA by pipetting 2 droplets of 5 µL of the actinobacterial inoculum; and plates were incubated at 28°C

for 5 days in dark. Later on, a suspension of the target isolate was atomized over the surface of the spot-inoculated plates. After 4 days at 28°C in dark, zones of growth inhibition of the target isolate around the spot-inoculated isolates were evaluated, if any.

To determine if the selected isolates do not inhibit each other by their volatile compounds, the method described by Payne et al. (2000) was used. Briefly, fresh OMYEA plates were inoculated by evenly spreading 0.2 mL of 10^8 cfu mL^{-1} of the isolate onto the surface of agar. Plates were incubated in dark at 28°C. After 5 days of incubation, another fresh plate of OMYEA was simultaneously inoculated with an actively growing culture of the tested isolate. The lids were removed and the plates containing the tested isolate were inverted over the previously grown isolate; and the two plate bases were taped together with Parafilm (American National Can TM, Greenwich, CT, United States).

Control plates were prepared the same way except that non-inoculated plate was used instead of a plate containing the target isolate. After another 5 days in incubator, the growth of the target isolate was compared to that of the control. In these two tests, four independent replicates were used for each isolate.

3.2.12 Preparation of Date Pits-Based Activated Carbon as Seed Adsorbents for Actinobacterial Isolates

For the preparation of activated carbon as seed adsorbents for the actinobacterial isolates to be used in greenhouse experiments, local date seeds from the fruits of date palm (Phoenix dactylifera) were dried and ground using an electric agitated mortar (JKG-250B2, Shanghi Jingke Scientific Instrument) (Mathew et al., 2018).

Physical activation of date seeds was performed in a tube furnace (GSL-1500X; MTI Corporation, VA, United States) with carbonization followed by activation. A carbonization step was started by allowing N_2 gas to pass through the furnace for 10 minutes when the temperature was gradually increased under a constant flow of N_2 at a rate of 5°C min^{-1} up to 600°C and maintained at this temperature for 4 hours (Sekirifa, Hadj-Mahammed et al., 2013). The carbonaceous material was activated at 900°C in the same furnace under the flow of CO_2 gas.

The activated carbon was then sieved using a testing mesh (size of 200–300 µm). To prepare the activated carbon nanomaterials, activated carbon was wet-ground in a grinder (Retsch RM 100, Germany) and dried in a freeze dryer (Telstar, Spain) at −55°C and 0.02 mbar for 6 hours (Mathew et al., 2018). The material was then filtered using a 0.45 µm polytetrafluoroethylene filter (Thomas Scientific, NJ, United States) prior to use as a seed adsorbent for actinobacterial isolates.

3.2.13 Production of *Inocula* For *In Vivo* Experiments

Inocula of each isolate were applied as seed coating and in soil for the greenhouse experiment described below as recommended by El-Tarabily (2008). For the seed coating, isolates grown in ISSB made with membrane filter-sterilized full-strength sweater were shaken at 250 rpm at 28°C for 5 days in dark. Cells and/or spores were collected and centrifuged for 20 minutes at 5,000 × g. Pellets were washed three times before being suspended in sterile 0.03 M $MgSO_4$ (buffer).

Instantly, surface-sterilized *S. bigelovii* seeds were immersed in beakers containing either each actinobacterial suspension (approximately 10^8 cfu mL^{-1}) in 0.03 M $MgSO_4$ (buffer) or buffer alone (no actinobacterial suspension; control) for 4 hours at 28°C. Activated carbon from date seeds (5 g L^{-1}) was added as an adsorbent

for the treated and the control seeds. The rest of the suspension was drained, and seeds were air-dried.

For each isolate, inocula were prepared for the soil application by adding 300 g of oat bran as a food source in Erlenmeyer flasks (500 mL) autoclaved for 20 minutes at 121°C on three successive days. The oat bran was then aseptically inoculated with spore suspensions (25 mL) of each isolate in 20% glycerol (10^8cfu mL^{-1}) and incubated in dark at 28°C for 3 weeks. Non-colonized oat bran, which had been autoclaved twice, served as a control. Colonized oat bran with each isolate (0.05 g colonized oat bran inoculum g^{-1} air-dried non-sterile soil) were mixed thoroughly using a cement mixer in all experiments described below.

3.2.14 Evaluation of Growth Promotion of *S. bigelovii* in the Greenhouse

S. bigelovii growth was *in vivo* tested to determine the effect of the three isolates #7, #11, and #21 either individually or combined three together under greenhouse conditions. Briefly, free draining plastic pots (23 cm in diameter) were filled with 7 kg soil sampled from the area (described above) and mixed with 0.05 g of colonized oat bran inoculum g^{-1} field soil. Surface-sterilized healthy *S. bigelovii* seeds were coated with each isolate and with the activated carbon from date pits (described above) or with activated carbon only (control).

In each pot, eight seeds were sown in soil at 5 mm deep, and seedlings were thinned to four/pot when emergence was complete. A total of five treatments were applied; where each treatment was replicated eight times with four seedlings/replicate as follows: non-inoculated control (C); individually inoculated with either isolate #21 (*Sc*), isolate #7 (*St*) or isolate #11 (*Sr*), producing auxins, PA or ACCD, respectively; and collectively inoculated with all three isolates (*Sc/St/Sr*). Pots were placed in the

greenhouse (photosynthetic photon flux density of 700 µmol $m^{-2}s^{-1}$) at 25 ± 2°C and RH of 60 ± 5%) in a Randomized Complete Block Design (RCBD) and were daily watered to container capacity with full strength seawater. Dry weight and length of shoots and roots were recorded at 12 weeks post-sowing (wps) the seeds, and seed dry weight was recorded 20 wps.

3.2.15 Extraction of Photosynthetic Pigments, Endogenous Auxins, PA, and ACC from *S. bigelovii*

The levels of photosynthetic pigments, including chlorophyll (chl a and chl b) and carotenoids, were determined in the succulent stems (Holden, 1965; Davies, 1965). Tissues of the terminal part of the root and shoot systems were used for the analysis of endogenous auxins, PA, and ACC. The free PA (Put, Spd, and Spm) were extracted according to Flores and Galston (1982). Benzoylation using benzoyl chloride (Sigma-Aldrich) and the HPLC for the plant extracts and the internal standard of PA were carried out as described by Redmond and Tseng (1979).

The extraction of endogenous IAA, IPYA was carried out as previously described (Guinn et al., 1986; Shindy & Smith, 1975). The HPLC parameters were applied as previously described (Tien et al., 1979). The extraction of endogenous ACC was carried out according to Lizada and Yang (1979). Derivatization of ACC was done by adding phenyl isothiocyanate (Sigma-Aldrich) and the HPLC chromatograms were produced as described (Lanneluc-Sanson et al., 1986). Eight replicate samples were analyzed for the detection of photosynthetic pigments and endogenous auxins, PA, and ACC. All procedures were carried out on seedlings at 12 wps.

3.2.16 Statistical Analyses

Treatments were arranged in a RCBD in all experiments. Data from the experiments were repeated with similar results, combined, and analyzed. Data of PD were transformed into $\log_{10}$ cfu g^{-1} dry soil, and R% were arcsine transformed before Analysis of Variance (ANOVA) was carried out. Data were subjected to ANOVA and means were compared using Fisher's Protected LSD Test (P= 0.05). For multidimensional analyses, a PCA was performed to determine the contribution of PGP to the experimental variance. Results were displayed in a biplot.

The PCA was carried out using XLSTAT version 2019.3.2 (Addinsoft, United States). Pearson's correlation was conducted between all pairs of studied variables within the same treatment of actinobacterial isolates and plant tissues. For all statistical analyses carried out in this study, SAS Software version 9 was used (SAS Institute Inc., NC, United States).

3.3 Results

3.3.1 Isolation of Halotolerant Actinobacteria from *Salicornia* Rhizosphere Soils

The density of actinobacteria populations in *S. bigelovii* rhizosphere was 5.36 ± SE 1.33 $\log_{10}$ cfu g^{-1} dry soil. Thirty-nine actinobacteria were isolated from the rhizosphere on ISSA plates (Supplementary Figure S1). According to their cultural and morphological characteristics, 27 (69.23%) and 12 (30.76%) were identified as SA and NSA isolates, respectively. All *Streptomyces* spp. and genera of the NSA *(Actinomadura, Actinoplanes, Microbispora, Micromonospora, Rhodococcus, Nocardia, Nocardiopsis, and Streptosporangium* spp.), were enumerated (Supplementary Figure S1) and purified on OMYEA plates. Even though all 39

isolates grew well and sporulated heavily on ISSA medium supplied with up to 40 g L^{-1} NaCl, only 22 (56.41%) showed increased tolerance to 80 g L^{-1} of NaCl (Supplementary Figure S1). This indicates the efficiency of the selected isolates to tolerate high concentration of NaCl (8%) and were considered to be true halotolerant isolates. Of the 22 halotolerant isolates, 13 (59.1%) and (9) (40.9%) isolates belonged to SA and NSA, respectively.

3.3.2 Preliminary Screening of Actinobacterial Isolates for Root Colonization of *S. bigelovii*

In order to determine the ability of the halotolerant actinobacterial isolates to colonize *S. bigelovii* roots, an *in vitro* indicator root colonization plate assay was performed. Eight of halotolerant actinobacterial isolates (#1, #3, #10, #14, #23, #29, #33, and #37) failed to colonize the roots of *S. bigelovii* at 8 days after emergence. Therefore, they were excluded from the subsequent studies. The remaining 14 isolates (#2, #4, #6, #7, #9, #11, #15, #18, #21, #25, #27, #31, #32, and #35) showed different degrees of root colonization after 8 days of radicle emergence; 10 isolates (#2, #4, #6, #7, #11, #18, #21, #25, #27, and #32) revealed 100% of root colonization, whilst the rest (#9, #15, #31, and #35) colonized 50–75% of the roots. The latter four isolates were excluded in further studies.

Only the 10 isolates showing whole root colonization (7 SA and 3 NSA) were selected. The full colonization of the 10 isolates for *S. bigelovii* root with plate assay was confirmed by using SEM. For example, it was evident that the actinobacterial isolates #7, #11, and #21 that fully colonized the root system when evaluated by the *in vitro* root colonization plate assay. They also showed extensive mycelial growth and spore chains on the root surface of *S. bigelovii* with the use of SEM (Figure 3.1).

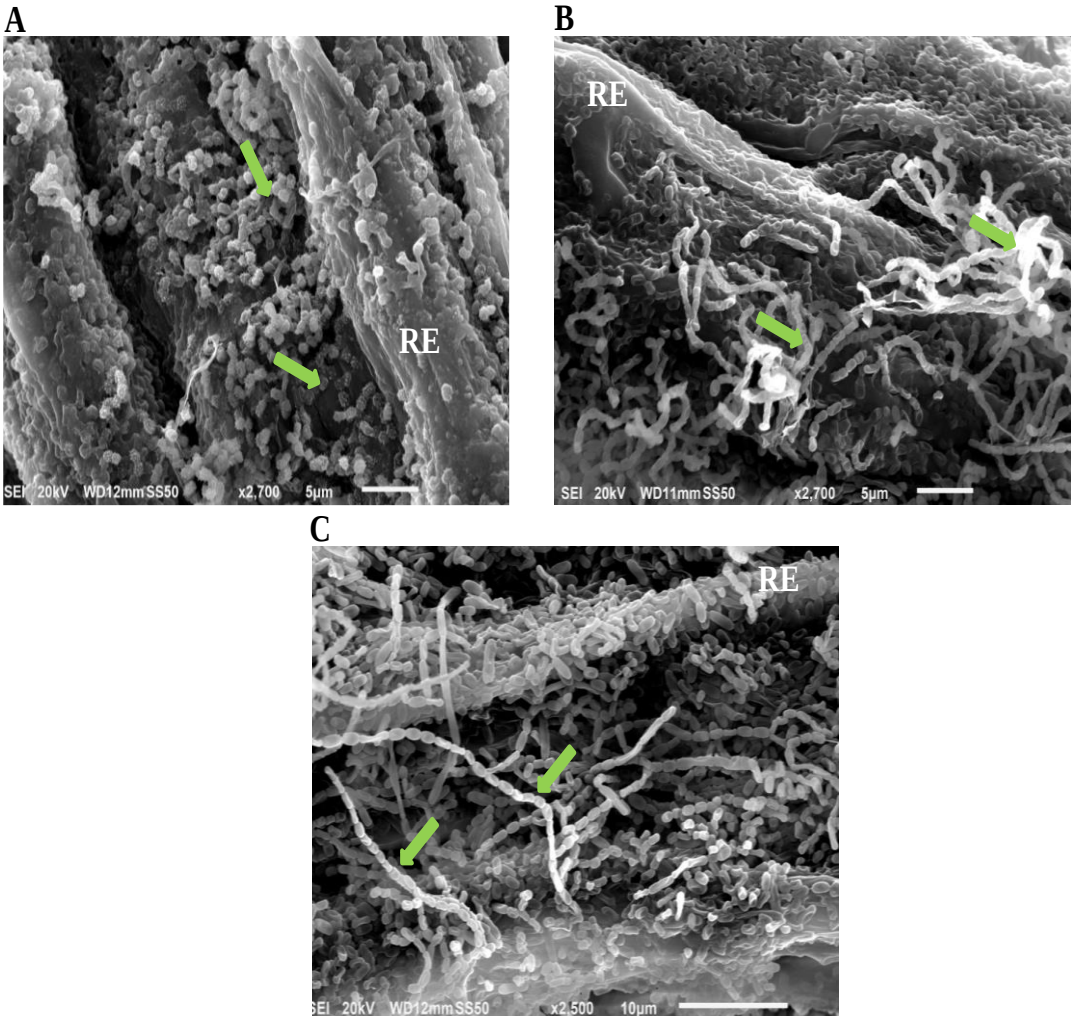

Figure 3.1: Root colonization of *Salicornia bigevolii* by selected halophilic actinobacterial isolates. Scanning electron micrograph of selected actinobacterial (A) auxin-producing isolate #21 (2,700X); (B) polyamine-producing isolate #7 (2,700X); and (C) ACCD-producing isolate #11 (2,500X) colonizing root of *S. bigevolii*. In (A-C), green arrows represent the chain and/or structure of spores. RE,

3.3.3 Production of IAA, PA, and ACCD by Actinobacteria

Using the colorimetric analysis, auxins were detected in the liquid cultures of isolates #4, #18, #21, #27, and #32 (Table 3.1). The efficiency of these isolates in their capability for IAA production varied greatly. The other five isolates did not produce IAA. The isolates that formed dark red color after the addition of Salkowski reagent

were considered as IAA-producing isolates (Supplementary Figure S2). We also screened the isolates for the ability to produce Put on MDAM plates amended with L-arginine-monohydrochloride. The relatively moderate to large dark red halo around and beneath the colonies in isolates #2, #4, #7, #25, and #32 indicated the production of Put (Table 3.1 and Supplementary Figure S2): but the absence of red halo was an indicator of inability of the remaining isolates to produce Put. From the HPLC analysis of the culture extracts of the 10 tested isolates grown on MDBM amended with L-arginine-monohydrochloride, the production of the PA (Put, Spd, and Spm) varied significantly ($P < 0.05$) (Table 3.1).

Five out of the 10 isolates grew and sporulated on DF+ACC agar (Supplementary Figure S2); the rest, however, grew only on DF control medium with $(NH_4)_2SO_4$ (Table 3.1). Quantitative estimation of ACCD activity revealed significant ($P < 0.05$) variations in the production of ACCD among the different isolates (Table 3.1). We noticed that isolates #2, #4, #6, #11, and #27 produced moderate to high levels of ACCD activity and were considered ACCD producers for further analyses.

Table 3.1: Production of Indole-3-Acetic Acid (IAA), polyamines and 1-AminoCyclopropane-1-Carboxylic acid Deaminase (ACCD) by the selected actinobacterial isolates obtained from *Salicornia bigelovii* rhizosphere

Isolate [a]	IAA equivalents (µg mL^{-1})	Polyamines			ACCD activity (Nanomoles α keto-butyrate mg^{-1} protein h^{-1})
		Put (mg L^{-1})	Spd (mg L^{-1})	Spm (mg L^{-1})	
#2	ND	312.13±7.48 *a*	71.75±4.69 *a*	ND	247.78±8.29 *a*
#4	29.76±1.92 *a*	385.50±6.89 *b*	95.87±4.65 *b*	25.79±2.40 *a*	402.98±5.78 *b*
#6	ND	ND	ND	ND	448.14±7.19 *c*
#7 [b]	ND	503.59±11.19 *c*	204.70±8.28 *c*	54.46±4.32 *b*	ND
#11 [b]	ND	ND	ND	ND	440.02±8.32 *c*
#18	20.26±1.21 *b*	ND	ND	ND	ND
#21 [b]	2.88±0.87 *c*	ND	ND	ND	ND
#25	ND	432.26±9.78 *c*	135.43±7.18 *d*	57.14±1.68 *b*	ND
#27	10.98±1.04 *d*	ND	ND	ND	118.67±5.22 *d*
#32	17.89±0.75 *e*	278.01±5.98 *d*	68.01±4.89 *a*	38.63±1.27 *c*	ND

[a]#7, #11 and #22 represent *Streptomyces tritolerans* UAE1, *S. rochei* UAE1 and *S. chartreusis* UAE1, respectively. [b]#3, #8, #14 and #27 produced negligible levels of Put, Spd or Spm were not included in subsequent experiments. Values are means of 8 independent replicates ± SE for each sampling from two independent experiments. Mean values followed by different letters are significantly ($P< 0.05$) different from each other according to Fisher's Protected LSD Test. Put, putrescine; Spd, spermidine; Spm, spermine; ND, non-detectable.

3.3.4 Rhizosphere Competence Assays Under Naturally Competitive Environment

The rhizosphere competence assays were carried out to evaluate the root colonization abilities under a naturally competitive greenhouse environment for the 10 isolates that initially colonized the entire root system *in vitro*. There was significant ($P< 0.05$) variation in the root colonizing abilities of the different isolates (Table 3.2). The root-colonization frequencies of actinobacterial strains in the rhizosphere soil were highest in isolates #7, #11, #21, and #27 that successfully colonized both the root and the rhizosphere up to 12 cm of root length (Table 3.2).

Although the 10 isolates colonized the rhizosphere soil at all soil depths, their abundancies were significantly ($P< 0.05$) greater at the top 8 cm in comparison to deeper roots (Table 3.2). All 10 isolates colonized the root system of *S. bigelovii* and the rhizosphere soil (up to 12 cm depth), but isolates #11, #7, #21, and #27 showed the highest colonized PD values. The strongest three rhizosphere-competent isolates #21, #7, and #11 that also were good producers for auxins, PA and ACCD, respectively, were selected to study their effects on *S. bigelovii* growth under greenhouse conditions.

Notably, isolates #2, #4, #6, #18, #25, and #32 produced high levels of auxins, PA and/or ACCD (Table 3.1). However, none of the isolates were selected for the greenhouse experiments because they showed low levels of rhizosphere competency (Table 3.2). Similarly, isolate #27 was eliminated due to its multiple modes of action albeit the excellent rhizosphere competency. In this study, the criteria used in choosing the isolates were (1) to solely possess a single mechanism of action such as producing high levels of auxins, PA or ACCD; and (2) to be able to show a strong rhizosphere competency as recommended by El-Tarabily et al. (2020).

Table 3.2: Root colonization frequencies (%) of the auxins, polyamines and the 1-aminocyclopropane-1-carboxylic acid deaminase producing actinobacterial isolates in Root segments (R) of *Salicornia bigelovii* and Population Densities. (PD) (Mean log10 cfu g-1 dry soil) of the actinobacterial isolates in rhizosphere soil of *S. bigelovii* at 3 weeks post sowing (wps) treated seeds in the non-sterile soil tube rhizosphere competence assay

port	**Isolate**																			
	#2		**#4**		**#6**		**#7** [b]		**#11** [b]		**#18**		**#21** [b]		**#25**		**#27**		**#32**	
	R	**PD**	**R**	**PD**	**R**	**PD**	**R**	**PD**	**R**	**PD**	**R**	**PD**	**R**	**PD**	**R**	**PD**	**R**	**PD**	**R**	**PD**
0-2	100 *a*	5.02 *a*	100 *a*	4.41 *a*	100 *a*	3.91 *a*	100 *a*	5.55 *a*	100 *a*	6.35 *a*	100 *a*	3.65 *a*	100 *a*	5.33 *a*	100 *a*	4.42 *a*	100 *a*	4.83 *a*	100 *a*	4.11 *a*
2-4	100 *a*	4.39 *b*	100 *a*	3.65 *b*	100 *a*	3.33 *b*	100 *a*	5.42 *a*	100 *a*	5.72 *b*	100 *a*	2.97 *b*	100 *a*	4.85 *b*	90 *a*	3.72 *b*	100 *a*	4.22 *b*	100 *a*	4.05 *a*
4-6	100 *a*	3.78 *c*	70 *b*	3.02 *c*	100 *a*	3.21 *b*	100 *a*	4.72 *b*	100 *a*	5.61 *b*	100 *a*	2.45 *c*	100 *a*	4.43 *c*	70 *b*	3.11 c	100 *a*	4.05 *b*	80 *b*	3.25 *b*
6-8	100 *a*	3.15 *d*	50 *c*	2.45 *d*	80 *b*	2.55 *c*	100 *a*	4.65 *b*	100 *a*	4.86 *c*	100 *a*	2.57 *c*	100 *a*	4.31 *c*	60 *b*	2.55 *d*	100 *a*	3.66 *c*	65 *c*	2.66 *c*
8-10	80 *b*	2.45 *e*	40 *c*	1.56 *e*	60 *c*	2.45 *c*	100 *a*	4.18 *c*	100 *a*	4.74 *c*	70 *b*	1.94 *d*	100 *a*	3.89 *d*	40 *c*	1.82 *e*	100 *a*	3.41 *c*	60 *c*	2.05 *d*
10-12	60 *c*	1.88 *f*	20 *d*	1.47 e	30 *d*	1.58 d	100 *a*	4.25 *c*	100 *a*	4.93 *c*	50 *c*	1.25 *e*	100 *a*	3.72 *d*	35 *c*	1.22 *f*	100 *a*	3.55 *c*	30 *d*	1.52 *e*

[a] *S. bigelovii* seeds were coated with each isolate and grown in non-sterile field sandy soils in plastic tubes in polystyrene boxes containing soil, in an evaporative-cooled greenhouse maintained at 25±2°C. Seedlings were harvested 3 wps the seeds. [b] Isolates #7, #11 and #21 represent *Streptomyces tritolerans* RAK1, *S. rochei* RAMS1 and ***S. chartreusis*** UAE1, respectively. Values are means of 16 independent replicates for each treatment from two independent experiments. Values with the same letter within a column are not significantly ($P > 0.05$) different according to Fisher's Protected LSD Test. Percentage data were arc-sine transformed before analysis.

3.3.5 Identification and Characterization of the Halotolerant Rhizosphere-Competent Isolates

The promising isolates that only produced either auxins, PA or ACCD isolates were further identified and characterized. Purified PCR products of the 16S rDNA gene was sequenced. The resulting sequence data of isolates #21 (Genbank accession number: MN795131), #7 (MN795132), and #11 (MN795133) were compared with representative 16S rRNA gene sequences of organisms belonging to the actinobacteria. Based on the evolutionary distance values, the phylogenetic tree was constructed according to the neighborhood joining method (Saitou & Nei, 1987). The 16S rRNA gene of isolates #21, #7, and #11 were compared with sequences in the GenBank, European Molecular Biology Laboratory (EMBL) or Ribosomal Database Project (RDP) database (Maidak et al., 1999), which showed that these actinobacterial candidates were all belonged to the genus *Streptomyces* spp.

The complete 16S rRNA gene sequence of isolate #21 showed full 100.0% similarity with *S. chartreusis* (NR 041216), although the remaining isolates of *Streptomyces* spp. showed less than 99.3% similarities Figure 3.2a. On ISP3 medium, pure cultures of isolate #21 produced powdery blue-green aerial mycelium with yellow substrate mycelial growth after 7 days of incubation Figure 3.2b and Supplementary Table S1. According to our observations, the isolate showed branched substrate mycelia from which aerial hyphae developed in the form of open spirals Figure 3.2c. The configuration of the spore chains of isolate #21 which belonged to spirales section of 10–25 mature, spiny spores per chain was detected Figure 3.2c and Supplementary Table S1. Our data suggest that isolate #21 can be recognized as *Streptomyces chartreusis* (Leach et

al., 1953) strain UAE1. The phylogenetic analysis of isolate #7 showed 99.6% similarity to *S. tritolerans* DAS 165 (NR 043745) and *S. tendae* ATCC (NR 025871) and NBRC 12822 (NR 112290); while the rest showed < 99.2% similarity with this particular strain (Figure 3.3a). This suggests that this isolate could be *S.* tritolerans, *S. tendae* or a strain of a new species within the genus *Streptomyces*.

The pure cultures produced dark yellow substrate mycelia and gray aerial mycelia when isolate #7 was incubated for 7 days on ISP3 medium (Figure 3.3b). The isolate did not produce any diffusible pigments in ISP3 medium, and it grew on plates of 7% of NaCl or more (Supplementary Table S2); all of these distinctive characteristics are common features of *S. tritolerans* (Syed et al., 2007). Spores of the isolate were smooth, oval-rod shaped (Figure 3.3c); and its spore chains arranged in long straight to flexous (rectiflexibiles) chains of 10–15 spores (Figure 3.3c and Supplementary Table S2). Our data further support the identification of isolate #7 can be recognized as *Streptomyces tritolerans* strain RAK1 (Syed et al., 2007). For isolate #11, it was phylogenetically grouped in the same clade as five other species, namely *S. geysiriensis* NRRL B-12102 (NR 043818), *S. vinaceusdrappus* BRC 13099 (NR 112368), *S. plicatus* NBRC 13071 (NR 112357), *S. enissocaesilis* NRRL B-16365 (NR 115668), and S. rochei NRRL B-1559 (NR 116078) with 100% similarity (Figure 3.4a).

To identify our isolate from the very closely related species, detailed morphological, cultural, biochemical, and physiological characterization were carried out to distinguish the ACCD-producing isolate. Light grayish-yellow color of aerial mycelium and pale grayish-yellow color of substrate mycelium were produced by isolate #11 on ISP3 medium without production of any diffusible pigments (Figure 3.4b). Except of

S. enissocaesilis, it was difficult to distinguish between our isolate and the other four species based on the aerial mass or substrate mycelium color on any of the ISP media (Supplementary Table S3). At high magnification of SEM, the strain clearly developed smooth, oval-rod shaped spores forming straight to flexuous long chains (rectiflexibiles) of 20–35 spores per chain (Figure 3.4c). The other *Streptomyces* strains, however, showed either retinaculum-apertum or spiral spore chains (Supplementary Table S3). The identification was further confirmed when other phenotypic, biochemical and physiological characteristics between isolate #21 and *S. rochei* NRRL B-1559 (NR 116078) (Kämpfer, 2012) were comparable (Supplementary Table S3); suggesting that isolate #11 can most probably be *Streptomyces rochei* strain RAMS1(Berger et al., 1953). Together, our data indicate that the auxins, PA, and ACCD-producing isolates were identified as *S. chartreusis, S. tritolerans* and *S. rochei,* respectively.

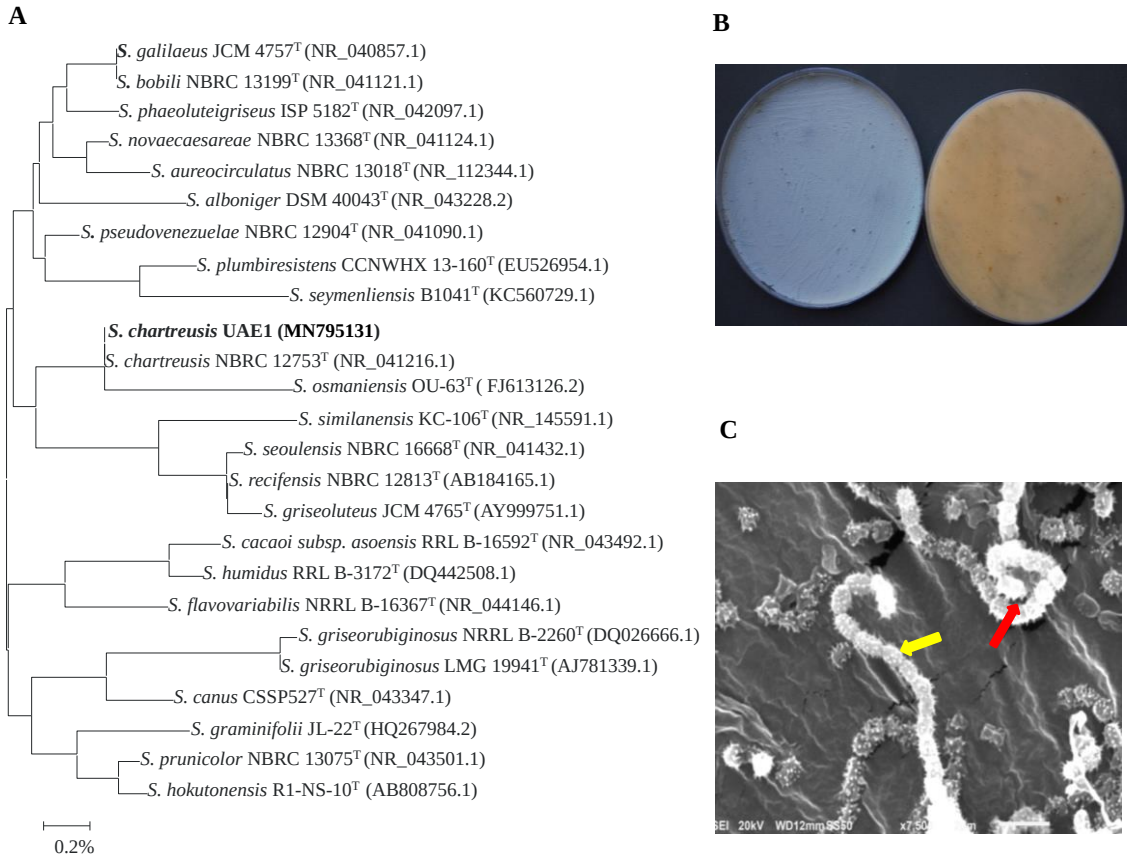

Figure 3.2: Taxonomic characterization of *Streptomyces chartreusis* UAE1. (A) The tree showing the phylogenetic relationships between the auxin-producing *S. chartreusis* UAE1 (isolate #21; MN795131; 1,519 bp) and other members of *Streptomyces* spp. on the basis of 16S rRNA sequences. (B) Aerial mycelia (left) and substrate mycelia (right) growing on ISP medium 3 supplemented with yeast extract; and (C) scanning electron micrograph (7,500X) showing spiral chains of spores (red arrow) with spiny spore structure (yellow arrow) of the strain of *S. chartreusis* UAE1. In (A) numbers at nodes indicate percentage levels of bootstrap support based on a neighbor-joining analysis of 1000 resampled datasets. Bar, 0.002 substitutions per site. GenBank accession numbers are given in parentheses

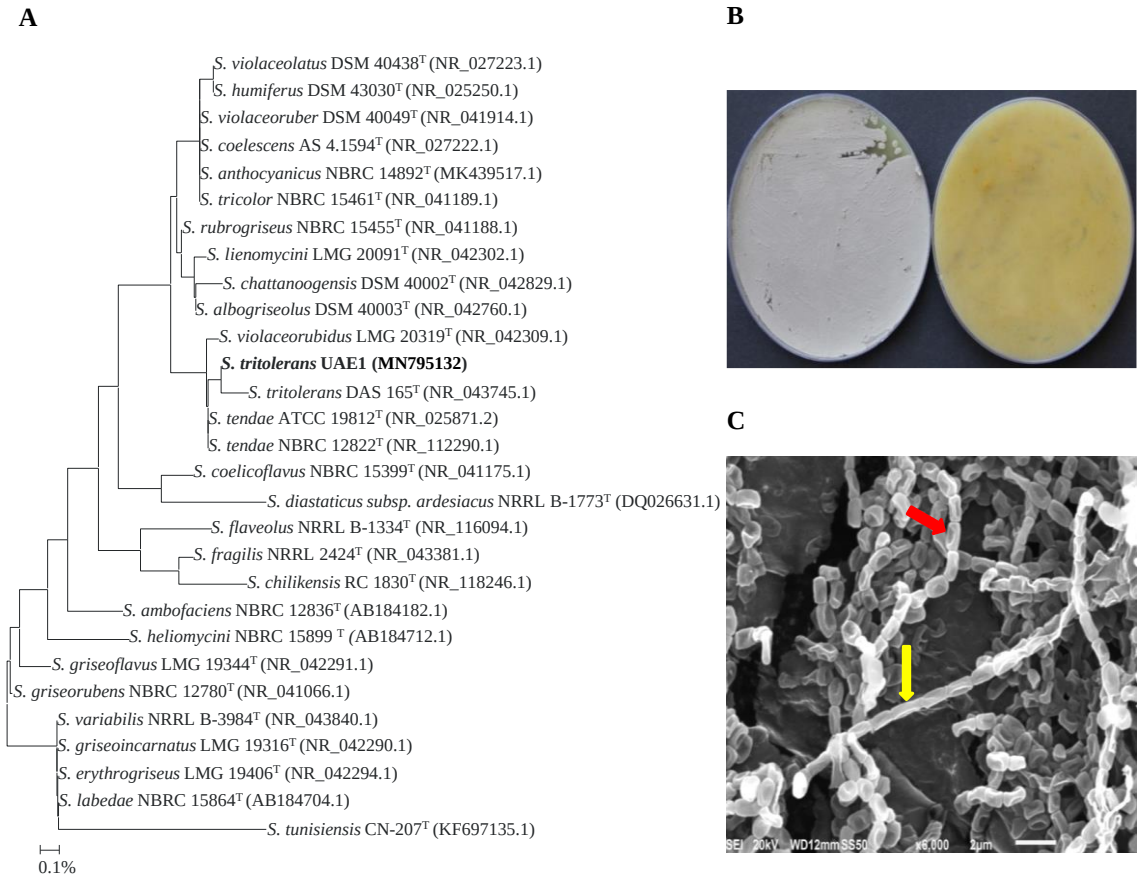

Figure 3.3: Taxonomic determination of *Streptomyces tritolerans* UAE1. (A) The tree showing the phylogenetic relationships between the polyamine-producing *S. tritolerans* UAE1 (isolate #7; MN795132; 1,516 bp) and other members of *Streptomyces* spp. on the basis of 16S rRNA sequences. (B) Aerial mycelia (left) and substrate mycelia (right) growing on ISP medium 3 supplemented with yeast extract, and (C) scanning electron micrograph (6,000X) showing closed straight to flexuous (rectus-flexibilis) chains of spores (red arrow) with smooth spore structure (yellow arrow) of the strain of *S. tritolerans* UAE1. In (A) numbers at nodes indicate percentage levels of bootstrap support based on a neighbor-joining analysis of 1000 resampled datasets. Bar, 0.001 substitutions per site. GenBank accession numbers are given in parentheses

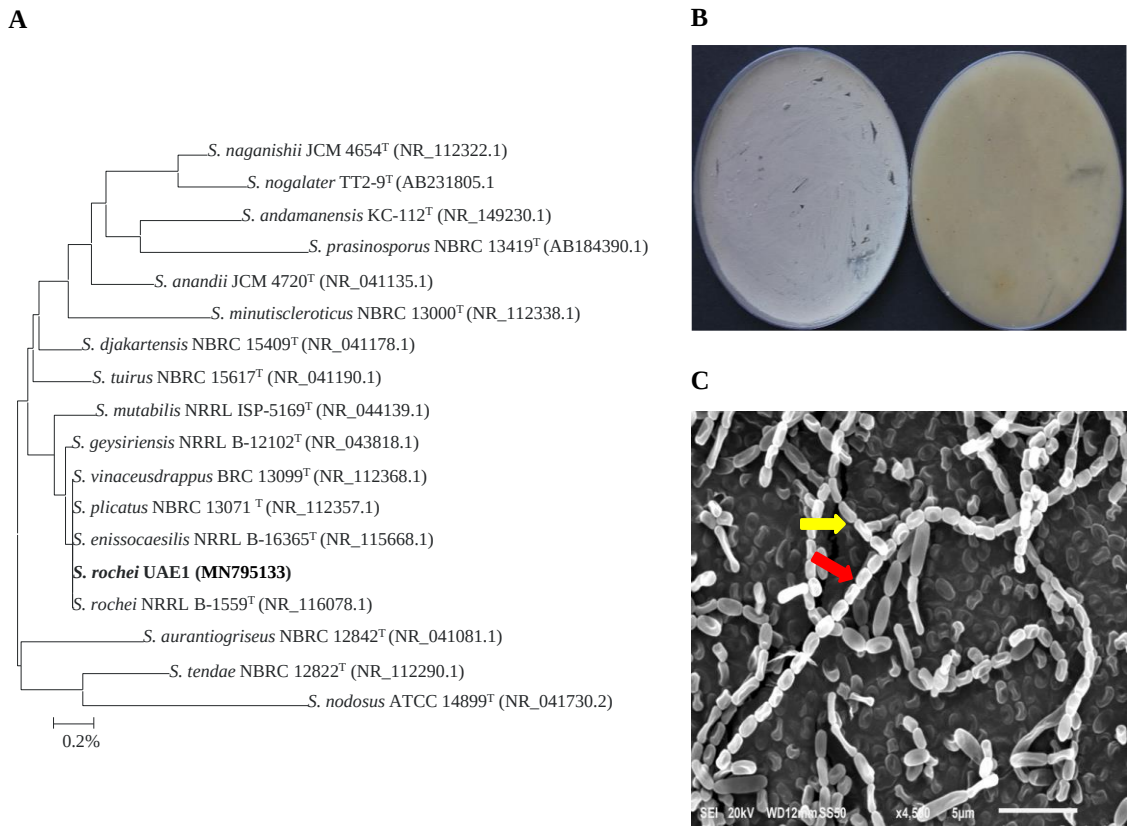

Figure 3.4: Identification of *Streptomyces rochei* UAE1 based on phylogenetic, cultural and morphological characteristics. (A) The tree showing the phylogenetic relationships between the 1-aminocyclopropane-1-carboxylic deaminase-producing *S. rochei* UAE1 (isolate #11; MN795133; 1,519 bp) and other members of *Streptomyces* spp. on the basis of 16S rRNA sequences. (B) Aerial mycelia (left) and substrate mycelia (right) growing on ISP medium 3 supplemented with yeast extract; and (C) scanning electron micrograph (6,000X) showing closed straight to flexuous (rectus-flexibilis) chains of spores (red arrow) with smooth spore structure (yellow arrow) of the strain of *S. rochei* UAE1. In (A) numbers at nodes indicate percentage levels of bootstrap support based on a neighbor-joining analysis of 1000 resampled datasets. Bar, 0.002 substitutions per site. GenBank accession numbers are given in parentheses

3.3.6 Assessment of PGP Activities by the Auxin-, PA-, and ACCD-Producing Isolates

The production of the PGRs, ACCD and siderophores, and P-solubilization abilities varied among *S. chartreusis, S. tritolerans, and S. rochei* (Table 3.3). Only the auxin-producing isolate *S. chartreusis* produced high levels of IAA and IPYA (44.35 and 9.11 μg mL^{-1}, respectively), but did not produce Put, Spd, Spm, or ACCD. Conversely, the PA-producing isolate *S. tritolerans* (#7) only produced high levels of Put, Spd, Spm (Tables 3.1, 3.3), but did not produce detectable levels of IAA, IPYA or ACCD (Tables 3.1, 3.3). Unlike the other two strains, the ACCD producing isolate *S. rochei* (#11) produced only ACCD without the production of detectable levels of IAA, IPYA, Put, Spd, or Spm (Tables 3.1, 3.3). I did not notice detectable levels of gibberellic acid in the culture extracts of any of the three isolates (Table 3.3). There was a variation in the production of cytokinins by the three isolates. Isolates #7 and #11 produced 1.12 and 1.32 μg mL^{-1} of iPa, respectively, and isolates #21 and #11 produced 0.95 and 1.52 μg mL^{-1} of iPA, respectively. The two isolates #21 and #7 produced 1.45 and 1.05 μg mL−1 of Z, respectively (Table 3.3).

The three tested isolates neither fixed N nor produced ammonia. Only two of the isolates (#7 and #21) were able to solubilize P and only one isolate (#21) was able to produce siderophores (Table 3.3 and Supplementary Figure S2). Interestingly, the growth of *S. chartreusis, S. tritolerans, and S. rochei* did not appear to be affected by the presence of each other; there was no evidence of inhibitory effects of the volatile metabolites on the isolates' growth. In addition, the sprayed target isolates were not inhibited by the spot-

inoculated isolate, indicating no observed inhibitory effect of the diffusible metabolites on the growth of the target isolates.

Table 3.3: In vitro production of plant growth regulators, 1-Aminocyclopropane-1-Carboxylic Acid Deaminase (ACCD), siderophores, nitrogenase enzyme, ammonia, and the Phosphorus (P) solubilization ability by *Streptomyces chartreusis*, *S. tritolerans* and *S. rochei* isolated from the rhizosphere of *Salicornia bigelovii*

Activity	***S. chartreusis* (#21)**	***S. tritolerans* (#7)**	***S. rochei* (#11)**
IAA	+	-	-
IPYA	+	-	-
Put	-	+	-
Spd	-	+	-
Spm	-	+	-
GA_3	-	-	-
iPa	-	+	+
iPA	+	-	+
Z	+	+	-
ACCD	-	-	+
Siderophores	+	-	-
Nitrogenase	-	-	-
Ammonia	-	-	-
P-solubilization	+	+	-
Tolerance to NaCl (8%)	++	++	++

Data are from eight independent replicates.

IAA, indole-3-acetic acid; IPYA, indole-3-pyruvic acid; Put, putrescine; Spd, spermidine; Spm, spermine; GA_3, gibberellic acid; iPa, isopentenyl adenine; iPA, isopentenyl adenoside; Z, Zeatin. + = producing; - = not producing detectable levels; ++, highly tolerant to NaCl (8%).

3.3.7 Assessment of Growth Promotion of *S. bigelovii* Under Greenhouse Conditions

In order to determine the effect of the three actinobacterial isolates as producers for specific PGP, we treated *S. bigelovii* with each isolate individually and in combinations (i.e., as a synergistic consortium). In general, the application of *S. chartreusis* (*Sc*), *S. tritolerans* (*St*), and *S. rochei* (*Sr*) either singly or in combination (*Sc/St/Sr*) significantly ($P< 0.05$) promoted growth of *S. bigelovii* compared to the control treatment after 12 wps of sowing *S. bigelovii* seeds (Figure 3.5a).

Compared to the non-inoculated control plants, *Sc* treatment increased shoot and root dry biomass by 32.3 and 42.3%, respectively (Figure 3.5b). When seawater-irrigated plants were treated with either *St* or *Sr*, there was a significant ($P< 0.05$) increase in the dry biomass of shoots (46.9% in *St* and 56.5% in *Sr*) and roots (62.4% in *St* and 71.9% in *Sr*) compared to the control treatment. Similar observations were found in shoot and root tissues when we measured their lengths. When we treated *S. bigelovii* seedlings with *Sc, St* or *Sr*, we found that the length of both shoots and roots increased significantly ($P< 0.05$) compared to control (Figure 3.5c). Thus, *Sc/St/Sr* revealed the greatest growth.

This was confirmed by the significant increases in the dry weights of shoots and roots by 62.2 and 77.9%, respectively (Figure 3.5b), and the length of shoots and root by 56.0 and 56.8%, respectively (Figure 3.5c) compared to non-inoculated control plants. Treatments of *S. bigelovii* with the three individual isolates (*Sc*, *St*, or *Sr*) or with the combined approach (*Sc/St/Sr*) had significantly ($P< 0.05$) increased levels of chl a, chl b and carotenoids as compared with control plants (Figure 3.5d). The combined effect of the three isolates (*Sc/St/Sr*) resulted in more production of photosynthetic pigments

compared the application of each isolate individually. Similarly, *S. bigelovii* yielded more seeds of 46.1% in *Sc*, 60.0% in *St* and 69.1% in *Sr* than that in the control plants watered with seawater at the harvest time (Figure 3.5e). Such increase in seed yield reached to 79.7% in the consortium treatment of *Sc/St/Sr* when compared to the control plants. In individual treatments, growth enhancement reflected as a set of morpho-physiological parameters (dry biomass, photosynthetic pigments, and seed yield), was most pronounced with the ACCD-producing *S. rochei* (Figure 3.5). This was followed by the PA-producing *S. tritolerans* and lastly by the auxin-producing isolate *S. chartreusis* compared to non-inoculated control plants. Interestingly, the consortium had the superiority in growth promotion effect in comparison with any other individual applications. This suggests that the consortium of actinobacterial isolates stimulated growth of *S. bigelovii*, most probably, due to the synergistic interactions between these isolates via multiple mechanisms.

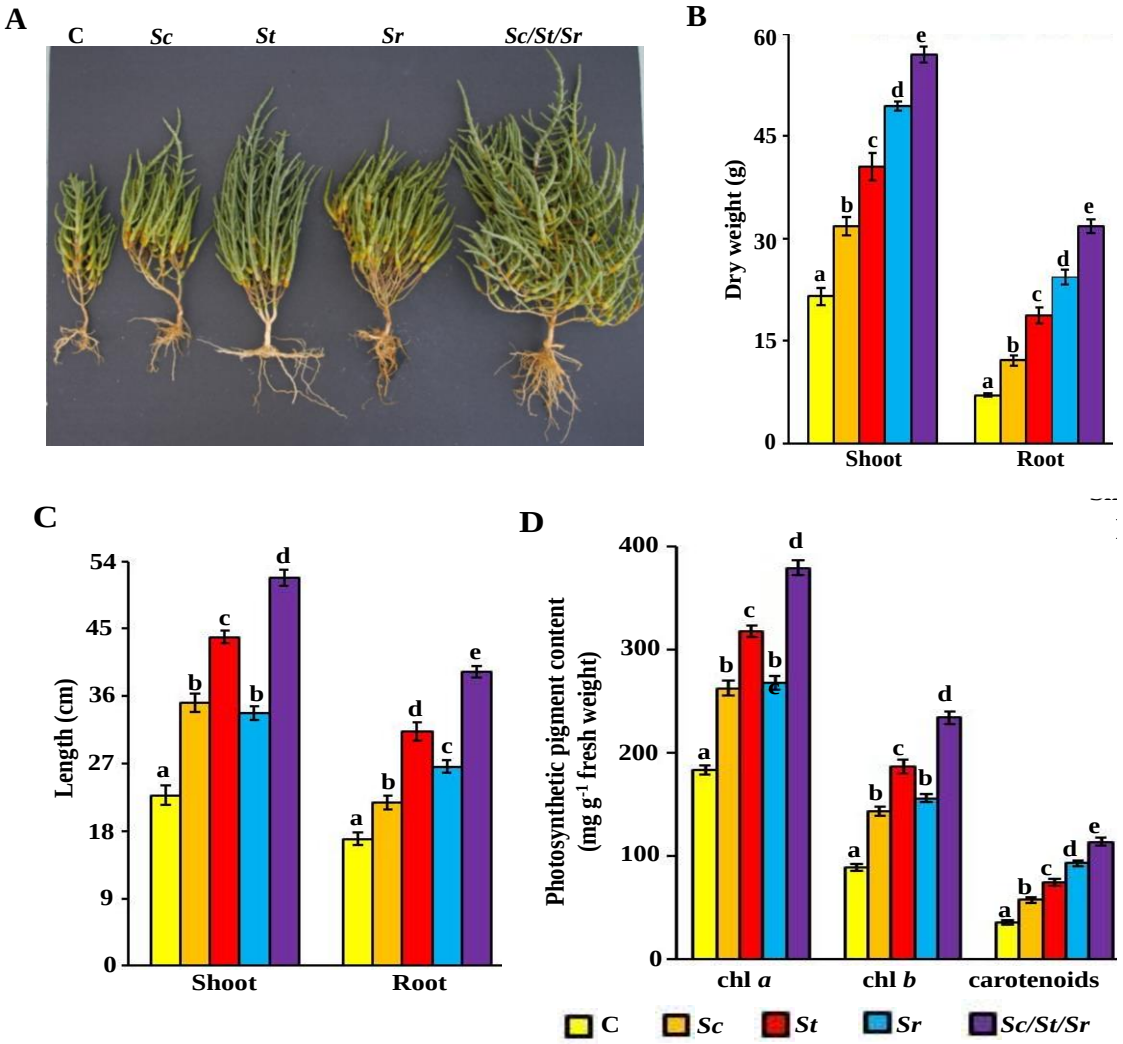

Figure 3.5: Effect of the individual and/or consortium of the rhizosphere-competent actinobacteria on growth and production of *Salicornia bigelovii*. Effect of soil and seed inoculation with the rhizosphere-competent auxin-, polyamine- and 1-aminocyclopropane-1-carboxylic deaminase-producing isolates on (A) formation, (B) dry weight and (C) length of shoot and root tissues; (D) photosynthetic pigment contents of chl a, chl b and carotenoids; and (E) dry weight of seeds, of *S. bigelovii*. In (A-D), the figure and measurements of dry weight and length of shoot and root tissues, and photosynthetic pigments were measured at 12 weeks after sowing the seeds; whereas dry weight of seeds was measured at 20 weeks after sowing. Values are means of 16 replicates ± SE for each sampling from two independent experiments. Mean values followed by different letters are significantly ($P < 0.05$) different from each other according to Fisher's Protected LSD Test. C, control (autoclaved non-inoculated oat bran); Sc, auxin-producing isolate #21 (*S. chartreusis* UAE1); St, polyamine-producing isolate #7 (*S. tritolerans* UAE1); Sr, ACCD-producing isolate #11 (*S. rochei* UAE1); Sc/St/Sr, consortium of the three rhizosphere-competent isolates. ACCD, 1-aminocyclopropane-1-carboxylic deaminase; chl, chlorophyll

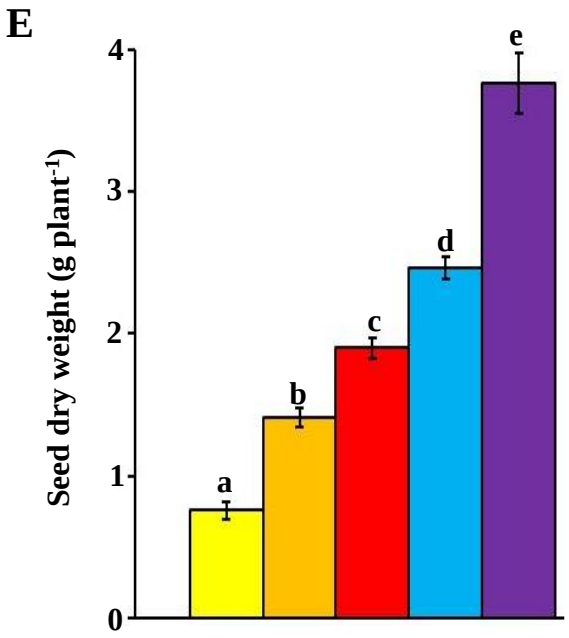

Figure 3.5: Effect of the individual and/or consortium of the rhizosphere-competent actinobacteria on growth and production of *Salicornia bigelovii*. Effect of soil and seed inoculation with the rhizosphere-competent auxin-, polyamine- and 1-aminocyclopropane-1-carboxylic deaminase-producing isolates on (A) formation, (B) dry weight and (C) length of shoot and root tissues; (D) photosynthetic pigment contents of chl a, chl b and carotenoids; and (E) dry weight of seeds, of *S. bigelovii*. In (A-D), the figure and measurements of dry weight and length of shoot and root tissues, and photosynthetic pigments were measured at 12 weeks after sowing the seeds; whereas dry weight of seeds was measured at 20 weeks after sowing. Values are means of 16 replicates ± SE for each sampling from two independent experiments. Mean values followed by different letters are significantly ($P< 0.05$) different from each other according to Fisher's Protected LSD Test. C, control (autoclaved non-inoculated oat bran); Sc, auxin-producing isolate #21 *(S. chartreusis* UAE1); St, polyamine-producing isolate #7 (*S. tritolerans* UAE1); Sr, ACCD-producing isolate #11 (*S. rochei* UAE1); Sc/St/Sr, consortium of the three rhizosphere-competent isolates. ACCD, 1-aminocyclopropane-1-carboxylic deaminase; chl, chlorophyll (Continued)

3.3.8 Determination of the Levels of Auxins, PA, and ACC in Planta

To study possible mechanisms leading to the growth enhancement of *S. bigelovii* after individual or combined treatments of isolates, we analysed the endogenous levels of

particular PGRs in shoot and root tissues of *S. bigelovii.* The application of *Sc* or *Sc/St/Sr* significantly ($P< 0.05$) increased the levels of IAA and IPYA in the tissues of *S. bigelovii* compared to control plants (Figures 3.6a, b).

Plants treated with either the *St* or the mixture of isolates significantly ($P< 0.05$) increased the levels of endogenous Put, Spd and Spm than any other treatment including the control in both roots and shoot tissues Figures 3.6c–e. Similarly, *S. bigelovii* treated with *Sr* or *Sc/St/Sr* significantly ($P< 0.05$) reduced the levels of ACC in the plant tissues compared to the control treatment Figure 3.6F. Application with the PA-producing isolate *S. tritolerans* (*St*) or the ACCD-producing *S. rochei* (*Sr*) significantly ($P< 0.05$) increased levels of endogenous auxins of *S. bigelovii* compared to control Figures 3.6A, B. Both *S. tritolerans* and *S. rochei* were, however, found to be non-auxin-producing isolates. This suggests that the production of PA and ACCD by these isolates may indirectly increase the auxins levels in planta.

In general, the overall endogenous levels of auxins and PA measured in both tissues of *S. bigelovii* were found to be high, but low levels of ACC in *Sc/St/Sr* treatment were detected compared with other treatments Figure 3.6. This suggests that the synergistic consortium of isolates positively regulated the activities of the endogenous hormone auxin and the PA with a concomitant decline in the level of ACC in planta more than those in the individual treatments. This ultimately could lead to better growth and performance of *S. bigelovii*. To lesser extent, the effects were also observed by the individual application of *Sc, St or Sr*.

3.3.9 Assessment of Plant Growth Promotion Using Multivariate Analysis

The PCA was performed to identify the Principal Components (PCs) to identify the most important morpho-physiological parameters that are responsible about the variation of both shoot and root growth and seed yield of *S. bigelovii* that best describe the growth promotion to the actinobacterial isolates individually or in combination. The first two PCs accounted for 60.8 and 17% of the total variation in shoots (77.8%; Figure 3.7a) and 56 and 20.5% of the total variation in roots (76.5%; Figure 3.7b).

Plants received the five different treatments were segregated into clear five clusters; plants that were not treated with any actinobacterial isolate (control) were on side, but plants inoculated with the combination of the three actinobacterial isolates (*Sc/St/Sr*) on the other side that had higher agronomic growth parameters associated positively with all PGRs in plant tissues. Plants treated with the auxin-producing *S. chartreusis* are located next to control plants followed by plants treated with ACCD-producing *S. rochei*.

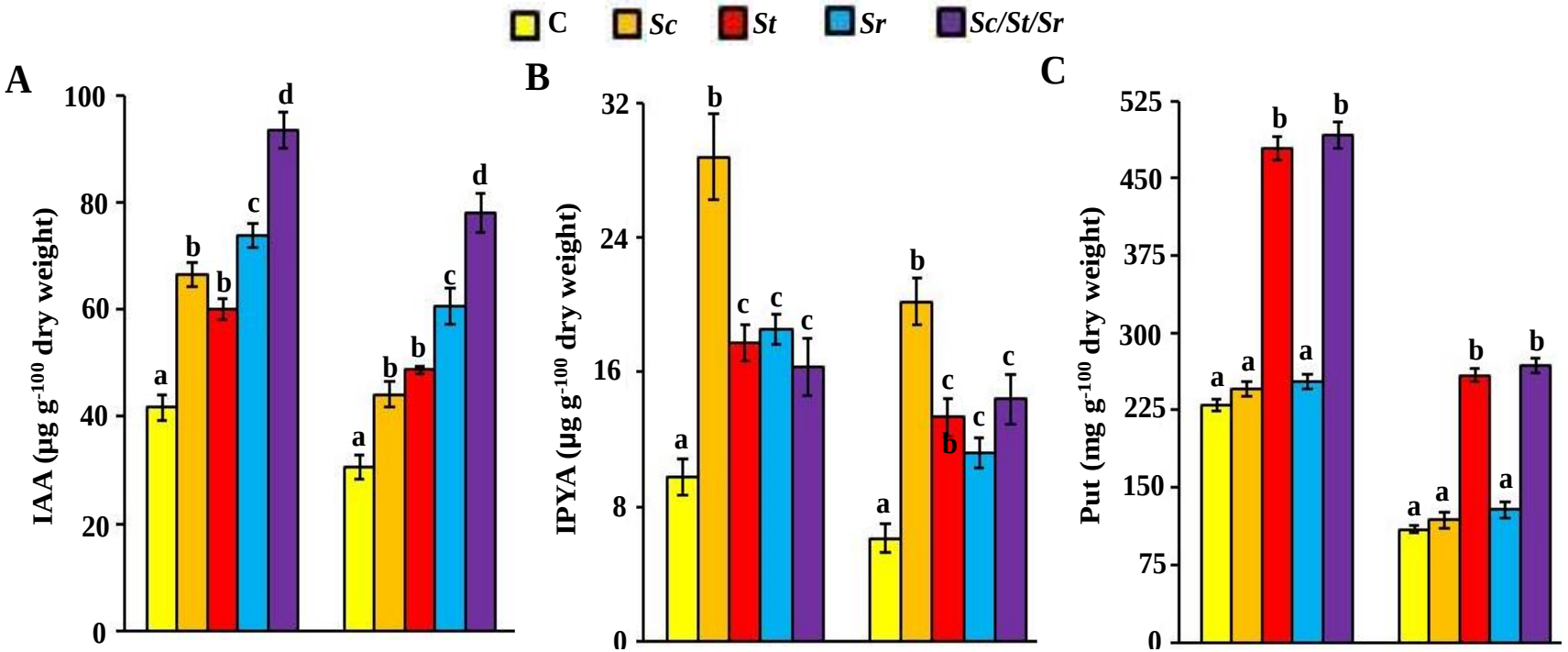

Figure 3.6: Effect of the individual and/or consortium of the rhizosphere-competent actinobacteria on endogenous auxins, polyamines and ACC content of *Salicornia bigelovii*. Endogenous contents of (A) IAA; (B) IPYA; (C) putrescine; (D) spermidine; (E) spermine and (F) ACC in *S. bigelovii* shoot and root tissues after soil and seed inoculation with autoclaved non-inoculated oat bran (control); Sc, auxin-producing isolate #21 (*S. chartreusis* UAE1); St, polyamine-producing isolate #7(*S. tritolerans* UAE1); Sr, ACCD-producing isolate #11 (*S. rochei* UAE1); Sc/St/Sr, consortium of the three rhizosphere-competent isolates. *S. bigelovii* seedlings were grown in an evaporative-cooled greenhouse and maintained at 25 ± 2°C. Values are means of 8 replicates ± SE for each sampling from two independent experiments. Mean values followed by different letters are significantly (P< 0.05) different from each other according to Fisher's Protected LSD Test. Endogenous contents of IAA, IPYA, putrescine, spermidine, spermine, and ACC were measured at 12 weeks after sowing the seeds of *S. bigelovii*. IAA, indole-3-acetic acid; IPYA, indole-3-pyruvic acid; ACCD, 1-aminocyclopropane-1-carboxylic deaminase

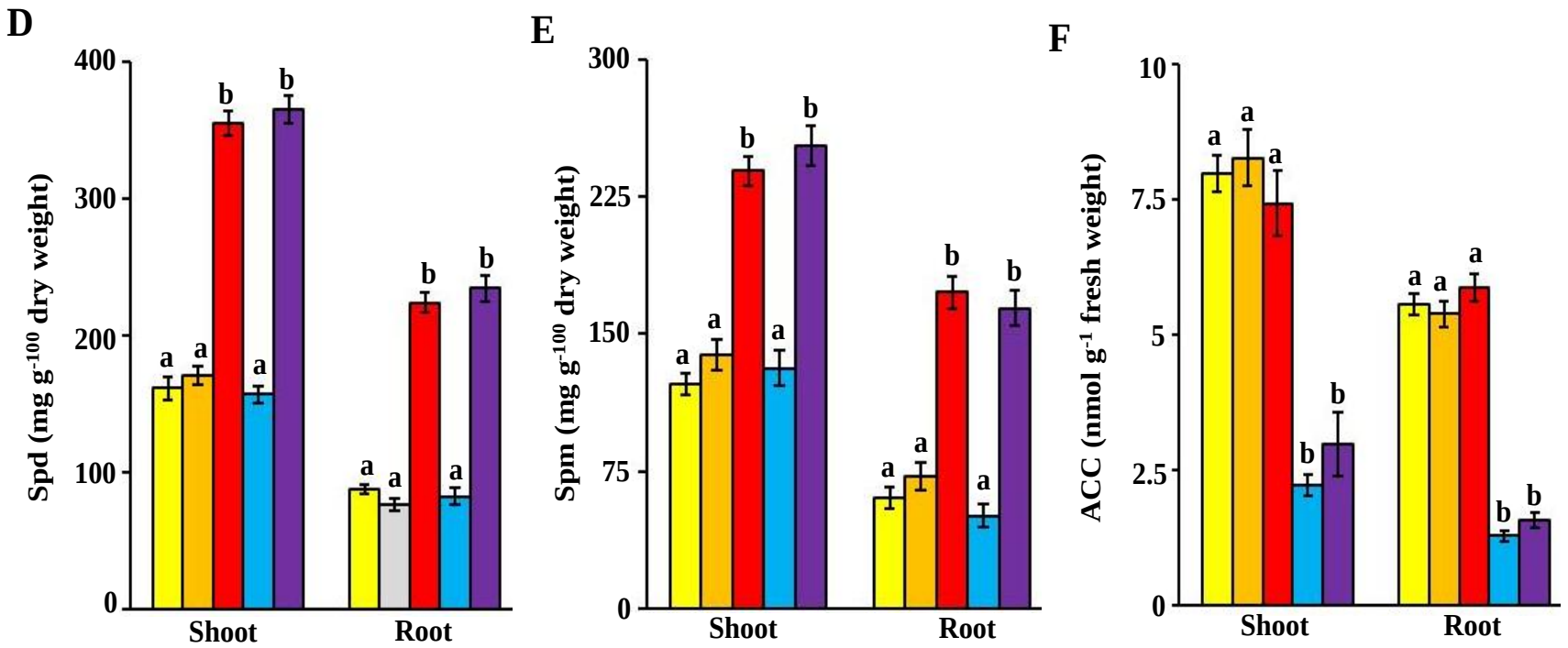

Figure 3.6: Effect of the individual and/or consortium of the rhizosphere-competent actinobacteria on endogenous auxins, polyamines and ACC content of *Salicornia bigelovii*. Endogenous contents of (A) IAA; (B) IPYA; (C) putrescine; (D) spermidine; (E) spermine and (F) ACC in *S. bigelovii* shoot and root tissues after soil and seed inoculation with autoclaved non-inoculated oat bran (control); Sc, auxin-producing isolate #21 (*S. chartreusis* UAE1); St, polyamine-producing isolate #7(*S. tritolerans* UAE1); Sr, ACCD-producing isolate #11 (*S. rochei* UAE1); Sc/St/Sr, consortium of the three rhizosphere-competent isolates. *S. bigelovii* seedlings were grown in an evaporative-cooled greenhouse and maintained at 25 ± 2°C. Values are means of 8 replicates ± SE for each sampling from two independent experiments. Mean values followed by different letters are significantly ($P < 0.05$) different from each other according to Fisher's Protected LSD Test. Endogenous contents of IAA, IPYA, putrescine, spermidine, spermine, and ACC were measured at 12 weeks after sowing the seeds of *S. bigelovii*. IAA, indole-3-acetic acid; IPYA, indole-3-pyruvic acid; ACCD, 1-aminocyclopropane-1-carboxylic deaminase (Continued)

The relatively slower growth and seed yield of *Sc* and *Sr* treated plants, as compared to those treated with *St* and *Sc/St/Sr* were not associated with insignificant productions of Put, Spd, Spm and ACC. In fact, ACC was negatively associated in roots of plants treated with *Sc* and both roots and shoots of plants treated with *Sr*. The Screen plots representing the eigenvalue of variance explained by each PC in shoot and root were also shown (Supplementary Figure S3). The effects of auxins, PA and/or ACCD produced by individual or combined isolates were also evaluated on plant growth parameters in shoot and root tissues. On the biplots, *Sc, St,* and *Sr* were closely located to auxins, PA, and ACCD, respectively (Figure 3.7). The consortium of isolates, on the other hand, was closely related to all growth parameters and PGRs. In general, the accumulation of growth parameters was positively correlated upon individual or mixed inoculations of isolates but was negatively correlated with the endogenous ACC content of shoot and root. This suggests that each strain of actinobacteria possessing different mechanisms can directly contribute to plant promotion; thus, the application of the consortium showing rhizosphere-competent abilities maximizes the growth and yield of *S. bigelovii*.

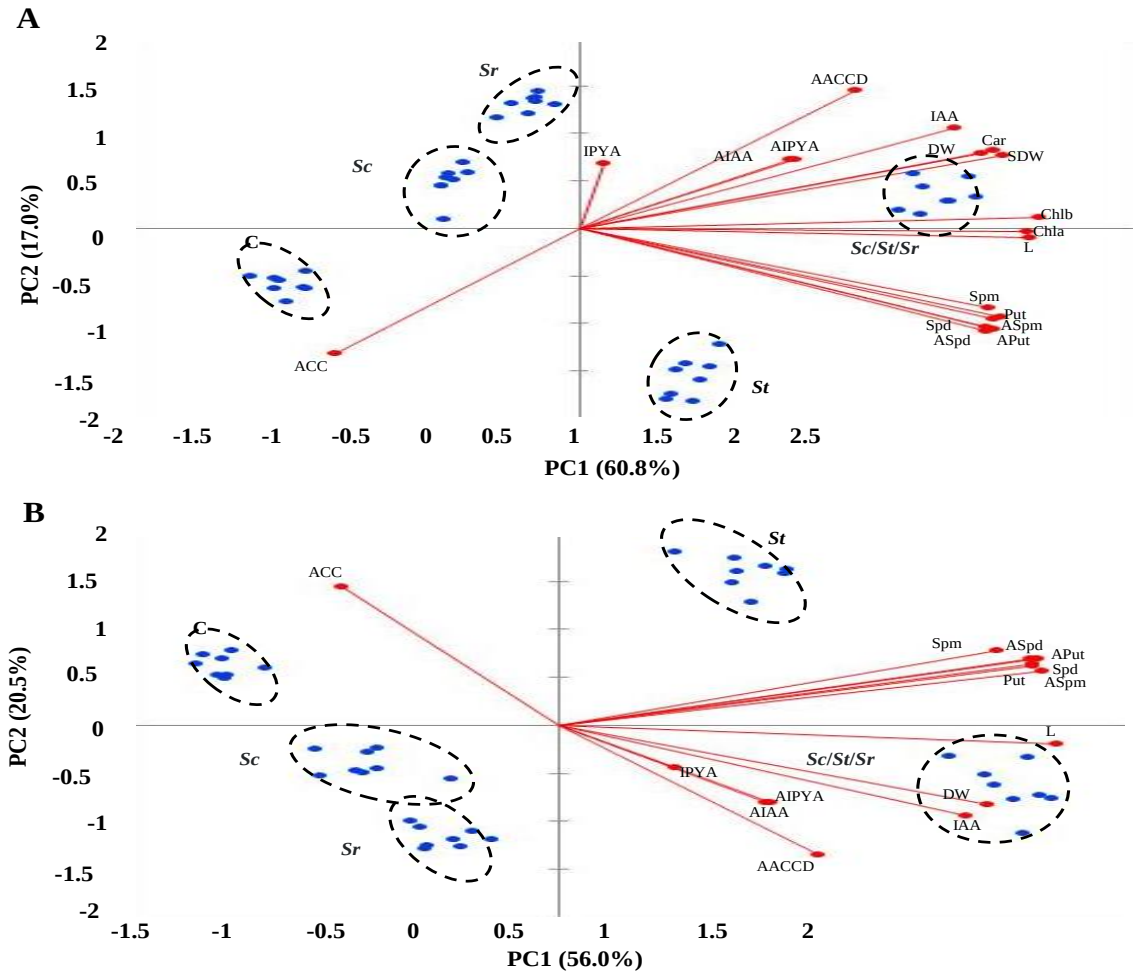

Figure 3.7: Multivariate statistical analyses of the endogenous PGRs of *Salicornia bigelovii* treated with actinobacterial isolates. Principal Component (PC) analysis on (A) shoot and (B) root tissues of *S. bigelovii* after treatment with autoclaved non-inoculated oat bran (control); auxin-producing isolate #21 (*S. chartreusis* UAE1, Sc); PA-producing isolate #7 (*S. tritolerans* RAK1, St); ACCD-producing isolate #11 (*S. rochei* RAMS1, Sr) consortium of the three rhizosphere-competent isolates (Sc/St/Sr). Two auxins (AIAA and AIPYA), three PA (Aput, ASpd and Aspm) and (AACCD) obtained from actinobacterial isolates, eight agronomic growth parameters (L and DW in shoot and root separately, chl a, chl b and Car in shoot, and SDW) and six plant growth regulators (IAA, IPYA, Put, Spd, Spm and ACC) obtained from *S. bigelovii*, were tested. *S. bigelovii* seedlings were grown in an evaporative-cooled greenhouse and maintained at 25±2°C. Values are means of eight replicates for each sampling from two independent experiments. IAA, indole-3-acetic acid; IPYA, indole-3-pyruvic acid; Put, putrescine; Spd, spermidine, Spm, spermine; ACC, 1-aminocyclopropane-1-carboxylic; PA, polyamines; ACCD, ACC deaminase; L, length; DW, dry weight; Chl, chlorophyll; Car, carotenoids; SDW, seed dry weight

The association across the morphophysiological and biochemical characteristics of *S. bigelovii* and the PGP produced by each isolate were also studied. The correlation coefficients (r-values) analysis showed that the auxin-producing *S. chartreusis* had significant ($P< 0.05$) correlation with all agronomic growth parameters, IAA and IPYA; but insignificant ($P> 0.05$) with the endogenous PA and ACC in both plant organs (Supplementary Tables S4, S5). Thus, 45 and 28 insignificant ($P> 0.05$) correlations with *Sc* in shoot and root, respectively. There were 14 and 10 insignificant ($P> 0.05$) correlations in shoots and roots of *S. bigelovii* inoculated with the PA-producing *S. tritolerans*, respectively (Supplementary Tables S6, S7); and 24 and 23 insignificant correlations in the same tissues with the ACCD-producing *S. rochei* treatment (Supplementary Tables S8, S9). Neither *Sc* nor *St* significantly correlated with ACC. *Sr* negatively correlated with ACC in planta.

It is noteworthy to mention that most endogenous PA in shoot and root tissues were insignificant ($P> 0.05$) in *S. bigelovii* tissues after *Sr* treatment. This was confirmed when the three isolates were combined to determine the correlation coefficients between plant growth attributes in shoots and roots of *S. bigelovii* and endogenous growth regulation compounds. The synergistic consortium significantly ($P< 0.01$) correlated with almost all agronomic growth parameters and PGRs in plant tissues; and thus, the insignificance was not observed between growth regulation parameters in root (Supplementary Tables S10, S11). This indicates that the promoting effects of the ACCD, three PA followed by the auxins detected in *S. rochei, S. tritolerans,* and *S. chartreusis*, respectively, were effective in enhancing different levels of growth regulating compounds.

Thus, the relative superiority in performance of the consortium can be attributed to the multiple modes of action that are known to enhance growth and relieve plants from environmental stresses.

3.4 Discussion

In the UAE, the production of aviation biofuel can be derived from halophytic plants such as *Salicornia spp*. that can successfully grow in salt marshes. However, the growth and seed yield of plants, even halophytes, under salt conditions are very low. It is known that PGPR can improve plant growth by enhancing nutrient recycling and producing PGRs; thus, minimizing the application of chemical fertilization (Hassan et al., 2019). Therefore, PGPR can play an essential role in the sustainable agriculture industry. Specifically, actinobacteria can be more suitable for dry, arid soils and extreme hot environments (Chaurasia et al., 2018) such as those in the UAE (Saeed et al., 2017; Kamil et al., 2018).

A recent study has compared growth promotion of *S. bigelovii* between rhizosphere competent versus rhizosphere-non-competent actinobacterial strains after irrigation with seawater (El-Tarabily et al., 2020). Although both isolates produced high levels of PA, PGP has been more remarkable in the presence of the rhizosphere-competent, *Streptomyces euryhalinus* than the rhizosphere-non-competent, *Actinoplanes deccanensis*. The outcomes imply the importance of rhizosphere competency as a criterion for PGPR selection. Herein, I hypothesized that activated carbon coated inoculation with a “consortium” of rhizosphere-competent actinobacteria possessing different PGP

activities can consequently improve the growth characteristics of *S. bigelovii* irrigated with seawater.

In this report, the performance of the three halotolerant marine rhizosphere-competent PGP actinobacterial isolates were assessed on seawater-irrigated *S. bigelovii* seedlings. *S. chartreusis* UAE1 (#21), *S. tritolerans* RAK1 (#7), and *S. rochei* RAMS1 (#11) that were isolated from *S. bigelovii* rhizosphere stimulated the growth of seedlings of this halophytic cash crop under greenhouse conditions. Moreover, the application of the mixture treatment consisting of the three isolates was more effective in promoting growth of *S. bigelovii*, indicating synergistic effects rather than individual effects. By using single actinobacterial strains, growth promotion-reflected growth characteristics in tissues of *S. bigelovii*- was most pronounced with *S. rochei* that produced high levels of ACCD. Although seawater-irrigated *S. bigelovii* showed increased length in shoots and roots when treated with the auxin-producing isolate *S. chartreusis*, seedlings treated with the PA-producing isolate *S. tritolerans* produced more biomass and seed yield than those treated with *S. chartreusis*.

Thus, the relative superiority in performance of the ACCD-producing isolate *S. rochei* and the PA-producing isolate *S. tritolerans* over the auxin-producing isolate *S. chartreusis* might be attributed to their abilities to produce ACCD and PA, respectively, which have been known to relieve plants from environmental stresses (Glick et al., 2007; Ghosh et al., 2018). Contributions of these components in growth enhancement are significant for the ability of PGPR to increase plant tolerance to salinity and facilitate plant growth. Although *S. chartreusis* was effective to a lesser extent than *S. tritolerans* or *S. rochei*, this auxin-producing isolate was still able to significantly improve seedling

growth compared with the control treatment. This study highlights, for the first time, the potential of using activated carbon coated mixture of marine rhizosphere-competent actinobacteria as biological inoculants to enhance growth and establishment of *Salicornia* in nutrient impoverished marine soils occurring in coastal environments. *Salicornia* thrive in environments that are N or P deficient.

Previous work on PGPR from *Salicornia* rhizosphere and their effects on *Salicornia* growth has dealt predominantly with N-fixing bacteria (Ozawa et al., 2007; Hrynkiewicz et al., 2019) or P-solubilizing bacteria (Bashan et al., 2000). Except of one study done by Jha et al. (2012), no reports have considered if PGPR capable of fixing-N or solubilizing-P can still promote *Salicornia* growth through the production of ACCD or other PGRs. The bacteria isolated from *Salicornia* roots which can fix N, and produce IAA and ACCD have only been tested on *Salicornia* seed germination and seedling performance under axenic conditions in petri dishes using various NaCl concentrations (Jha et al., 2012). Under gnotobiotic and greenhouse conditions, the endophytic ACCD-producing actinobacterium, *M. chalcea*, and the two PA-producing actinobacteria, *S. euryhalinus* and *A. deccanensis*, enhanced seedling growth when irrigated with full strength seawater (El-Tarabily et al., 2019, El-Tarabily et al., 2020).

In the current study, the three isolates were selected through a series of tests, which included screening for salinity tolerance, rhizosphere-competency under naturally competitive environment and PGP traits. It is well-known that effective PGP, PGPR strains must colonize the roots and the introduced inoculum must establish and grow in an ecological habitat that includes indigenous rhizosphere microbial community (Hassan et al., 2019; Rilling et al., 2019). In our study, the potential PGPR isolates were initially

selected based on their ability to *in vitro* colonize *S. bigelovii* roots; followed by a rhizosphere competence screening in the greenhouse under naturally competitive environment. Halophilic/halotolerant marine non-actinobacterial isolates colonizing *Salicornia* roots under *in vitro* conditions have previously been reported (Mapelli et al., 2013). Non-actinobacterial isolates from native sediments have also been tested for their abilities to colonize mangrove roots *in vitro* and under non-competitive environments (Bashan et al., 1998; Rojas et al., 2006).

On the other hand, the abilities of the halotolerant actinobacteria reported in the current study colonizing the rhizosphere of *Salicornia* and showing effective levels of rhizosphere-competency have rarely been screened under naturally competitive environments. Only one study exists in which rhizosphere-competent PA-producing isolates have been used to promote *S. bigelovii* growth under naturally competitive environment (El-Tarabily et al., 2020). Additional emphasis on rhizosphere-competency was deliberately set to the niche around the root zone critical for the physiological activities of roots in the soil. It was not surprising that isolates producing PGRs and possessing high rhizosphere competency were effective in helping the host plant overcome root growth inhibition in the inhospitable environment. We argue that the success of the rhizosphere-competent PGP actinobacterial isolates was most likely attributed to their abilities to produce relatively high levels of PGRs and/or the activity of ACCD. In order to be considered as an effective root-colonizing isolate, PGPR should have the ability to colonize the entire root system (Hassan et al., 2019; Rilling et al., 2019).

There were 10 isolates that exhibited 100% of root colonization in the preliminary plate assay. Under naturally competitive saline conditions, many isolates were strongly

deliberated as rhizosphere-competent; despite others showed no or inadequate levels of competency (Table 3.2). This confirms the importance of testing the isolates in competitive environment. I noticed that all isolates recovered from the rhizosphere on the whole root with different levels of frequency; thus, the PD were highly detected in the top 8 cm of the root system. Notably, *S. chartreusis, S. tritolerans*, and *S. rochei* reached as deep as to 12 cm colonizing *S. bigelovii* root system. This indicates that these isolates were favored to be excellent rhizosphere-competent and prominently suitable for seed and soil inoculations.

The three-outstanding rhizosphere-competent isolates were chosen based on their exceptional abilities to produce auxins, PA and ACCD *in vitro*. Thus, these isolates were neither N-fixers nor ammonia-producers. In addition, they did not produce any detectable levels of GA3. Several marine bacteria have been reported to produce auxins (Jha et al., 2012; Mapelli et al., 2013), cytokinines (Maruyama et al., 1986), PA (Suzuki et al., 1990), GA3, or ACCD (Sgroy et al., 2009; Mapelli et al., 2013). Some actinobacteria from the coast of the Arabian Gulf have also been reported to produce PGRs in chemically-defined medium (El-Tarabily et al., 2019, El-Tarabily et al., 2020).

In the greenhouse trials, inoculations with the auxin producing *S. chartreus* are resulted in a significant increase in the levels of endogenous IAA and IPYA in *S. bigelovii* (Figure 3.6). Consistent with that, Fallik et al. (1989) have reported increases in the level of auxins in corn following the application of IAA-producing rhizosphere bacteria. *S. tritolerans* produced considerable amount of the three PA (Put, Spd, and Spm) also stimulated growth of *S. bigelovii*. This was evident when there were significant increases in endogenous PA in the tissues of *S. bigelovii* inoculated with *S. tritolerans* in comparison

to plants without inoculation. Similarly, the non-marine PA producing *Streptomyces griseoluteus* enhanced the growth of bean plants under greenhouse conditions by increasing the endogenous levels of PA (Nassar et al., 2003). Some studies have reported that marine and non-marine bacterial isolates produce PA only (Cassán et al., 2009; Zhou et al., 2016). The third isolate, *S. rochei* with elevated ACCD activity caused significant reduction in the levels of endogenous ACC in roots and shoots; most likely through the cleavage of ACC (the ET precursor) to NH_3 and α-ketobutyrate (Handa et al., 2011).

The growth enhancement in *S. bigelovii* treated with *S. rochei* is supported by other observations of ACCD-producing (actino) bacteria that have also shown to promote plant growth by lowering ET levels (Glick et al., 2007; El-Tarabily, 2008; El-Tarabily et al., 2019). It is known that ET is a major player in plant responses to biotic and abiotic stresses (Mengiste et al., 2009; Sham et al., 2019). As a result, preventing the synthesis of the stress hormone ET to levels inhibitory for the root growth by *S. rochei* could help plant to grow normally as described by Glick et al. (2007). Thus, the activity of ACCD alone was insufficient to reach to the degrees of growth enhancement achieved in the presence of the three isolates together. Previous studies have reported the advantages of the use of mixed versus individual cultures of PGPR for better growth in mangrove (Bashan et al., 2004).

In *Salicornia spp.,* growth promotion and salinity tolerance in the combined treatment were more obvious than in the individual treatment of the rhizosphere or the endophytic bacterial strains (Komaresofla et al., 2019). Consistent with that, the application of the actinobacterial consortium increased seed production by 79.7% compared to the control treatment. Mangrove seedlings treated with mixed cultures of *Phyllobacterium* sp. and *Bacillus licheniformis* developed more leaves than by the

individual cultures of bacteria (Rojas et al., 2006). The actinobacterial isolates in our study mostly achieved the growth promotion through their ability to solely produce auxins, PA, ACCD and may be certain growth promoting factors other than those assayed on and/or adjacent to the root system. It may also be of interest for future work to study combinations of other isolates belonging to different rhizosphere competency to determine the ranking of importance of various growth factors evaluated.

This is the first study to report *S. chartreusis, S. tritolerans, and S. rochei* being isolated from Salicornia rhizosphere. The PCA and correlation analysis demonstrated the reproducibility of the measurements performed and allowed us to identify possible traits related to treatments of individual or combined inoculation on *S. bigelovii*. I believe this study was successful in obtaining suitable bio-inoculants of *S. bigelovii* seedlings in the UAE or elsewhere.

The current study draws the public attention to the feasibility of using halotolerant actinobacteria to promote growth of *S. bigelovii* cultivated in the greenhouse, particularly as a consortium that can potentially be applied in marine farming agricultural systems (Mathew et al., 2020). Thus, this is expected to increase the largescale production of *Salicornia* seeds under the recently termed integrated Seawater Energy and Agriculture System (iSEAS) 2 in order to promote the supply of sustainable aviation biofuels.

Chapter 4: Conclusion

The flow of this work includes evaluation of Activated Carbon (AC) in both biomedical and environmental applications. The first part of the current thesis demonstrates utilization of physical activation produced phytomaterials based activated carbon as adsorbent for bilirubin adsorption in artificial liver devices. Herein, utilization of activated carbon produced via physical activation method from different phytomaterials available in UAE such as date seeds, jojoba seeds and microalgae for bilirubin detoxification were used for its application in biomedical research domain.

The chemical structure and morphology of the activated carbons obtained from different phytomaterials demonstrated highly selective bilirubin adsorption comparable to the commercial collagen and matrigel as revealed from isotherm modelling analysis. I identified highly selective and effective capacity of bilirubin detoxification using date pits based activated carbon compared to other two phytomaterials based activated carbon due to its superior physio-chemical properties. In addition, date pits based activated carbon revealed preservation of liver cells integrity and cytocompatibility through *in vitro* cell culture studies.

The findings of this study conclude date-pit-based AC as a novel alternative biomaterial for removal of protein-bound toxins in bioartificial liver devices. Future investigation would include development of date pits based activated carbon through different activation methods such as chemical or physio-chemical methods, optimization of different activation parameters, its thorough characterization for applications in acute poisoning detoxification, as drug carriers, biosensors, and in tissue regeneration.

The second part of the current thesis reported the environmental applications of activated carbon as adsorbent for promotion of growth and seed production of halophilic plant, *Salicornia.* In this work, I have successfully isolated three outstanding rhizosphere-competent isolates from rhizospheric soils of halophytic plant, *Salicornia bigelovii* for evaluation of Plant Growth Promoting (PGP) capabilities as biological inoculants on seawater-irrigated *S. bigelovii* plants. The three rhizosphere-competent isolates, *Streptomyces chartreusis* (*Sc*), *S. tritolerans* (*St*) and *S. rochei* (*Sr*) capable of producing growth hormones were investigated individually and as consortium (*Sc/St/Sr*) to determine their effects on the performance of *S. bigelovii* growth in the greenhouse.

All the inoculants and plant seeds were coated with earlier established date pits based activated carbon and utilized as bioinoculant for further evaluation of growth promotion capabilities. Individual applications of strains on seawater-irrigated plants significantly enhanced shoot and root dry biomass by 32.3-56.5% and 42.3-71.9%, respectively, in comparison to non-inoculated plants (control). Additionally, plants individually treated with *Sc*, *St* and *Sr* resulted in 46.1%, 60.0% and 69.1% increase in seed yield, respectively compared to control plants.

Furthermore, the synergetic combination of activated carbon coated all three strains demonstrated significant effects on *S. bigelovii* biomass (62.2% and 77.9% increase in shoot and root dry biomass, respectively) and seed yield (79.7% increase), compared to the individual strains. The results from this work indicated role of activated carbon coated bioinoculants towards growth promotion and increasing yield of *S. bigelovii*. Therefore, these halotolerant actinobacterial strains coated with activated

carbon could potentially be exploited as biofertilizers in order to sustain crop production in arid coastal areas.

Taken together, the key findings of this work opened various avenues for applications of activated carbon in different environmental domains besides having their individual potentialities. Activated carbon may be employed for adsorption of inhibitory substances such as sucrose breakdown products or phenolic compounds which are released in cultures or present in the medium. The addition of 0.01% of activated carbon in the culture medium demonstrated significant increase in the root number per explant. Therefore, this provides a base for further evaluating the effect of addition of date pits based activated charcoal to the culture medium along with the optimized plant growth promoting rhizosphere-competent bacterial strains. Besides the action, optimized bacterial strains used in conjunction with date seed activated carbon produced by physical activation offers an all-green approach towards detoxification of contaminated soil, food materials and feed raw materials.

Overall, this work emphasizes the potential role of date pits based activated carbon in biomedical and environmental applications and open doors for applications in diverse domains such as healthcare sector and environmental issues.

References

Abdelaziz, D. H. A., Ali, S. A., & Mostafa, M. M. A. (2015). *Phoenix dactylifera* seeds ameliorate early diabetic complications in streptozotocin-induced diabetic rats. *Pharmaceutical Biology*, 53, 792-799. https://doi.org/10.3109/13880209.2014.942790.

Abideen, Z., Qasim, M., Rizvi, R. F., Gul, B., Ansari, R., & Khan, M. A. (2015). Oilseed halophytes: A potential source of biodiesel using saline degraded lands. *Biofuels*, 6, 241-248. https://doi.org/10.1080/17597269.2015.1090812.

Ahmad, J. S., & Baker, R. (1987). Rhizosphere competence of *Trichoderma harzianum*. *Phytopathology*, 77, 182-189. https://doi.org/10.1094/phyto-77-182.

Ahmad, T., Danish, M., Rafatullah, M., Ghazali, A., Sulaiman, O., Hashim, R., & Ibrahim, M. N. M. (2012). The use of date palm as a potential adsorbent for wastewater treatment: A review. *Environmental Science and Pollution Research*, 19, 1464-1484. https://doi.org/10.1007/s11356-011-0709-8.

Ahmed, M. J., & Dhedan, S. K. (2012). Equilibrium isotherms and kinetics modeling of methylene blue adsorption on agricultural wastes-based activated carbons. *Fluid Phase Equilibria*, 317, 9-14. https://doi.org/10.1016/j.fluid.2011.12.026.

Ahmed, M. J., & Theydan, S. K. (2012). Physical and chemical characteristics of activated carbon prepared by pyrolysis of chemically treated date stones and its ability to adsorb organics. *Powder Technology*, 229, 237-245. https://doi.org/10.1016/j.powtec.2012.06.043.

Al-Alawi, R., Al-Mashiqri, J. H., Al-Nadabi, J. S. M., Al-Shihi, B. I., & Baqi, Y. (2017). Date palm tree (*Phoenix dactylifera L.*): Natural products and therapeutic options. *Frontiers in Plant Science*, 8, 845. https://doi.org/10.3389/Fpls.2017.00845/Bibtex.

Al-Yamani, W., Kennedy, S., Sgouridis, S., & Yousef, L. F. (2013). A land suitability study for the sustainable cultivation of the halophyte *Salicornia bigelovii*: The case of Abu Dhabi, UAE. *Arid Land Research and Management*, 27, 349-360. https://doi.org/10.1080/15324982.2013.771230.

Alhamed, Y. A., & Bamufleh, H. S. (2009). Sulfur removal from model diesel fuel using granular activated carbon from dates' stones activated by ZnCl2. *Fuel*, 88, 87-94. https://doi.org/10.1016/j.fuel.2008.07.019.

Alharbi, K. L., Raman, J., & Shin, H. J. (2021). Date fruit and seed in nutricosmetics. *Cosmetics*, 8, 59. https://doi.org/10.3390/cosmetics8030059.

Almutary, A., & Sanderson, B. J. S. (2016). The MTT and crystal violet assays: potential confounders in nanoparticle toxicity testing. *International Journal of Toxicology*, 35, 454-462. https://doi.org/10.1177/1091581816648906.

Alqaragully, M. B. (2014). Removal of textile dyes (maxilon blue, and methyl orange) by date stones activated carbon. *International Journal of Advanced Research in Chemical Science*, 1, 48-59. Retrieved September 18, 2019, from https://www.arcjournals.org/pdfs/ijarcs/v1-i1/ijarcs-v1-i1-5.pdf.

Alyileili, S. R., Belal, I., Hussein, A. S., & El-Tarabily, K. A. (2020). Effect of Inclusion of Degraded and Non-Degraded Date Pits in Broilers' Diet on their Intestinal Microbiota and Growth Performance. *Animals*, 10, 2041. https://doi.org/10.3390/ani10112041.

Alyileili, S. R., El-Tarabily, K. A., Belal, I. E. H., Ibrahim, W. H., Sulaiman, M., & Hussein, A. S. (2020). Effect of *Trichoderma reesei* degraded date pits on antioxidant enzyme activities and biochemical responses of broiler chickens. *Frontiers in Veterinary Science*, 7, 1-10. https://doi.org/10.3389/fvets.2020.00338.

Ameh, P. O. (2013). Modelling of the adsorption of Cu (II) and Cd (II) from aqueous solution by Iraqi palm-date activated carbon (IPDAC). *International Journal of Modern Chemistry*, 5(3), 136-144. Retrieved October 19, 2019, from http://www.modernscientificpress.com/Journals/ViewArticle.aspx?H86Z5Noa2iKDNvH/0wRKWuhbGhOjZO3z0QwByeD8DEpLMpWIgMNdVCh2cXbLfPY.

Annesini, M. C., Piemonte, V., & Turchetti, L. (2010). Removal of albumin-bound toxins from albumin-containing solutions: Tryptophan fixed-bed adsorption on activated carbon. *Chemical Engineering Research and Design*, 88, 1018-1023. https://doi.org/10.1016/j.cherd.2010.01.022.

Annesini, M Cristina, Piemonte, V., & Turchetti, L. (2013). Simultaneous removal of albumin-bound toxins in liver support devices: bilirubin and tryptophan adsorption on activated carbon. *Chemical Engineering Transactions*, 32, 1069-1074. https://doi.org/10.3303/cet1332179.

Archana, Bastian, Yogesh, T., & Kumaraswamy, K. (2013). Various methods available for detection of apoptotic cells- A review. *Indian Journal of Cancer*, 50, 274. https://doi.org/10.4103/0019-509X.118720.

Arena, M. E., & Nadra, M. C. M. de. (2001). Biogenic amine production by *Lactobacillus. Journal of Applied Microbiology*, 90, 158-162. https://doi.org/10.1046/J.1365-2672.2001.01223.X.

Aron, J., Agarwal, B., & Davenport, A. (2016). Extracorporeal support for patients with acute and acute on chronic liver failure. *Expert Review of Medical Devices*, 13, 367-380. https://doi.org/10.1586/17434440.2016.1154455.

Artym, V. V., & Matsumoto, K. (2010). Imaging cells in three-dimensional collagen matrix. *Current Protocols in Cell Biology*, 48, 10-18. https://doi.org/10.1002/0471143030.cb1018s48.

Arumugaswami, V., & Svendsen, C. (2016). *US20160256672A1* - Induced pluripotent stem cell-derived hepatocyte based bioartificial liver device - *Google Patents*. Retrieved October 19, 2019, from https://patents.google.com/patent/US20160256672A1/en.

Atale, N., Gupta, S., Yadav, U. C. S., & Rani, V. (2014). Cell-death assessment by fluorescent and nonfluorescent cytosolic and nuclear staining techniques. *Journal of Microscopy*, 255, 7-19. https://doi.org/10.1111/JMI.12133.

Awwad, N. S., El-Zahhar, A. A., Fouda, A. M., & Ibrahium, H. A. (2013). Removal of heavy metal ions from ground and surface water samples using carbons derived from date pits. *Journal of Environmental Chemical Engineering*, 1, 416-423. https://doi.org/10.1016/j.jece.2013.06.006.

Ayinla, R. T., Dennis, J. O., Zaid, H. M., Sanusi, Y. K., Usman, F., & Adebayo, L. L. (2019). A review of technical advances of recent palm bio-waste conversion to activated carbon for energy storage. *Journal of Cleaner Production*, 229, 1427-1442. https://doi.org/10.1016/j.jclepro.2019.04.116.

Babaghayou, M. I., Mourad, A. H. I., Lorenzo, V., de la Orden, M. U., Urreaga, J. M., Chabira, S. F., & Sebaa, M. (2016). Photodegradation characterization and heterogeneity evaluation of the exposed and unexposed faces of stabilized and unstabilized LDPE films. *Materials & Design*, 111, 279-290. https://doi.org/10.1016/j.matdes.2016.08.065.

Backer, R., Rokem, J. S., Ilangumaran, G., Lamont, J., Praslickova, D., Ricci, E., Subramanian, S., & Smith, D. L. (2018). Plant growth-promoting rhizobacteria: context, mechanisms of action, and roadmap to commercialization of biostimulants for sustainable agriculture. *Frontiers in Plant Science*, 9, 1473. https://doi.org/10.3389/FPLS.2018.01473.

Balahmar, N., Al-Jumialy, A. S., & Mokaya, R. (2017). Biomass to porous carbon in one step: directly activated biomass for high performance CO2 storage. *Journal of Materials Chemistry A*, 5, 12330-12339. https://doi.org/10.1039/c7ta01722g.

Bañuelos, J. A., Velázquez-Hernández, I., Guerra-Balcázar, M., & Arjona, N. (2018). Production, characterization and evaluation of the energetic capability of bioethanol from *Salicornia bigelovii* as a renewable energy source. *Renewable Energy*, 123, 125-134. https://doi.org/10.1016/j.renene.2018.02.031.

Bashan, Y., Holguin, G., & De-Bashan, L. E. (2004). *Azospirillum*-plant relationships: physiological, molecular, agricultural, and environmental advances (1997-2003). *Canadian Journal of Microbiology*, 50, 521-577. https://doi.org/10.1139/W04-035.

Bashan, Y., Moreno, M., & Troyo, E. (2000). Growth promotion of the seawater-irrigated oilseed halophyte *Salicornia bigelovii* inoculated with mangrove rhizosphere bacteria and halotolerant *Azospirillum spp*. *Biology and Fertility of Soils*, 32, 265-272. https://doi.org/10.1007/S003740000246.

Bashan, Y, de-Bashan, L. E., Prabhu, S. R., & Hernandez, J.-P. (2013). Advances in plant growth-promoting bacterial inoculant technology: formulations and practical perspectives (1998–2013). *Plant and Soil*, 378,1-33. https://doi.org/10.1007/S11104-013-1956-X.

Bashan, Y., & Holguin, G. (2002). Plant growth-promoting bacteria: A potential tool for arid mangrove reforestation. *Trees*, 16, 159-166. https://doi.org/10.1007/s00468-001-0152-4.

Bashan, Y., Puente, M.E., Myrold, D.D., & Toledo, G. (1989). *In vitro* transfer of fixed nitrogen from diazotropic filamentous cyanobacteria to black mangrove seedlings. *FEMS Microbiology Ecology*, 26, 165-170. https://doi.org/10.1111/j.1574-6941.1998.tb00502.x.

Bayer, P., Heuer, E., Karl, U., & Finkel, M. (2005). Economical and ecological comparison of granular activated carbon (GAC) adsorber refill strategies. *Water Research*, 39, 1719-1728. https://doi.org/10.1007/s00468-001.

Belhachemi, M., Rios, R. V. R. A., Addoun, F., Silvestre-Albero, J., Sepúlveda-Escribano, A., & Rodríguez-Reinoso, F. (2009). Preparation of activated carbon from date pits: Effect of the activation agent and liquid phase oxidation. *Journal of Analytical and Applied Pyrolysis*, 86, 168-172. https://doi.org/10.1016/j.jaap.2009.05.004.

Ben Amor, H., & Ismail, M. (2015). Adsorption of chromium (VI) on activated carbon prepared by acid activation of date stones. *International Journal of Science and Research (IJSR)*, 4(3), 309-314. Retrieved September 22, 2019, from https://www.ijsr.net/get_abstract.php?paper_id=SUB15697.

Beneduzi, A., Ambrosini, A., & Passaglia, L. M. P. (2012). Plant growth-promoting rhizobacteria (PGPR): Their potential as antagonists and biocontrol agents. *Genetics and Molecular Biology*, 35, 1044. https://doi.org/10.1590/s1415-47572012000600020

Berger, J., Jampolsky, L. M., & Goldberg, M. W. (1953). A Guide to the Classification of the Actinomycetes and their Antibiotics. *A Guide to the Classification of the Actinomycetes and their Antibiotics.* Williams &Wilkins, Baltimore, pp.1-246. https://doi.org/10.5962/bhl.title.7279.

Bernal, W., & Wendon, J. (2013). Acute Liver Failure. *The New England Journal of Medicine*, 369, 2525-2534. https://doi.org/10.1056/nejmra1208937.

Bernardo, M., Lapa, N., Matos, I., & Fonseca, I. (2016). Critical discussion on activated carbons from bio-wastes: environmental risk assessment. *Boletín Del Grupo Español Del Carbón*, 2, 18-21. Retrieved September 22, 2017, from http://www.gecarbon.org/boletines/articulos/BoletinGEC_040-art4.pdf.

Besbes, S., Blecker, C., Deroanne, C., Lognay, G., Drira, N. E., & Attia, H. (2005). Heating effects on some quality characteristics of date seed oil. *Food Chemistry*, 91, 469-476. https://doi.org/10.1016/J.foodchem.2004.04.037.

Boyd, S. A., Sallach, J. B., Zhang, Y., Crawford, R., Li, H., Johnston, C. T., Teppen, B. J., & Kaminski, N. E. (2017). Sequestration of TCDD by activated carbon eliminates bioavailability and the suppression of immune function in mice. *Environmental Toxicology and Chemistry*, 36, 2671. https://doi.org/10.1002/etc.3815.

Bradford, M. M. (1976). A rapid and sensitive method for the quantitation of microgram quantities of protein utilizing the principle of protein-dye binding. *Analytical Biochemistry*, 72, 248-254. https://doi.org/10.1016/0003-2697(76)90527-3.

Brito, M. J. P., Veloso, C. M., Santos, L. S., Bonomo, R. C. F., & Fontan, R. da C. I. (2018). Adsorption of the textile dye Dianix® royal blue CC onto carbons obtained from yellow mombin fruit stones and activated with KOH and H3PO4: kinetics, adsorption equilibrium and thermodynamic studies. *Powder Technology*, 339(1), 334-343. https://doi.org/10.1016/j.powtec.2018.08.017.

Cassán, F., Maiale, S., Masciarelli, O., Vidal, A., Luna, V., & Ruiz, O. (2009). Cadaverine production by *Azospirillum brasilense* and its possible role in plant growth promotion and osmotic stress mitigation. *European Journal of Soil Biology*, 45, 12-19. https://doi.org/10.1016/J.ejsobi.2008.08.003.

Chamuleau, R. A. F. M., Deurholt, T., & Hoekstra, R. (2005). Which are the right cells to be used in a bioartificial liver?. *Metabolic Brain Disease*, 20, 327-335. https://doi.org/10.1007/S11011-005-7914-4.

Chaurasia, A., Meena, B. R., Tripathi, A. N., Pandey, K. K., Rai, A. B., & Singh, B. (2018). Actinomycetes: an unexplored microorganisms for plant growth promotion and biocontrol in vegetable crops. *World Journal of Microbiology & Biotechnology*, 34, 132. https://doi.org/10.1007/S11274-018-2517-5.

Chen, J., Han, W., Chen, J., Zong, W., Wang, W., Wang, Y., Cheng, G., Li, C., Ou, L. & Yu, Y. (2017). High performance of a unique mesoporous polystyrene-based adsorbent for blood purification. *Regenerative Biomaterials*, 4, 31-37. https://doi.org/10.1093/rb/rbw038.

Chen, Y., Wu, Y., Hua, D., Li, C., Harold, M. P., Wang, J., & Yang, M. (2015). Thermochemical conversion of low-lipid microalgae for the production of liquid fuels: challenges and opportunities. *RSC Advances*, 5, 18673-18701. https://doi.org/10.1039/c4ra13359e.

Cross, T. (1989). Growth and examination of actinomycete-some guidelines. *Bergey's Manual of Systematic Bacteriology*. Williams &Wilkins, Baltimore, pp. 2340-2343.

Cukierman, A. L. (2013). Development and environmental applications of activated carbon cloths. *ISRN Chemical Engineering*, 2013, 1-31. https://doi.org/10.1155/2013/261523.

Dai, J., Tian, S., Jiang, Y., Chang, Z., Xie, A., Zhang, R., & Yan, Y. (2018). Facile synthesis of porous carbon sheets from potassium acetate via in-situ template and self-activation for highly efficient chloramphenicol removal. *Journal of Alloys and Compounds*, 732, 222-232. https://doi.org/10.1016/j.jallcom.2017.10.237.

Damania, A., Hassan, M., Shirakigawa, N., Mizumoto, H., Kumar, A., Sarin, S. K., Ijima, H., Kamihira, M., & Kumar, A. (2017). Alleviating liver failure conditions using an integrated hybrid cryogel based cellular bioreactor as a bioartificial liver support. *Scientific Reports*, 7, 1-11. https://doi.org/10.1038/srep40323.

Damania, A., Kumar, A., Sarin, S. K., & Kumar, A. (2018). Optimized performance of the integrated hepatic cell-loaded cryogel-based bioreactor with intermittent perfusion of acute liver failure plasma. *Journal of Biomedical Materials Research Part B: Applied Biomaterials*, 106, 259-269. https://doi.org/10.1002/jbm.b.33851.

Danish, M., & Ahmad, T. (2018). A review on utilization of wood biomass as a sustainable precursor for activated carbon production and application. *Renewable and Sustainable Energy Reviews*, 87, 1-21. https://doi.org/10.1016/j.rser.2018.02.003.

Das Purkayastha, M., Manhar, A. K., Mandal, M., & Mahanta, C. L. (2014). Industrial waste-derived nanoparticles and microspheres can be potent antimicrobial and functional ingredients. *Journal of Applied Chemistry*, 2014, 1-12. https://doi.org/10.1155/2014/171427.

Davies, B. H. (1965). Analysis of carotenoid pigments. *Chemistry and Biochemistry of Plant Pigments*. Academic Press, London, pp. 489-532.

Davy, A. J., Bishop, G. F., & Costa, C. S. B. (2001). *Salicornia L.*(*Salicornia pusilla* J. woods, *S. ramosissima* J. woods, *S. europaea L., S. obscura* PW ball & tutin, *S. nitens* PW ball & tutin, *S. fragilis* PW ball & tutin *and S. dolichostachya* moss). *Journal of Ecology*, 89, 681-707. https://doi.org/10.1046/j.0022-0477.2001.00607.x.

de Boer, M., van der Sluis, I., van Loon, L. C., & Bakker, P. A. H. M. (1991). Combining fluorescent *Pseudomonas spp*. strains to enhance suppression of *Fusarium* wilt of radish. *European Journal of Plant Pathology*, 105, 201-210. https://doi.org/10.1023/A:1008761729073.

Diab, K. A. S., & Aboul-Ela, E. I. (2012). *In vivo* comparative studies on antigenotoxicity of date palm (*Phoenix dactylifera L*.) pits extract against DNA damage induced by N-Nitroso-N-methylurea in mice. *Toxicology International*, 19, 279. https://doi.org/10.4103/0971-6580.103669.

Ding, W., Zou, L., Sun, S., Li, W., & Gao, D. (2014). A new method to increase the adsorption of protein-bound toxins in artificial liver support systems. *Artificial Organs*, 38, 954-962. https://doi.org/10.1111/aor.12291.

Doncato, K. B., & Costa, C. S. B. (2018). Nutritional potential of a novel sea asparagus, *Salicornia neei* Lag., for human and animal diets. *Biotemas*, 31, 57-63. https://doi.org/10.5007/2175-7925.2018v31n4p57.

Dworkin, M., & Foster, J. W. (1958). Experiments with some microorganisms which utilize ethane and hydrogen. *Journal of Bacteriology*, 75, 592. https://doi.org/10.1128/jb.75.5.592-603.1958.

Dye, D. W. (1962). The inadequacy of the usual determinative tests for the identification of *Xanthomonas spp. New Zealand Journal of Science*, 393-416. Retrieved October 19, 2019, from https://www.scinapse.io/papers/150151505.

Edmondson, R., Jenkins Broglie, J., Adcock, A. F., & Yang, L. (2014). Three-dimensional cell culture systems and their applications in drug discovery and cell-based biosensors. *Assay and Drug Development Technologies*, 12, 207-218. https://doi.org/10.1089/adt.2014.573.

El-Hendawy, A. N. A. (2009). The role of surface chemistry and solution pH on the removal of Pb2+ and Cd2+ ions via effective adsorbents from low-cost biomass. *Journal of Hazardous Materials*, 167, 260-267. https://doi.org/10.1016/j.jhazmat.2008.12.118.

El-Naas, M. H., Al-Zuhair, S., & Alhaija, M. A. (2010). Reduction of COD in refinery wastewater through adsorption on date-pit activated carbon. *Journal of Hazardous Materials*, 173, 750-757. https://doi.org/10.1016/j.jhazmat.2009.09.002.

El-Tarabily, K. A. (2008). Promotion of tomato (*Lycopersicon esculentum* Mill.) plant growth by rhizosphere competent 1-aminocyclopropane-1-carboxylic acid deaminase-producing *Streptomycete actinomycetes*. *Plant and Soil*, 308, 161-174. https://doi.org/10.1007/s11104-008-9616-2.

El-Tarabily, K. A., AlKhajeh, A. S., Ayyash, M. M., Alnuaimi, L. H., Sham, A., ElBaghdady, K. Z., Tariq, S., & AbuQamar, S. F. (2019). Growth promotion of *Salicornia bigelovii* by *Micromonospora chalcea* UAE1, an endophytic 1-aminocyclopropane-1-carboxylic acid deaminase-producing actinobacterial isolate. *Frontiers in Microbiology*, 10,1694. https://doi.org/10.3389/fmicb.2019.01694.

El-Tarabily, K. A., ElBaghdady, K. Z., AlKhajeh, A. S., Ayyash, M. M., Aljneibi, R. S., El-Keblawy, A., & AbuQamar, S. F. (2020). Polyamine-producing actinobacteria enhance biomass production and seed yield in *Salicornia bigelovii*. *Biology and Fertility of Soils*, 56, 499-519. https://doi.org/10.1007/S00374-020-01450-3.

El Bakouri, H., Usero, J., Morillo, J., Rojas, R., & Ouassini, A. (2009). Drin pesticides removal from aqueous solutions using acid-treated date stones. *Bioresource Technology*, 100, 2676-2684. https://doi.org/10.1016/j.biortech.2008.12.051.

English, J. P., & Colmer, T. D. (2011). Salinity and waterlogging tolerances in three stem-succulent halophytes (*Tecticornia* species) from the margins of ephemeral salt lakes. *Plant and Soil*, 348, 379-396. https://doi.org/10.1007/s11104-011-0924-6.

Ettlinger, L., Corbaz, R., & Hutter, R. (1958). Species classification of the genus *Streptomyces* Waksman et Henrici. *Experientia*, 14, 334-335. https://doi.org/10.1007/bf02160394.

Fallik, E., Okon, Y., Epstein, E., Goldman, A., & Fischer, M. (1989). Identification and quantification of IAA and IBA in *Azospirillum brasilense*-inoculated maize roots. *Soil Biology and Biochemistry*, 21, 147-153. https://doi.org/10.1016/0038-0717(89)90024-2.

Figueira, C., Ferreira, M. J., Silva, H., & Cunha, A. (2019). Improved germination efficiency of *Salicornia ramosissima* seeds inoculated with *Bacillus aryabhattai* SP1016-20. *Annals of Applied Biology*, 174, 319-328. https://doi.org/10.1111/aab.12495.

Foo, K. Y., & Hameed, B. H. (2009). Utilization of biodiesel waste as a renewable resource for activated carbon: application to environmental problems. *Renewable and Sustainable Energy Reviews*, 13, 2495-2504. https://doi.org/10.1016/j.rser.2009.06.009.

Foo, K. Y., & Hameed, B. H. (2011). Preparation of activated carbon from date stones by microwave induced chemical activation: Application for methylene blue adsorption. *Chemical Engineering Journal*, 170, 338-341. https://doi.org/10.1016/j.cej.2011.02.068.

Flores, H. E., & Galston, A. W. (1982). Analysis of polyamines in higher plants by high performance liquid chromatography. *Plant Physiology*, 69, 701-706. https://doi.org/10.1104/pp.69.3.701.

Frickmann, H., Schröpfer, E., & Dobler, G. (2013). Actin assessment in addition to specific immuno-fluorescence staining to demonstrate rickettsial growth in cell culture. *European Journal of Microbiology and Immunology*, 3, 198-203. https://doi.org/10.1556/eujmi.3.2013.3.8.

Gao, Y., Yue, Q., Gao, B., & Li, A. (2020). Insight into activated carbon from different kinds of chemical activating agents: A review. *Science of the Total Environment*, 746, 141094. https://doi.org/10.1016/j.scitotenv.2020.141094.

Gautam, R. K., Mudhoo, A., Lofrano, G., & Chattopadhyaya, M. C. (2014). Biomass-derived biosorbents for metal ions sequestration: Adsorbent modification and activation methods and adsorbent regeneration. *Journal of Environmental Chemical Engineering*, 2, 239-259. https://doi.org/10.1016/j.jece.2013.12.019.

Ghnimi, S., Umer, S., Karim, A., & Kamal-Eldin, A. (2017). Date fruit (*Phoenix dactylifera* L.): an underutilized food seeking industrial valorization. *NFS Journal*, 6, 1-10. https://doi.org/10.1016/j.nfs.2016.12.001.

Ghosh, P. K., De, T. K., & Maiti, T. K. (2018). Role of ACC deaminase as a stress ameliorating enzyme of plant growth-promoting rhizobacteria useful in stress agriculture: a review. *Role of Rhizospheric Microbes in Soil.* Springer, Singapore, pp. 57-106. https://dx.doi.org/10.1007/978-981-10-8402-7_3.

Glenn, E. P., Brown, J. J., & O'Leary, J. W. (1998). Irrigating crops with seawater. *Scientific American*, 279, 76-81. https://doi.org/10.1038/scientificamerican0898-76.

Glick, B. R., Todorovic, B., Czarny, J., Cheng, Z., Duan, J., & McConkey, B. (2007). Promotion of plant growth by bacterial ACC deaminase. *Critical Reviews in Plant Sciences*, 26, 227-242. https://doi.org/10.1080/07352680701572966.

Gonçalves, S. P. C., Strauss, M., Delite, F. S., Clemente, Z., Castro, V. L., & Martinez, D. S. T. (2015). Activated carbon from pyrolysed sugarcane bagasse: silver nanoparticle modification and ecotoxicity assessment. *Science of the Total Environment*, 565, 833-840. https://doi.org/10.1016/j.scitotenv.2016.03.041.

González-García, P. (2018). Activated carbon from lignocellulosics precursors: A review of the synthesis methods, characterization techniques and applications. *Renewable and Sustainable Energy Reviews*, 82(1), 1393-1414. https://doi.org/10.1016/j.rser.2017.04.117.

Gordon, S. A., & Weber, R. P. (1951). Colorimetric estimation of indoleacetic acid. *Plant Physiology*, 26(1), 192-195. https://dx.doi.org/10.1104%2Fpp.26.1.192.

Guinn, G., Brummett, D. L., & Beier, R. C. (1986). Purification and measurement of abscisic acid and indole-acetic acid by high performance liquid chromatography. *Plant Physiology*, 81, 997-1002. Retrieved October 19, 2019, from https://academic.oup.com/plphys/article/81/4/997/6082060.

Guo, J., & Lua, A. C. (2003). Surface functional groups on oil-palm-shell adsorbents prepared by H3PO4 and KOH activation and their effects on adsorptive capacity. *Chemical Engineering Research and Design*, 81, 585-590. https://doi.org/10.1205/026387603765444537.

Guo, L., Dial, S., Shi, L., Branham, W., Liu, J., Fang, J.-L., Green, B., Deng, H., Kaput, J., & Ning, B. (2011). Similarities and differences in the expression of drug-metabolizing enzymes between human hepatic cell lines and primary human hepatocytes. *Drug Metabolism and Disposition*, 39, 528-538. https://dx.doi.org/10.1124%2Fdmd.110.035873.

Halaby, M. S., Farag, M. H., & Gerges, A. H. (2014). Potential effect of date pits fortified bread on diabetic rats. *International Journal of Nutrition and Food Sciences*, 3, 49-59. https://doi.org/10.11648/j.ijnfs.20140302.16.

Hameed, B. H., Salman, J. M., & Ahmad, A. L. (2009). Adsorption isotherm and kinetic modeling of 2,4-D pesticide on activated carbon derived from date stones. *Journal of Hazardous Materials*, 163, 121-126. https://doi.org/10.1016/j.jhazmat.2008.06.069.

Hamid, R., Rotshteyn, Y., Rabadi, L., Parikh, R., & Bullock, P. (2004). Comparison of alamar blue and MTT assays for high through-put screening. *Toxicology in Vitro : An International Journal Published in Association with BIBRA*, 18, 703-710. https://doi.org/10.1016/j.tiv.2004.03.012.

Handa, A. K., Nambeesan, S., Abu Qamar, S., Mengiste, T., Laluk, K., & Mattoo, A. K. (2011). Polyamine spermidine is an upstream negator of ethylene-regulated pathogenesis of *Botrytis cinerea* in tomato leaf. *Acta Horticulturae*, 914, 109-112. https://doi.org/10.17660/actahortic.2011.914.18.

Harm, S., Falkenhagen, D., & Hartmann, J. (2014). Pore size--a key property for selective toxin removal in blood purification. *The International Journal of Artificial Organs*, 37, 668-678. https://doi.org/10.5301/ijao.5000354.

Hassan, M. K., McInroy, J. A., & Kloepper, J. W. (2019). The interactions of rhizodeposits with plant growth-promoting rhizobacteria in the rhizosphere: a review. *Agriculture*, 9, 142. https://doi.org/10.3390/agriculture9070142.

Hazourli, S., Ziati, M., & Hazourli, A. (2009). Characterization of activated carbon prepared from lignocellulosic natural residue:-Example of date stones-. *Physics Procedia*, 3, 1039-1043. https://doi.org/10.1016/j.phpro.2009.11.060.

Hazzaa, R., & Hussein, M. (2015). Adsorption of cationic dye from aqueous solution onto activated carbon prepared from olive stones. *Environmental Technology and Innovation*, 4, 36-51. https://doi.org/10.1016/j.eti.2015.04.002.

Heidarinejad, Z., Dehghani, M. H., Heidari, M., Javedan, G., Ali, I., & Sillanpää, M. (2020). Methods for preparation and activation of activated carbon: a review. *Environmental Chemistry Letters*, 18, 393-415. https://doi.org/10.1007/s10311-019-00955-0.

Hilal-Alnaqbi, A., Yousuf, B., & Gaylor, J. D. S. (2011). Fiber in fiber (FIF) bioartificial liver device: initial design and prototyping. *Computer-Aided Design & Applications*, 8, 99-109. https://doi.org/10.3722/cadaps.2011.99-109.

Hilal-Alnaqbi, A., Mourad, A.-H. I., Yousef, B. F., & Gaylor, J. D. S. (2013). Experimental evaluation and theoretical modeling of oxygen transfer rate for the newly developed hollow fiber bioreactor with three compartments. *Bio-Medical Materials and Engineering*, 23, 387-403. https://doi.org/10.3233/bme-130762.

Holden, M. (1965). Chlorophylls: chemistry and biochemistry of plant pigments. *Chemistry and Biochemistry of Plant Pigments.* Academic Press, London, pp. 462-488.

Holguin, G., Guzman, M. A., & Bashan, Y. (1992). Two new nitrogen-fixing bacteria from the rhizosphere of mangrove trees: their isolation, identification and *in vitro* interaction with rhizosphere *Staphylococcus sp. FEMS Microbiology Ecology*,101, 207-216. https://doi.org/10.1111/j.1574-6941.1992.tb01657.x.

Honma, M., & Shimomura, T. (2014). Metabolism of 1-Aminocyclopropane-1-carboxylic Acid. *Agricultural and Biological Chemistry*, 42(10), 1825-1831. https://doi.org/10.1080/00021369.1978.10863261.

Hossain, M. F., & Park, J. Y. (2016). Plain to point network reduced graphene oxide-activated carbon composites decorated with platinum nanoparticles for urine glucose detection. *Scientific Reports*, 6, 1-10. https://doi.org/10.1038/srep21009.

Hrynkiewicz, K., Patz, S., & Ruppel, S. (2019). *Salicornia europaea* L. as an underutilized saline-tolerant plant inhabited by endophytic diazotrophs. *Journal of Advanced Research*, 19, 49. https://doi.org/10.1016/j.jare.2019.05.002.

Htwe, W. M., Kyawt, Y. Y., Thaikua, S., Imai, Y., Mizumachi, S., & Kawamoto, Y. (2016). Effects of liming on dry biomass, lead concentration and accumulated amounts in roots and shoots of three tropical pasture grasses from lead contaminated acidic soils. *Grassland Science*, 62, 257-261. https://doi.org/10.1111/grs.12136.

Hu, Y., Hamed, O., Salghi, R., Abidi, N., Jodeh, S., & Hattb, R. (2017). Extraction and characterization of cellulose from agricultural waste argan press cake. *Cellulose Chemistry and Technology*, 51, 263-272. Retrieved September 22, 2019, from https://www.researchgate.net/publication/316241357_EXTRACTION_AND_CHARACTERIZATION_OF_CELLULOSE_FROM_AGRICULTURAL_WASTE_ARGAN_PRESS_CAKE.

Hussein, F. H., Halbus, A. F., Lafta, A. J., & Athab, Z. H. (2015). Preparation and characterization of activated carbon from Iraqi Khestawy date palm. *Journal of Chemistry*, 2015. https://doi.org/10.1155/2015/295748.

Hussein, A.S., Belal, I.H., Alyalyali, S. R. A., & El-Tarabily, K. A. (2017). Date pit composition for the treatment of animals. *U.S. Patent No. 9682116. Washington, DC: U.S. Patent and Trademark Office.* Retrieved September 22, 2019, from https://patents.justia.com/patent/9682116.

Idowu, A. T., Igiehon, O. O., Adekoya, A. E., Idowu, S., Idowu, A. T., Igiehon, O. O., Adekoya, A. E., & Idowu, S. (2020). Dates palm fruits: a review of their nutritional components, bioactivities and functional food applications. *AIMS Agriculture and Food*, 5, 734-755. https://doi.org/10.3934/agrfood.2020.4.734.

Iguchi, S., Yamaguchi, N., Takami, H., Komatsu, T., Ookubo, H., Sekii, H., Inoue, K., Okazaki, S., Okai, I., Maruyama, S., Nomura, T., & Sugita, M. (2017). Higher efficacy of direct hemoperfusion using coated activated-charcoal column for disopyramide poisoning: A case report. *Medicine*, 96, 1-4. https://doi.org/10.1097/MD.0000000000008755.

Islam, M. A., Tan, I. A. W., Benhouria, A., Asif, M., & Hameed, B. H. (2015). Mesoporous and adsorptive properties of palm date seed activated carbon prepared via sequential hydrothermal carbonization and sodium hydroxide activation. *Chemical Engineering Journal*, 270, 187-195. https://doi.org/10.1016/j.cej.2015.01.058.

Jain, E., Damania, A., Shakya, A. K., Kumar, A., Sarin, S. K., & Kumar, A. (2015). Fabrication of macroporous cryogels as potential hepatocyte carriers for bioartificial liver support. *Colloids and Surfaces. B, Biointerfaces*, 136, 761-771. https://doi.org/10.1016/J.colsurfb.2015.10.012.

Jain, A., Balasubramanian, R., & Srinivasan, M. P. (2016). Hydrothermal conversion of biomass waste to activated carbon with high porosity: A review. *Chemical Engineering Journal*, 283, 789-805. https://doi.org/10.1016/j.cej.2015.08.014.

Jalan, R., Sen, S., & Williams, R. (2004). Recent advances in clinical practice prospects for extracorporeal liver support. *Gut*, 53, 890-898. https://doi.org/10.1136/gut.2003.024919.

Jassim, S. A. A., & Naji, M. A. (2010). *In vitro* Evaluation of the antiviral activity of an extract of date palm (*Phoenix dactylifera* L.) pits on a *Pseudomonas* Phage. *Evidence-Based Complementary and Alternative Medicine : ECAM*, 7, 57. https://doi.org/10.1093/ecam/nem160.

Jha, B., Gontia, I., & Hartmann, A. (2012). The roots of the halophyte *Salicornia brachiata* are a source of new halotolerant diazotrophic bacteria with plant growth-promoting potential. *Plant and Soil*, 356, 265-277. https://doi.org/10.1007/S11104-011-0877-9.

Jonoobi, M., Shafie, M., Shirmohammadli, Y., Ashori, A., Zarea-Hosseinabadi, H., & Mekonnen, T. (2019). A review on date palm tree: Properties, characterization and its potential applications. *Journal of Renewable Materials*, 7, 1055-1075. https://doi.org/10.32604/jrm.2019.08188.

Kamil, F. H., Saeed, E. E., El-Tarabily, K. A., & AbuQamar, S. F. (2018). Biological control of mango dieback disease caused by *Lasiodiplodia theobromae* using streptomycete and non-streptomycete actinobacteria in the united arab emirates. *Frontiers in Microbiology*, 9, 829. https://doi.org/10.3389/fmicb.2018.00829.

Kämpfer, P. (2012). Genus I. Streptomyces. *Bergey's Manual of Systematic Bacteriology*, Springer, New York, pp. 1455-1767. https://doi.org/10.1002/9781118960608.gbm00191.

Khalid, A., Arshad, M., & Zahir, Z. A. (2004). Screening plant growth-promoting rhizobacteria for improving growth and yield of wheat. *Journal of Applied Microbiology*, 96, 473-480. https://doi.org/10.1046/j.1365-2672.2003.02161.x.

Khare, E., Mishra, J., & Arora, N. K. (2018). Multifaceted interactions between endophytes and plant: developments and prospects. *Frontiers in Microbiology*, 9, 2732. https://doi.org/10.3389/fmicb.2018.02732.

Kjaergard, L. L., Liu, J., Als-Nielsen, B., & Gluud, C. (2003). Artificial and bioartificial support systems for acute and acute-on-chronic liver failure: a systematic review. *JAMA*, 289, 217-222. https://doi.org/10.1001/jama.289.2.217.

Kołtowski, M., & Oleszczuk, P. (2016). Effect of activated carbon or biochars on toxicity of different soils contaminated by mixture of native polycyclic aromatic hydrocarbons and heavy metals. *Environmental Toxicology and Chemistry*, 35, 1321-1328. https://doi.org/10.1002/etc.3246.

Komaresofla, B. R., Alikhania, H. A., Etesamia, H., & Khoshkholgh-Sima, N. A. (2019). Improved growth and salinity tolerance of the halophyte *Salicornia sp.* by co–inoculation with endophytic and rhizosphere bacteria. *Applied Soil Ecology*, 138, 160-170. http://dx.doi.org/10.1016/j.apsoil.2019.02.022.

Kortemaa, H., Rita, H., Haahtela, K., & Smolander, A. (1994). Root-colonization ability of antagonistic *Streptomyces griseoviridis. Plant and Soil*, 163, 77-83. https://doi.org/10.1007/bf00033943.

Küster, E. (1959). Outline of a comparative study of criteria used in characterization of the actinomycetes. *International Bulletin of Bacterial Nomenclature and Taxonomy*, 9, 97-104. https://doi.org/https://dx.doi.org/10.1099/0096266X-9-2-97.

Kumar, A., Patel, J. S., Meena, V. S., & Ramteke, P. W. (2019). Plant growth-promoting rhizobacteria: strategies to improve abiotic stresses under sustainable agriculture. *Journal of Plant Nutrition*, 42, 1402-1415. https://doi.org/10.1080/01904167.2019.1616757.

Kumar, A., & Jena, H. M. (2015). High surface area microporous activated carbons prepared from Fox nut (*Euryale ferox*) shell by zinc chloride activation. *Applied Surface Science*, 356, 753-761. https://doi.org/10.1016/j.apsusc.2015.08.074.

Kumar, A., Tripathi, A., & Jain, S. (2011). Extracorporeal bioartificial liver for treating acute liver diseases. *The Journal of Extra-Corporeal Technology*, 43, 195. Retrieved September 22, 2019, from https://www.ncbi.nlm.nih.gov/pubmed/22416599.

Kumar, S., Stecher, G., & Tamura, K. (2016). MEGA7: Molecular Evolutionary Genetics Analysis Version 7.0 for Bigger Datasets. *Molecular Biology and Evolution*, 33, 1870-1874. https://doi.org/10.1093/molbev/msw054.

Lakshmi, S. D., Avti, P. K., & Hegde, G. (2018). Activated carbon nanoparticles from biowaste as new generation antimicrobial agents: A review. *Nano-Structures and Nano-Objects*, 16, 306-321. https://doi.org/10.1016/j.nanoso.2018.08.001.

Lanneluc-Sanson, D., Phan, C. T., & Granger, R. L. (1986). Analysis by reverse-phase high-pressure liquid chromatography of phenylisothiocyanate-derivatized 1-aminocyclopropane-1-carboxylic acid in apple extracts. *Analytical Biochemistry*, 155, 322-327. https://doi.org/10.1016/0003-2697(86)90441-0.

Leach, B. E., Calhoun, K. M., Johnson, L. E., Teeters, C. M., & Jackson, W. G. (1953). Chartreusin, a new antibiotic the oxime (VII) was prepared by refluxing for one hour. *Journal of the American Chemical Society*, 75, 4011-4012. https://doi.org/10.1021/ja01112a040.

Lee, K. C. L., Stadlbauer, V., & Jalan, R. (2016). Extracorporeal liver support devices for listed patients. *Liver Transplantation*, 22, 839-848. https://doi.org/10.1002/lt.24396.

Lizada, M. C., & Yang, S. F. (1979). A simple and sensitive assay for 1-aminocyclopropane- 1-carboxylic acid. *Analytical Biochemistry*, 100, 140-145. https://doi.org/10.1016/0003-2697(79)90123-4.

Loconsole, D., Cristiano, G., & De Lucia, B. (2019). Glassworts: from wild salt marsh species to sustainable edible crops. *Agriculture*, 9,14. https://doi.org/10.3390/agriculture9010014.

Luckert, C., Schulz, C., Lehmann, N., Thomas, M., Hofmann, U., Hammad, S., Hengstler, J. G., Braeuning, A., Lampen, A., & Hessel, S. (2017). Comparative analysis of 3D culture methods on human HepG2 cells. *Archives of Toxicology*, 91, 393-406. https://doi.org/10.1007/S00204-016-1677-Z.

Maidak, B. L., Cole, J. R., Parker, C. T. Jr., Garrity, G. M., & Larsen, N., Li, B. (1999). A new version of the RDP (Ribosomal Database Project). *Nucleic Acids Research*, 27, 171-173. https://doi.org/10.1093/nar/27.1.171.

Mahmoudi, K., Hamdi, N., & Srasra, E. (2014). Preparation and characterization of activated carbon from date pits chemical activation with zinc chloride for methyl orange adsorption. *Journal of Materials and Environmental Science*, 5, 1758-1769. Retrieved september 22, 2019, from http://www.jmaterenvironsci.com/Document/vol5/vol5_N6/215-JMES-774-2014-Mahmoudi.pdf.

Mandal, S., Sahu, M. K., & Patel, R. K. (2013). Adsorption studies of arsenic(III) removal from water by zirconium polyacrylamide hybrid material (ZrPACM-43). *Water Resources and Industry*, 4, 51-67. https://doi.org/10.1016/J.WRI.2013.09.003.

Mapelli, F., Marasco, R., Rolli, E., Barbato, M., Cherif, H., Guesmi, A., Ouzari, I., & Daffonchio, D.S. (2013). Potential for plant growth promotion of rhizobacteria associated with *Salicornia* growing in Tunisian hypersaline soils. *Biomedical Research International*, 2013, 248078. http://dx.doi.org/10.1155/2013/248078.

Maruyama, A., Maeda, M., & Simidu, U. (1986). Occurrence of plant hormone (cytokinin)-producing bacteria in the sea. *Journal of Applied Bacteriology*, 61, 569-574. https://doi.org/10.1111/j.1365-2672.1986.tb01731.x.

Mathew, B. T., Torky, Y., Amin, A., Mourad, A. I., Ayyash, M. M., El-Keblawy, A., Hilal-Alnaqbi, A., Abu Qamar, S. F., & El-Tarabily, K. A. (2020). Halotolerant marine rhizosphere-competent actinobacteria promote *Salicornia bigelovii* growth and seed production using seawater irrigation. *Frontiers in Microbiology*, 11, 552. https://doi.org/10.3389/fmicb.2020.00552.

Mathew, B. T., Raji, S., Dagher, S., Hilal-Alnaqbi, A., Mourad, A. I., Al-Zuhair, S., Al Ahmad, M., El-Tarabily, K. A., & Amin, A. (2018). Bilirubin detoxification using different phytomaterials: characterization and in vitro studies. *International Journal of Nanomedicine*, 13, 2997-3010. https://doi.org/10.2147/ijn.s160968.

Matos, J., Nahas, C., Rojas, L., & Rosales, M. (2011). Synthesis and characterization of activated carbon from sawdust of Algarroba wood. 1. Physical activation and pyrolysis. *Journal of Hazardous Materials*, 196, 360-369. https://doi.org/10.1016/j.jhazmat.2011.09.046.

Maulina, S., Handika, G., Irvan, I., & Iswanto, A. H. (2020). Quality comparison of activated carbon produced from oil palm fronds by chemical activation using sodium carbonate versus sodium chloride. *Journal of the Korean Wood Science and Technology*, 48, 503-512. https://doi.org/10.5658/wood.2020.48.4.503.

Mayak, S., Tirosh, T., & Glick, B. R. (2004). Plant growth-promoting bacteria confer resistance in tomato plants to salt stress. *Plant Physiology and Biochemistry*, 42, 565-572. https://doi.org/10.1016/j.plaphy.2004.05.009.

Mansurov, Z.A., Jandosov, J., Chenchik, D., Azat, S., Savitskaya, I.S., Kistaubaeva, A., Akimbekov, N., Digel, I. & Zhubanova, A. A. (2020). Biocomposite materials based on carbonized rice husk in biomedicine and environmental applications. *Carbon Nanomaterials in Biomedicine and the Environment*. Jenny Stanford Publishing, Boca Raton, pp. 3-32. https://doi.org/10.1201/9780429428647.

Mayyas, M., & Sahajwalla, V. (2019). Carbon nano-sponge with enhanced electrochemical properties: A new understanding of carbon activation. *Chemical Engineering Journal*, 358, 980-991. https://doi.org/10.1016/j.cej.2018.10.094.

Menéndez-Díaz, J. A., & Martín-Gullón, I. (2006). Types of carbon adsorbents and their production. *Interface Science and Technology*, 7, 1-47. https://doi.org/10.1016/S1573-4285(06)80010-4.

Meng, A., Yang, Z., Li, Z., Yuan, X., & Zhao, J. (2018). Nanochain architectures constructed by hydrangea-like MoS2 nanoflowers and SiC nanowires: Synthesis, mechanism and the enhanced electrochemical and wide-temperature properties as an additive-free negative electrode for supercapacitors. *Journal of Alloys and Compounds*, 746, 93-101. https://doi.org/10.1016/j.jallcom.2018.02.280.

Mengiste, T., Laluk, K., & Abu Qamar, S. (2009). Mechanisms of induced resistance against *B. cinerea*. *Post-Harvest Pathology*. Springer, Dordrecht, pp.13-30. http://dx.doi.org/10.1007/978-1-4020-8930-5_2.

Merzougui, Z., & Addoun, F. (2008). Effect of oxidant treatment of date pit activated carbons application to the treatment of waters. *Desalination*, 222, 394-403. https://doi.org/10.1016/j.desal.2007.01.134.

Mesa-Marín, J., Pérez-Romero, J. A., Mateos-Naranjo, E., Bernabeu-Meana, M., Pajuelo, E., Rodríguez-Llorente, I. D., & Redondo-Gómez, S. (2019). Effect of plant growth promoting Rhizobacteria on *Salicornia ramosissima* seed germination under salinity, CO2 and temperature stress. *Agronomy*, 9(10),655. https://doi.org/10.3390/agronomy9100655.

Mikhalovsky, S., Sandeman, S., Howell, C., Phillips, G., & Nikolaev, V. G. (2012). Biomedical applications of carbon adsorbents. *Novel Carbon Adsorbents*. Elsevier, Oxford, UK, pp. 639-669. http://www.elsevier.com/books/novel-carbon-adsorbents/tascandampoacuten/978-0-08-097744-7#.

Misaghi, I. J. & Donndelinger, C.R. (1990). Endophytic bacteria in symptom-free cotton plants. *Phytopathology*, 80, 808. https://doi.org/10.1094/phyto-80-808.

Mourad, A.-H. I., Akkad, R. O., Soliman, A. A., & Madkour, T. M. (2013). Characterisation of thermally treated and untreated polyethylene–polypropylene blends using DSC, TGA and IR techniques. *Plastics, Rubber and Composites*, 38, 265-278. https://doi.org/10.1179/146580109x12473409436625.

Mrabet, A., Jiménez-Araujo, A., Guillén-Bejarano, R., Rodríguez-Arcos, R., & Sindic, M. (2020). Date seeds: a promising source of oil with functional properties. *Foods*, 9. https://doi.org/10.3390/FOODS9060787.

Mui, E. L. K., Cheung, W. H., Valix, M., & Mckay, G. (2010). Activated carbons from bamboo scaffolding using acid activation. *Separation and Purification Technology*, 74, 213-218. https://doi.org/10.1016/j.seppur.2010.06.007.

Müller, B. R. (2010). Effect of particle size and surface area on the adsorption of albumin-bonded bilirubin on activated carbon. *Carbon*, 48, 3607-3615. https://doi.org/10.1016/j.carbon.2010.06.011.

Murphy, J., & Riley, J. P. (1962). A modified single solution method for the determination of phosphate in natural waters. *Analytica Chimica Acta*, 27, 31-36. http://dx.doi.org/10.1016/S0003-2670(00)88444-5.

Nassar, A. H., El-Tarabily, K. A., & Sivasithamparam, K. (2003). Growth promotion of bean (*Phaseolus vulgaris* L.) by a polyamine-producing isolate of *Streptomyces griseoluteus. Plant Growth Regulation*, 40, 97-106. https://doi.org/10.1023/A:1024233303526.

Nasser, R. A., Salem, M. Z. M., Hiziroglu, S., Al-Mefarrej, H. A., Mohareb, A. S., Alam, M., & Aref, I. M. (2016). Chemical analysis of different parts of date palm (*Phoenix dactylifera* L.) using ultimate, proximate and thermo-gravimetric techniques for energy production. *Energies*, 9, 374. https://doi.org/10.3390/en9050374.

Nautiyal, C. A. (1997). A method for selection and characterization of rhizosphere-competent bacteria of chickpea. *Current Microbiology*, 34, 12-17. https://doi.org/10.1007/S002849900136.

Nayak, A., Bhushan, B., Gupta, V., & Sharma, P. (2017). Chemically activated carbon from lignocellulosic wastes for heavy metal wastewater remediation: Effect of activation conditions. *Journal of Colloid and Interface Science*, 493, 228-240. https://doi.org/10.1016/j.jcis.2017.01.031.

Nicolas, C. T., Hickey, R. D., Chen, H. S., Mao, S. A., Higuita, M. L., Wang, Y., & Nyberg, S. L. (2017). Liver regenerative medicine: from hepatocyte transplantation tobioartificial livers and bioengineered grafts. *Stem Cells*, 35, 42. https://doi.org/10.1002/STEM.2500.

Odhiambo, G. O. (2016). Water scarcity in the Arabian peninsula and socio-economic implications. *Applied Water Science*, 7, 2479-2492. https://doi.org/10.1007/S13201-016-0440-1.

Oginni, O., Singh, K., Oporto, G., Dawson-Andoh, B., McDonald, L., & Sabolsky, E. (2019). Influence of one-step and two-step KOH activation on activated carbon characteristics. *Bioresource Technology Reports*, 7, 100266. https://doi.org/10.1016/j.biteb.2019.100266

Ogungbenro, A. E., Quang, D. V., Al-Ali, K., & Abu-Zahra, M. R. M. (2017). Activated carbon from date seeds for CO2 capture applications. *Energy Procedia*, 114, 2313-2321. https://dx.doi.org/10.1016/j.egypro.2017.03.1370.

Ortega, I., McKean, R., Ryan, A. J., MacNeil, S., & Claeyssens, F. (2014). Characterisation and evaluation of the impact of microfabricated pockets on the performance of limbal epithelial stem cells in biodegradable PLGA membranes for corneal regeneration. *Biomaterials Science*, 2, 723-734. https://doi.org/10.1039/C3BM60268K.

Ozawa, T., Wu, J., & Fujii, S. (2007). Effect of inoculation with a strain of *Pseudomonas pseudoalcaligenes* isolated from the endorhizosphere of *Salicornia europea* on salt tolerance of the glasswort. *Soil Science and Plant Nutrition*, 53, 12-16. https://doi.org/10.1111/J.1747-0765.2007.00098.X.

Payne, C., Bruce, A., & Staines, H. (2000). Yeast and bacteria as biological control agents against fungal discolouration of *Pinus sylvestris* blocks in laboratory-based tests and the roleof antifungal volatiles. *Holzforschung*, 54, 563-569. https://doi.org/10.1515/HF.2000.096.

Peñaloza, J. P., Márquez-Miranda, V., Cabaña-Brunod, M., Reyes-Ramírez, R., Llancalahuen, F. M., Vilos, C., Maldonado-Biermann, F., Velásquez, L. A., Fuentes, J. A., González-Nilo, F. D., Rodríguez-Díaz, M., & Otero, C. (2017). Intracellular trafficking and cellular uptake mechanism of PHBV nanoparticles for targeted delivery in epithelial cell lines. *Journal of Nanobiotechnology*, 15,1-15. https://doi.org/10.1186/S12951-016-0241-6.

Petkovic, L. M., Ginosar, D. M., Rollins, H. W., Burch, K. C., Deiana, C., Silva, H. S., Sardella, M. F., & Granados, D. (2009). Activated carbon catalysts for the production of hydrogen via the sulfur-iodine thermochemical water splitting cycle. *International Journal of Hydrogen Energy*, 34, 4057-4064. https://doi.org/10.1016/j.ijhydene.2008.07.075.

Petuhov, O., Lupascu, T., Behunová, D., Povar, I., Mitina, T., & Rusu, M. (2019). Microbiological properties of microwave-activated carbons impregnated with Enoxil and nanoparticles of Ag and Se. *C*, 5(2), 31. https://doi.org/10.3390/c5020031.

Pfab, R., Schmoll, S., Dostal, G., Stenzel, J., Hapfelmeier, A., & Eyer, F. (2017). Single dose activated charcoal for gut decontamination: application by medical non-professionals -a prospective study on availability and practicability. *Toxicology Reports*, 4, 49-54. https://doi.org/10.1016/j.toxrep.2016.12.007.

Phiri, J., Dou, J., Vuorinen, T., Gane, P. A. C., & Maloney, T. C. (2019). Highly Porous Willow Wood-Derived Activated Carbon for High-Performance Supercapacitor Electrodes. *ACS Omega*, 4, 18108-18117. https://doi.org/10.1021/acsomega.9b01977.

Pikovskaya, R. I. (1948). Mobilization of phosphorus in soil in connection with the vital activity of some microbial species. *Mikrobiologiya*, pp. 362-370. Retrieved September 22, 2019, from https://www.scienceopen.com/document?-1.ILinkListener-header-action~bar-public~button~container-bookmark~button-bookmark~button&vid=44a8aa7f-fad0-4038-a97b-a766d1a3b6fb.

Pinyou, P., Blay, V., Muresan, L. M., & Noguer, T. (2019). Enzyme-modified electrodes for biosensors and biofuel cells. *Materials Horizons*, 6, 1336-1358. https://doi.org/10.1039/c9mh00013e.

Rainey, F. A., Ward-Rainey, N., Kroppenstedt, R. M., & Stackebrandt, E. (1996). The genus *Nocardiopsis* represents a phylogenetically coherent taxon and a distinct actinomycete lineage: Proposal of Nocardiopsaceae fam. nov. *International Journal of Systematic Bacteriology*, 46, 1088-1092. https://doi.org/10.1099/00207713-46-4-1088.

Rahman, S. F., Min, K., Park, S. H., Park, J. H., Yoo, J. C., & Park, D. H. (2016). Selective determination of dopamine with an amperometric biosensor using electrochemically pretreated and activated carbon/tyrosinase/Nafion®-modified glassy carbon electrode. *Biotechnology and Bioprocess Engineering*, 21, 627-633. https://doi.org/10.1007/s12257-016-0382-3.

Ramalingam, R. J., Sivachidambaram, M., Vijaya, J. J., Al-Lohedan, H. A., & Muthumareeswaran, M. R. (2020). Synthesis of porous activated carbon powder formation from fruit peel and cow dung waste for modified electrode fabrication and application. *Biomass and Bioenergy*, 142, 105800. https://doi.org/10.1016/j.biombioe.2020.105800.

Ramanujan, R. V., Purushotham, S., & Chia, M. H. (2007). Processing and characterization of activated carbon coated magnetic particles for biomedical applications. *Materials Science and Engineering C*, 27, 659- 664. https://doi.org/10.1016/j.msec.2006.06.007.

Rashidi, N. A., & Yusup, S. (2017). A review on recent technological advancement in the activated carbon production from oil palm wastes. *Chemical Engineering Journal*, 314, 277-290. https://doi.org/10.1016/j.cej.2016.11.059.

Ray, A., & Anumakonda, A. (2011). Production of green liquid hydrocarbon fuels. *Biofuels*. Academic Press, Oxford, UK, pp. 587-608. https://doi.org/10.1016/B978-0-12-385099-7.00027-9.

Reddy, K. S. K., Al Shoaibi, A., & Srinivasakannan, C. (2015). Preparation of porous carbon from date palm seeds and process optimization. *International Journal of Environmental Science and Technology*, 12, 959-966. https://doi.org/10.1007/s13762-013-0468-9.

Reddy, K. S. K., Al Shoaibi, A., & Srinivasakannan, C. (2012). A comparison of microstructure and adsorption characteristics of activated carbons by CO2 and H3PO4 activation from date palm pits. *New Carbon Materials*, 27, 344-351. https://doi.org/10.1016/s1872-5805(12)60020-1.

Redmond, J. W., & Tseng, A. (1979). High-pressure liquid chromatographic determination of putrescine, cadaverine, spermidine and spermine. *Journal of Chromatography A*, 170, 479-481. https://doi.org/10.1016/S0021-9673(00)95481-5.

Rilling, J. I., Acuña, J. J., Nannipieri, P., Cassan, F., Maruyama, F., & Jorquera, M. A. (2019). Current opinion and perspectives on the methods for tracking and monitoring plant growth–promoting bacteria. *Soil Biology and Biochemistry*, 130, 205-219. https://doi.org/10.1016/j.soilbio.2018.12.012.

Ríos, A. (2014). UAE's home-grown biofuel is important milestone in aviation. Retrieved January 14, 2020, from https://www.ku.ac.ae/uae-s-home-grown-biofuel-is-important-milestone-in-aviation/.

Rodríguez-Reinoso, F., & Molina-Sabio, M. (1992). Activated carbons from lignocellulosic materials by chemical and/or physical activation: an overview. *Carbon*, 30, 1111-1118. https://doi.org/10.1016/0008-6223(92)90143-K.

Rojas, A., Holguin, G., Glick, B. R., & Bashan, Y. (2006). Synergism between *Phyllobacterium sp.* (N2-fixer) and *Bacillus licheniformis* (P-solubilizer), both from a semiarid mangrove rhizosphere. *FEMS Microbiology Ecology*, 35, 181-187. https://doi.org/10.1111/j.1574-6941.2001.tb00802.x.

Rozga, J., Umehara, Y., Trofimenko, A., Sadahiro, T., & Demetriou, A. A. (2006). A novel plasma filtration therapy for hepatic failure: preclinical studies. *Therapeutic Apheresis and Dialysis*, 10, 138-144. https://doi.org/10.1111/j.1744-9987.2006.00355.x.

Rueda-Puente, E. O., Castellanos, T., Troyo-Diéguez, E., & Díaz De León-Alvarez, J. L. (2004). Effect of *Klebsiella pneumoniae* and *Azospirillum halopraeferens* on the growth and development of two *Salicornia bigelovii* genotypes. *Australian Journal of Experimental Agriculture*, 44, 65-74. https://doi.org/10.1071/ea03012.

Saeed, E. E., Sham, A., Salmin, Z., Abdelmowla, Y., Iratni, R., El-Tarabily, K., & AbuQamar, S. (2017). *Streptomyces globosus* UAE1, a Potential Effective Biocontrol Agent for Black Scorch Disease in Date Palm Plantations. *Frontiers in Microbiology*, 8, 1455. https://doi.org/10.3389/fmicb.2017.01455.

Saitou, N., & Nei, M. (1987). The neighbor-joining method: a new method for reconstructing phylogenetic trees. *Molecular Biology and Evolution*, 4, 406-425. https://doi.org/10.1093/oxfordjournals.molbev.a040454.

Salman, J. M., & Hussein, F. H. (2014). Batch adsorber design for different solution volume/adsorbate mass ratios of bentazon, carbofuran and 2,4-d adsorption on to date seeds activated carbon. *Journal of Environmental Analytical Chemistry*, 2, 120. https://doi.org/10.4172/2380-2391.1000120.

Sarnatskaya, V. V., Lindup, W. E., Walther, P., Maslenny, V. N., Yushko, L. A., Sidorenko, A. S., Nikolaev, A. V., & Nikolaev, V. G. (2002). Albumin, bilirubin, and activated carbon: New edges of an old triangle. *Artificial Cells, Blood Substitutes, and Immobilization Biotechnology*, 30, 113-126. https://doi.org/10.1081/BIO-120003192.

Schwyn, B., & Neilands, J. B. (1987). Universal chemical assay for the detection and determination of siderophores. *Analytical Biochemistry*, 160, 47-56. https://doi.org/10.1016/0003-2697(87)90612-9.

Sekirifa, M. L., Pallier, S., Hadj-Mahammed, M., Richard, D., Baameur, L., & Al-Dujaili, A. H. (2013). Measurement of the performance of an agricultural residue-based activated carbon aiming at the removal of 4-chlophenol from aqueous solutions. *Energy Procedia*, 36, 94-103. https://doi.org/10.1016/j.egypro.2013.07.012.

Sekirifa, M. L., Hadj-Mahammed, M., Pallier, S., Baameur, L., Richard, D., & Al-Dujaili, A. H. (2013). Preparation and characterization of an activated carbon from a date stones variety by physical activation with carbon dioxide. *Journal of Analytical and Applied Pyrolysis*, 99, 155-160. https://doi.org/10.1016/J.JAAP.2012.10.007.

Sevilla, M., & Mokaya, R. (2014). Energy storage applications of activated carbons: Supercapacitors and hydrogen storage. *Energy and Environmental Science*, 7, 1250-1280. https://doi.org/10.1039/c3ee43525c.

Sgroy, V., Cassán, F., Masciarelli, O., Del Papa, M. F., Lagares, A., & Luna, V. (2009). Isolation and characterization of endophytic plant growth-promoting (PGPB) or stress homeostasis-regulating (PSHB) bacteria associated to the halophyte *Prosopis strombulifera*. *Applied Microbiology and Biotechnology*, 85, 371-381. https://doi.org/10.1007/S00253-009-2116-3.

Sha, Y., Lou, J., Bai, S., Wu, D., Liu, B., & Ling, Y. (2015). Facile preparation of nitrogen-doped porous carbon from waste tobacco by a simple pre-treatment process and their application in electrochemical capacitor and CO2 capture. *Materials Research Bulletin*, 64, 327-332. https://doi.org/10.1016/j.materresbull.2015.01.015.

Shah, S., Li, J., Moffatt, B. A., & Glick, B. R. (1998). Isolation and characterization of ACC deaminase gene from two different plant growth-promoting rhizobacteria. *Canadian Journal of Microbiology*, 44, 833-843. http://dx.doi.org/10.1139/w98-074.

Shahid, M., Jaradat, A. A., & Rao, N. K. (2013). Use of marginal water for *Salicornia bigelovii* Torr. planting in the United Arab Emirates. *Developments In Soil Salinity Assessment and Reclamation*. Springer, Netherlands, pp. 451-462. https://doi.org/10.1007/978-94-007-5684-7_31.

Sham, A., Al-Ashram, H., Whitley, K., Iratni, R., El-Tarabily, K. A., & AbuQamar, S. F. (2019). Metatranscriptomic analysis of multiple environmental stresses identifies RAP2.4 gene associated with arabidopsis immunity to *Botrytis cinerea. Scientific Reports*, 9, 17010. https://doi.org/10.1038/S41598-019-53694-1.

Sharma, R., Wungrampha, S., Singh, V., Pareek, A., & Sharma, M. K. (2016). Halophytes as bioenergy crops. *Frontiers in Plant Science*, 7, 1372. https://doi.org/10.3389/fpls.2016.01372.

Shepherd, K. A., Macfarlane, T. D., & Colmer, T. D. (2005). Morphology, anatomy and histochemistry of salicornioideae (chenopodiaceae) fruits and seeds. *Annals of Botany*, 95, 917-933. https://doi.org/10.1093/aob/mci101.

Shindy, W. W., & Smith, O. E. (1975). Identification of plant hormones from cotton ovules. *Plant Physiology*, 55, 550. https://doi.org/10.1104/pp.55.3.550.

Shirling, E. B., & Gottlieb, D. (1966). Methods for characterization of *Streptomyces* species1. *International Journal of Systematic and Evolutionary Microbiology*, 16, 313-340. https://doi.org/10.1099/00207713-16-3-313.

Sichula, J., Makasa, M. L., Nkonde, G. K., Kefi, A. S., & Katongo, C. (2011). Removal of ammonia from aquaculture water using maize cob activated carbon. *Malawi Journal of Aquaculture and Fisheries*, 1, 10-15. Retrieved September 22, 2019, from https://www.researchgate.net/publication/235734379_REMOVAL_OF_AMMONIA_FROM_AQUACULTURE_WATER_USING_MAIZE_COB_ACTIVATED_CARBON.

Slater, T. F., Sawyer, B., & Sträuli, U. (1963). Studies On Succinate-Tetrazolium Reductase Systems: III. Points Of Coupling Of Four Different Tetrazolium Salts. *Biochimica et Biophysica Acta*, 77, 383-393. https://doi.org/10.1016/0006-3002(63)90513-4.

Smith, M. A., & Davies, P. J. (1985). Separation and quantitation of polyamines in plant tissue by high performance liquid chromatography of their dansyl derivatives. *Plant Physiology*, 78, 89-91. https://doi.org/10.1104/pp.78.1.89.

Stange, J., Mitzner, S. R., Risler, T., Erley, C. M., Lauchart, W., Goehl, H., Klammt, S., Peszynski, P., Freytag, J., Hickstein, H., Löhr, M., Liebe, S., Schareck, W., Hopt, U. T., & Schmidt, R. (1999). Molecular adsorbent recycling system (MARS): clinical results of a new membrane-based blood purification system for bioartificial liver support. *Artificial Organs*, 23, 319-330. https://doi.org/10.1046/j.1525-1594.1999.06122.x.

Strzelczyk, E., & Pokojska-Burdziej, A. (1984). Production of auxins and gibberellin-like substances by mycorrhizal fungi, bacteria and actinomycetes isolated from soil and the mycorrhizosphere of pine (Pinus silvestris L.). Plant and Soil, 185-194. https://doi.org/10.1007/BF02197150.

Suzuki, S., Noda, j., & Takama, k. (1990). Growth and Polyamine Production of Alteromonas spp in Fish Meat Extracts Under Modified Atmosphere. *Bulletin of Faculty of Fisheries, Hokkaido University*, 41, 213-220. Retrieved September 22, 2019, from http://hdl.handle.net/2115/24066.

Syed, D. G., Agasar, D., Kim, C.-J., Li, W.-J., Lee, J.-C., Park, D.-J., Xu, L.-H., Tian, X.-P., & Jiang, C.-L. (2007). *Streptomyces tritolerans* sp. nov., a novel actinomycete isolated from soil in Karnataka, India. *Antonie van Leeuwenhoek*, 92, 391-397. https://doi.org/10.1007/s10482-007-9166-2.

Taha, E., Abd-Elkarim, N., & Ahmed, Z. (2019). Date seed oil as a potential natural additive to improve oxidative stability of edible vegetable oils. *Egyptian Journal of Food Science*, 47, 105-113. https://doi.org/10.21608/ejfs.2019.13050.1007.

Tan, I. A. W., Ahmad, A. L., & Hameed, B. H. (2008). Adsorption of basic dye on high-surface-area activated carbon prepared from coconut husk: equilibrium, kinetic and thermodynamic studies. *Journal of Hazardous Materials*, 154, 337-346. https://doi.org/10.1016/j.jhazmat.2007.10.031.

Tawalbeh, M., Allawzi, M. A., & Kandah, M. I. (2005). Production of activated carbon from Jojoba seed residue by chemical activation residue using a static bed reactor. *Journal of Applied Sciences*, 5, 482-487. https://doi.org/10.3923/JAS.2005.482.487.

Temdrara, L., Addoun, A., & Khelifi, A. (2015). Development of olivestones-activated carbons by physical, chemical and physicochemical methods for phenol removal: a comparative study. *Desalination and Water Treatment*, 53, 452-461. https://doi.org/10.1080/19443994.2013.838523.

Teotia, R. S., Kalita, D., Singh, A. K., Verma, S. K., Kadam, S. S., & Bellare, J. R. (2015). Bifunctional polysulfone-chitosan composite hollow fiber membrane for bioartificial liver. *ACS Biomaterials Science and Engineering*, 1, 372-381. https://doi.org/10.1021/ab500061j.

Theydan, S. K., & Ahmed, M. J. (2012). Adsorption of methylene blue onto biomass-based activated carbon by FeCl3 activation: Equilibrium, kinetics, and thermodynamic studies. *Journal of Analytical and Applied Pyrolysis*, 97, 116-122. https://doi.org/10.1016/j.jaap.2012.05.008.

Thomas, B. N., & George, S. C. (2015). Production of activated carbon from natural sources. *Trends in Green Chemistry*, 1-5. Retrieved September 22, 2019, from https://www.primescholars.com/articles/production-of-activated-carbon-fromnatural-sources.pdf.

Thompson, J. D., Gibson, T. J., Plewniak, F., Jeanmougin, F., & Higgins, D. G. (1997). The CLUSTAL_X windows interface: flexible strategies for multiple sequence alignment aided by quality analysis tools. *Nucleic Acids Research*, 25, 4876-4882. https://doi.org/10.1093/nar/25.24.4876.

Thurnherr, T., Brandenberger, C., Fischer, K., Diener, L., Manser, P., Maeder-Althaus, X., Kaiser, J.P., Krug, H.F., Rothen-Rutishauser, B. & Wick, P. (2011). A comparison of acute and long-term effects of industrial multiwalled carbon nanotubes on human lung and immune cells in vitro. *Toxicology Letters*, 200, 176-186. https://doi.org/10.1016/j.toxlet.2010.11.012.

Tien, T. M., Gaskins, M. H., & Hubbell, D. H. (1979). Plant growth substances produced by *Azospirillum brasilense* and their effect on the growth of pearl millet (*Pennisetum americanum* l.). *Applied and Environmental Microbiology*, 37, 1016-1024. https://doi.org/10.1128/aem.37.5.1016-1024.1979.

Togibasa, O., Ansanay, Y. O., Dahlan, K., & Erari, M. (2021). Identification of surface functional group on activated carbon from waste sago. *Journal of Physics: Theories and Applications*, 5, 1-8. https://doi.org/10.20961/jphystheor-appl.v5i1.49885.

van de Kerkhove, M. P., Hoekstra, R., Chamuleau, R. A. F. M., & van Gulik, T. M. (2004). Clinical application of bioartificial liver support systems. *Annals of Surgery*, 240, 216. https://doi.org/10.1097/01.sla.0000132986.75257.19.

van Wenum, M., Adam, A. A. A., Hakvoort, T. B. M., Hendriks, E. J., Shevchenko, V., van Gulik, T. M., Chamuleau, R. A. F. M., & Hoekstra, R. (2016). Selecting cells for bioartificial liver devices and the importance of a 3D culture environment: A functional comparison between the hepaRG and C3A cell lines. *International Journal of Biological Sciences*, 12, 964-978. https://doi.org/10.7150/IJBS.15165.

Ventura, Y., & Sagi, M. (2013). Halophyte crop cultivation: The case for *Salicornia* and *Sarcocornia. Environmental and Experimental Botany*, 92, 144-153. https://doi.org/10.1016/j.envexpbot.2012.07.010.

Verma, P., Yadav, A. N., Kumar, V., Singh, D. P., & Saxena, A. K. (2017). Beneficial plant-microbes interactions: Biodiversity of microbes from diverse extreme environments and its impact for crop improvement. *Plant-Microbe Interactions in Agro-Ecological Perspectives.* Springer, Singapore, pp. 543-580. https://doi.org/10.1007/978-981-10-6593-4_22.

Wellington, E. M. H., & Williams, S. T. (1977). Preservation of actinomycete inoculum in frozen glycerol. *Microbios Letters*, pp.151-157. Retrieved September 18, 2014, from https://eurekamag.com/research/000/723/000723816.php.

Williams, S. T., Shameemullah, M., Watson, E. T., & Mayfield, C. I. (1972). Studies on the ecology of actinomycetes in soil—VI. The influence of moisture tension on growth and survival. *Soil Biology and Biochemistry*, 4, 215-225. https://doi.org/10.1016/0038-0717(72)90014-4.

Xu, Z., Yuan, Z., Zhang, D., Chen, W., Huang, Y., Zhang, T., Tian, D., Deng, H., Zhou, Y., & Sun, Z. (2018). Highly mesoporous activated carbon synthesized by pyrolysis of waste polyester textiles and MgCl2: Physiochemical characteristics and pore-forming mechanism. *Journal of Cleaner Production*, 192, 453-461. https://doi.org/10.1016/j.jclepro.2018.05.007.

Yahya, M. A., Al-Qodah, Z., & Ngah, C. W. Z. (2015). Agricultural bio-waste materials as potential sustainable precursors used for activated carbon production: A review. *Renewable and Sustainable Energy Reviews*, 46, 218-235. https://doi.org/10.1016/j.rser.2015.02.051.

Yan, H., Endo, Y., Shen, Y., Rotstein, D., Dokmanovic, M., Mohan, N., Mukhopadhyay, P., Gao, B., Pacher, P., & Wu, W. J. (2016). Ado-trastuzumab emtansine targets hepatocytes via human epidermal growth factor receptor 2 to induce hepatotoxicity. *Molecular Cancer Therapeutics*, 15, 480-490. https://doi.org/10.1158/1535-7163.mct-15-0580.

Zakrzewska, K. E., Samluk, A., Wierzbicki, M., Jaworski, S., Kutwin, M., Sawosz, E., Chwalibog, A., Pijanowska, D. G., & Pluta, K. D. (2015). Analysis of the cytotoxicity of carbon-based nanoparticles, diamond and graphite, in human glioblastoma and hepatoma cell lines. *PLOS ONE*, 10, e0122579. https://doi.org/10.1371/Journal.Phone.0122579.

Zellner, T., Prasa, D., Färber, E., Hoffmann-Walbeck, P., Genser, D., & Eyer, F. (2019). The use of activated charcoal to treat intoxications. *Deutsches Arzteblatt International*, 116, 311-317. https://doi.org/10.3238/arztebl.2019.0311.

Zhang, N., & Shen, Y. (2019). One-step pyrolysis of lignin and polyvinyl chloride for synthesis of porous carbon and its application for toluene sorption. *Bioresource Technology*, 284, 325-332. https://doi.org/10.1016/j.biortech.2019.03.149.

Zhang, X., Guo, W., Ngo, H. H., Wen, H., Li, N., & Wu, W. (2016). Performance evaluation of powdered activated carbon for removing 28 types of antibiotics from water. *Journal of Environmental Management*, 172, 193-200. https://doi.org/10.1016/j.biortech.2019.03.149.

Zhang, Y., Song, X., Zhang, P., Gao, H., Ou, C., & Kong, X. (2019). Production of activated carbons from four wastes via one-step activation and their applications in Pb2+ adsorption: Insight of ash content. *Chemosphere*, 245, 125587. https://doi.org/10.1016/j.chemosphere.2019.125587.

Zhang, Z., Lei, Y., Li, D., Zhao, J., Wang, Y., Zhou, G., Yan, C., & He, Q. (2020). Sudden heating of H3PO4-loaded coconut shell in CO2 flow to produce super activated carbon and its application for benzene adsorption. *Renewable Energy*, 153, 1091-1099. https://doi.org/10.1016/j.renene.2020.02.059.

Zhao, Y., Wang, Z. Q., Zhao, X., Li, W., & Liu, S. X. (2013). Antibacterial action of silver-doped activated carbon prepared by vacuum impregnation. *Applied Surface Science*, 266, 67-72. https://doi.org/10.1016/j.apsusc.2012.11.084.

Zhou, Cheng, Ma, Z., Zhu, L., Xiao, X., Xie, Y., Zhu, J., & Wang, J. (2016). Rhizobacterial strain *Bacillus megaterium* bofc15 induces cellular polyamine changes that improve plant growth and drought resistance. *International Journal of Molecular Sciences*, 17, 976. https://doi.org/10.3390/Ijms17060976.

Zhou, C., & Wang, Y. (2020) Recent progress in the conversion of biomass wastes into functional materials for value-added applications, *Science and Technology of Advanced Materials*, 21, 787-804. https://dx.doi.org/10.1080%2F14686996.2020.1848213.

Zhou, L., Yu, Q., Cui, Y., Xie, F., Li, W., Li, Y., & Chen, M. (2017). Adsorption properties of activated carbon from reed with a high adsorption capacity. *Ecological Engineering*, 102, 443-450. https://doi.org/10.1016/j.ecoleng.2017.02.036.

List of Publications

Mathew, B.T., Raji, S., Dagher, S., Hilal-Alnaqbi, A., Mourad, A.H.I., Al-Zuhair, S., Al Ahmad, M., El-Tarabily, K.A. & Amin, A. (2018). Bilirubin detoxification using different phytomaterials: characterization and in vitro studies. *International Journal of Nanomedicine*, 13, 2997-3010. https://doi.org/10.2147/IJN.S160968.

Mathew, B. T., Torky, Y., Amin, A., Mourad, A. H. I., Ayyash, M. M., El-Keblawy, A., Hilal-Alnaqbi, A., AbuQamar, S. F., & El-Tarabily, K. A. (2020). Halotolerant Marine Rhizosphere-Competent Actinobacteria Promote *Salicornia bigelovii* Growth and Seed Production Using Seawater Irrigation. *Frontiers in Microbiology*, 11, 552. https://doi.org/10.3389/fmicb.2020.00552.

Appendix

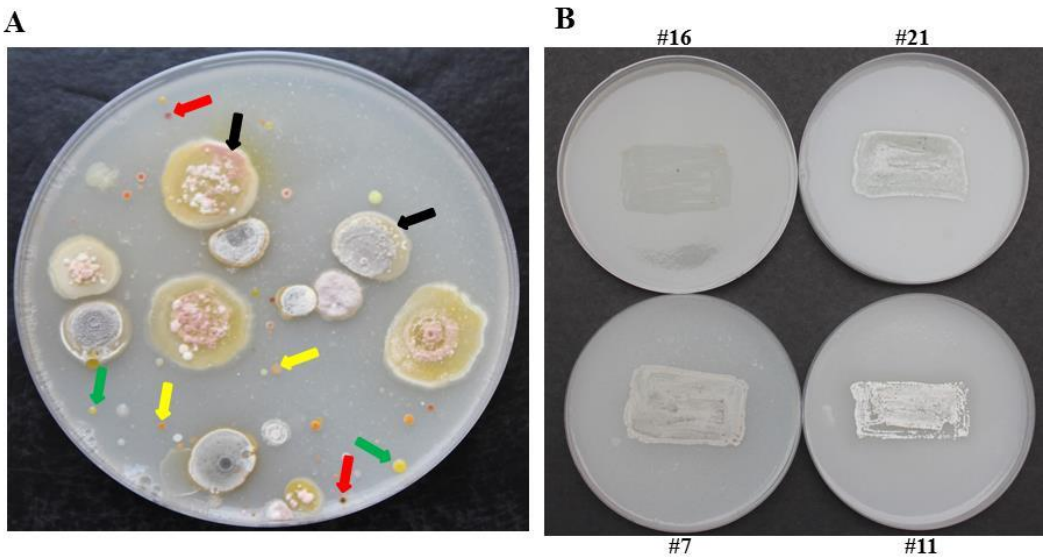

Figure S1: *In vitro* growth of selected actinobacteria isolated from *Salicornia bigelovii* rhizosphere. (a) Colonies of SA and NSA isolated from *S. bigelovii* grown on inorganic salt starch agar plates; and (b) selected actinobacterial isolates possessing salinity tolerance. In (a), black arrows represent the SA colonies, whereas red, yellow and green arrows represent the NSA colonies of *Micromonospora*, *Actinoplanes* and *Nocardia* spp., respectively. In (b), actinobacteria #21, #7 and #11, but not #16 (control), were considered halotolerant isolates due to growth and sporulation on inorganic salt starch agar supplemented with 8% NaCl. SA, streptomycete actinobacteria; NSA, non-streptomycete actinobacteria

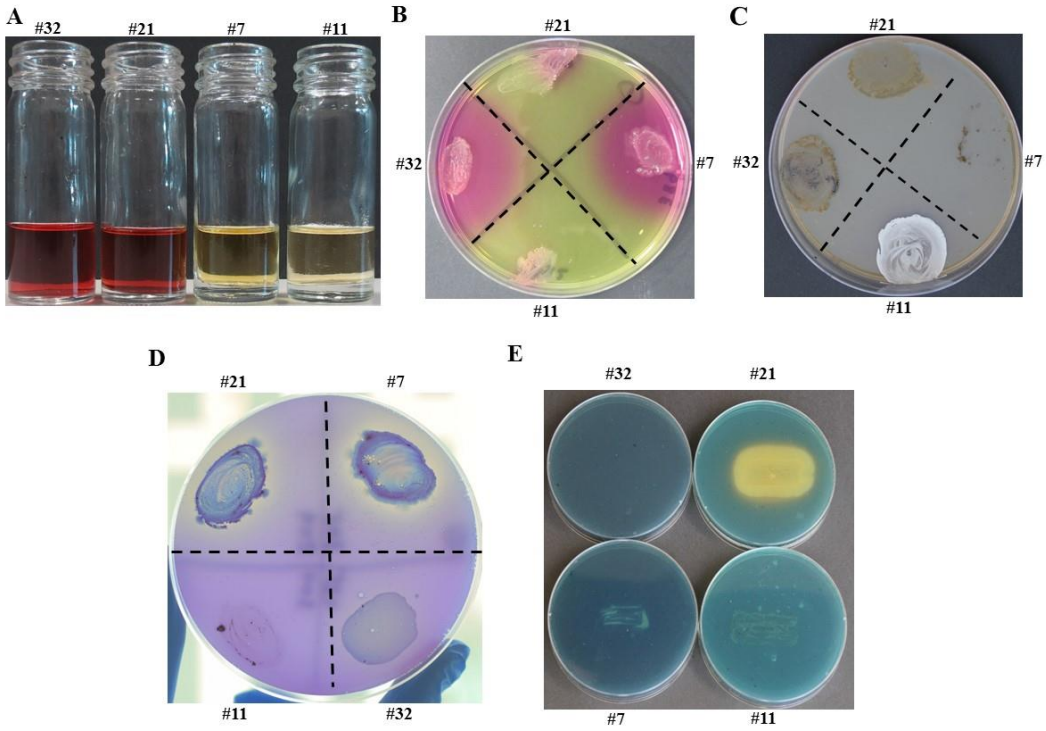

Figure S2: *In vitro* plant growth promoting characteristics of selected halotolerant actinobacterial isolates. Selected actinobacterial strains isolated from *Salicornia bigelovii* rhizosphere possessing the production of (a) IAA; (b) Put; (c) ACCD; (e) siderophores; and (d) solubilization of P. In (a), addition of Salkowski reagent to cultures grown in inorganic salt starch broth amended with L-tryptophan; and the formation of red color indicated the production of the auxin, IAA. In (b) isolates were tested on Moeller's decarboxylase agar medium amended with L-arginine monohydrochloride; and the change from yellow to red color of the phenol-red indicated production of the polyamine, Put. In (c) isolates were tested in N-free Dworkin and Foster's salts minimal agar medium amended with ACC; where growth and sporulation indicated the efficiency to utilize ACC and the production of ACCD. In (d), isolates were tested on Pikovskaya's agar medium amended with rock phosphate and bromophenol blue; and production of clear zone surrounding the colony was used as an indicator of P-solubilization. In (e), isolates were tested on chrome azurol S agar plates; and yellow halo surrounding the colony indicates the excretion of siderophores. In (a-e), isolates #21, #7 and #11 were considered as auxin-, polyamine and ACCD-producing isolates, respectively. In (d & e), isolates #21 and #7 were considered as P-solubilizing isolates, whereas #21 was considered as a siderophore-producing isolate. Actinobacterial strain #32 was used as a control isolate. IAA, indole-3-acetic acid; Put, putrescine; ACC, 1-aminocyclopropane-1-carboxylic; ACCD, 1-aminocyclopropane-1-carboxylic deaminase; P, phosphorus

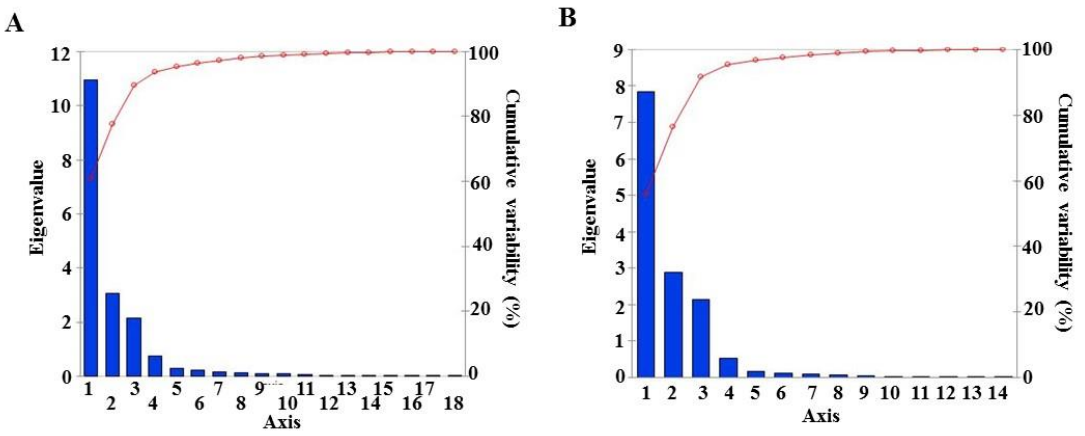

Figure S3: Screen plots representing the eigenvalue of variance accounted for each principal component in (a) shoot and (b) root. *S. bigelovii* seedlings were grown in an evaporative-cooled greenhouse and maintained at 25±2°C

Table S1: Comparison of morphological, cultural, and phenotypic characteristics that distinguish auxin-producing isolate #21 from very closely related species *Streptomyces chartreusis*

Characteristics	**Isolate #21**	***S. chartreusis***
Morphological		
Spore chain	Spirales (open spiral) having 10-25 spores/chain.	Spirales (open spiral) having 10-50 spores/chain.
Spore surface	Spiny	Spiny
Cultural		
ISP3		
Aerial mass color	Powdery blue-green	Powdery blue-green
Substrate mycelium color	Yellowish white	Yellowish white
Production of soluble pigment	No distinctive pigments	No distinctive pigments
Phenotypic		
Growth on carbon sources		
Xylose	+	+
Arabinose	+	+
Glucose	+	+
Fructose	+	+
Rhamnose	+	+
Iso-inositol	+	+
Mannitol	+	+
Sucrose	+	+
Raffinose	-	-
Melanin production in		
Peptone yeast iron agar	+	+
Tyrosine agar	-	-
Citrate utilization	+	+
Nitrate reduction	+	+
Hydrolysis of		
Starch	+	+
Gelatin	+	+
Casein	+	+
Production of hydrogen sulfide	-	-
Reference	This study	(Leach et al, 1953)

+, growth or positive reaction; -, no growth or negative reaction.

Table S2: Comparison of morphological, cultural and phenotypic characteristics that distinguish polyamine-producing isolate #7 from very closely related species *Streptomyces tritolerans* and *S. tendae*

Characteristics	**Isolate #7**	***S. tritolerans***	***S. tendae***
Morphological			
Spore chains	Straight to flexuous (Rectus-flexibilis)	Straight to flexuous (Rectus-flexibilis)	Retinaculiperti-spirals
Spore surface	Smooth	Smooth	warty
Cultural			
ISP3			
Aerial mycelium color	Gray	Gray	Gray
Substrate mycelium color	Dark yellow	Dark yellow	Yellow
Diffusible pigment color	-	-	Yellow
Growth at 7% NaCl	+	+	-
Phenotypic			
Growth on sole carbon sources			
Glucose	+	+	+
Rhamnose	-	-	+
Sucrose	+	+	+
Mannitol	+	+	+
Meso-inositol	-	-	+
Raffinose	-	-	-
Production of melanin pigments on			
Peptone-yeast extract-iron agar	+	+	-
Tyrosine agar	+	+	-
Hydrolysis of			
Casein	+	+	-
Cellulose	+	+	-
Pectin	-	-	+
Starch	+	+	+
Growth on sole nitrogen sources			
L- phenylalanine	+	+	+
L-histidine	-	-	-
Reference	This study	(Syed et al., 2007)	(Ettlinger et al., 1958)

+, growth or positive reaction; -, no growth or negative reaction.

Table S3: Comparison of morphological, cultural and phenotypic characteristics that distinguish 1-aminocyclopropane-1-carboxylic deaminase-producing isolate #11 from very closely related species *Streptomyces rochei*, *S. plicatus*, *S. enissocaesilis*, and *S. vinaceusdrappus*

Characteristic	**Isolate #11**	***S. rochei***	***S. plicatus***	***S. enissocaesilis***	***S. vinaceusdrappus***
Morphological					
Spore chain	Straight to flexuous (Rectus-flexibilis)	Straight to flexuous (Rectus-flexibilis)	Retinaculum-apertum	Spiral	Spiral
Spore surface	Smooth	Smooth	Smooth	Smooth	Smooth
Cultural					
ISP3					
Aerial mass color	Light grayish yellow	Grayish yellow	Light brownish gray	Poorly developed	Grayish reddish brown
Substrate mycelium color	Pale grayish yellow	Pale grayish yellow	Pale grayish yellow	Brown	Yellow
Diffusible pigment	-	-	-	Brown	-
ISP4					
Aerial mass color	Dark grayish yellow	Dark grayish yellow	Light grayish reddish brown	- or poorly developed	Grayish yellowish pink
Substrate mycelium color	Pale grayish yellow	Grayish yellow	Yellowish brown	Colorless	Yellowish brown
Diffusible pigment	-	-	-	-	-
ISP5					
Aerial mass color	Light grayish yellow	Light grayish yellow	Light grayish reddish brown	Absent or poorly developed	Grayish reddish brown
Substrate mycelium color	Grayish yellow	Pale grayish yellow	Dark grayish brown	Black grayish brown	Yellowish brown
Diffusible pigment	-	-	-	-	-
Characteristic	**Isolate #11**	***S. rochei***	***S. plicatus***	***S. enissocaesilis***	***S. vinaceusdrappus***
Phenotypic					
Growth on sole carbon sources					
Glucose	+	+	+	+	+
Arabinose	+	+	+	+	+
Xylose	+	+	+	+	+
Mannitol	+	+	+	+	+

Table S3: Comparison of morphological, cultural and phenotypic characteristics that distinguish 1-aminocyclopropane-1-carboxylic deaminase-producing isolate #11 from very closely related species *Streptomyces rochei*, *S. plicatus*, *S. enissocaesilis*, and *S. vinaceusdrappus* (continued)

Characteristic	**Isolate #11**	***S. rochei***	***S. plicatus***	***S. enissocaesilis***	***S. vinaceusdrappus***
Phenotypic					
Sucrose	-	-	-	-	+
Rhamnose	+	+	+	-	+
Raffinose	-	-	-	-	+
Fructose	+	+	+	+	+
Production of melanin pigments on Peptone-yeast extract-iron agar	-	-	-	-	-
Tyrosine agar	-	-	-	-	-
Production of hydrogen sulfide	-	-	-	-	-
Nitrate reduction	-	-	-	-	-
Hydrolysis of					
Starch	+	+	+	+	+
Gelatin	+	+	+	+	+
Casein	-	-	-	-	-
Reference	This study	(Kämpfer, 2012)	(Kämpfer, 2012)	(Kämpfer, 2012)	(Kämpfer, 2012)

+, growth or positive reaction; -, no growth or negative reaction

Table S4: Pearson correlation coefficient (n= 8) of 14 variables, including two actinobacterial auxins, six agronomic traits and six plant growth regulators obtained from shoots of *S. bigelovii*. Seedlings were seed- and soil-inoculated with *Streptomyces chartreusis* (*Sc*) grown in an evaporative-cooled greenhouse and maintained at 25±2°C (*, P< 0.05, **, P< 0.01 and ***, P< 0.001)

Parameter		*Sc*		Shoot											
		IAA	IPYA	L	DW	SWD	Chla	Chlb	Car	IAA	IPYA	Put	Spd	Spm	ACC
Sc	IAA	1													
	IPYA	0.996 ***	1												
Shoot	L	0.842 ***	0.842 ***	1											
	DW	0.793 ***	0.778 ***	0.747 ***	1										
	SDW	0.891 ***	0.896 ***	0.693 **	0.830 ***	1									
	Chla	0.675 **	0.693 **	0.561 *	0.597 *	0.675 **	1								
	Chlb	0.870 ***	0.868 ***	0.805 ***	0.745 ***	0.670 **	0.536	1							
	Car	0.797 ***	0.806 ***	0.810 ***	0.633 **	0.701 **	0.636 **	0.757 ***	1						
	IAA	0.829 ***	0.835 ***	0.760 ***	0.685 **	0.737 **	0.688 **	0.866 ***	0.773 ***	1					
	IPYA	0.835 ***	0.849 ***	0.853 ***	0.581 *	0.690 *	0.588 *	0.816 ***	0.886 ***	0.751 ***	1				
	Put	0.262	0.290	0.496	0.388	0.154	0.392	0.497	0.335	0.359	0.496	1			
	Spd	0.313	0.309	0.274	0.417	0.263	0.104	0.234	0.027	0.049	-0.048	0.148	1		
	Spm	0.317	0.335	0.269	0.171	0.191	0.346	0.380	0.689 **	0.335	0.481	0.208	-0.090	1	
	ACC	0.040	0.010	0.254	0.294	0.014	-0.112	0.259	0.021	0.199	0.099	0.335	-0.043	-0.202	1

Table S5: Pearson correlation coefficient (*n*= 8) of 10 variables, including two actinobacterial auxins, two agronomic traits and six plant growth regulators obtained from roots of *S. bigelovii*. Seedlings were seed- and soil-inoculated with *Streptomyces chartreusis* (*Sc*) grown in an evaporative-cooled greenhouse and maintained at 25±2°C (*, *P*< 0.05, **, *P*< 0.01 and ***, *P*< 0.001)

Parameter		*Sc*		Root							
		IAA	IPYA	L	DW	IAA	IPYA	Put	Spd	Spm	ACC
Sc	IAA	1									
	IPYA	0.996 ***	1								
Root	L	0.693 **	0.715 **	1							
	DW	0.816 ***	0.847 ***	0.766 ***	1						
	IAA	0.715 **	0.703 **	0.651 **	0.714 **	1					
	IPYA	0.866 ***	0.852 ***	0.465	0.713 **	0.612 *	1				
	Put	0.144	0.182	0.484	0.473	0.221	0.043	1			
	Spd	-0.402	-0.425	-0.013	-0.387	0.041	-0.538 *	-0.083	1		
	Spm	0.344	0.338	0.516 *	0.452	0.743 ***	0.152	0.029	0.349	1	
	ACC	-0.154	-0.141	-0.132	-0.118	-0.391	-0.066	-0.245	-0.310	-0.323	1

Table S6: Pearson correlation coefficient (*n*= 8) of 15 variables, including three actinobacterial polyamines, six agronomic traits and six plant growth regulators obtained from shoots of *S. bigelovii*. Seedlings were seed- and soil-inoculated with *Streptomyces tritolerans* (*St*) grown in an evaporative-cooled greenhouse and maintained at 25±2°C (*, *P*< 0.05, **, *P*< 0.01 and ***, *P*< 0.001)

Parameter		*St*			Shoot											
		Put	Spd	Spm	L	DW	SWD	Chla	Chlb	Car	IAA	IPYA	Put	Spd	Spm	ACC
St	Put	1														
	Spd	0.986 ***	1													
	Spm	0.952 ***	0.934 ***	1												
Shoot	L	0.957 ***	0.961 ***	0.919 ***	1											
	DW	0.916 ***	0.896 ***	0.850 ***	0.890 ***	1										
	SDW	0.944 ***	0.924 ***	0.942 ***	0.921 ***	0.901 ***	1									
	Chla	0.891 ***	0.884 ***	0.830 ***	0.840 ***	0.825 ***	0.858 ***	1								
	Chlb	0.948 ***	0.926 ***	0.930 ***	0.942 ***	0.863 ***	0.934 ***	0.848 ***	1							
	Car	0.906 ***	0.889 ***	0.911 ***	0.893 ***	0.786 ***	0.917 ***	0.812 ***	0.936 ***	1						
	IAA	0.851 ***	0.844 ***	0.757 ***	0.743 ***	0.722 **	0.781 ***	0.810 ***	0.755 ***	0.767 ***	1					
	IPYA	0.789 ***	0.804 ***	0.773 ***	0.794 ***	0.679 **	0.748 ***	0.670 **	0.828 ***	0.778 ***	0.529 *	1				
	Put	0.977 ***	0.964 ***	0.923 ***	0.961 ***	0.897 ***	0.948 ***	0.888 ***	0.964 ***	0.937 ***	0.804 ***	0.828 ***	1			
	Spd	0.976 ***	0.961 ***	0.966 ***	0.960 ***	0.891 ***	0.915 ***	0.856 ***	0.918 ***	0.887 r***	0.802 ***	0.747 ***	0.941 ***	1		
	Spm	0.943 ***	0.923 ***	0.911 ***	0.895 ***	0.823 ***	0.884 ***	0.850 ***	0.939 ***	0.958 ***	0.828 ***	0.825 ***	0.947 ***	0.918 ***	1	
	ACC	-0.155	-0.174	-0.184	-0.240	-0.036	-0.266	-0.287	-0.346	-0.382	-0.258	-0.176	-0.248	-0.104	-0.263	1

Table S7: Pearson correlation coefficient (n= 8) of 11 variables, including three actinobacterial polyamines, two agronomic traits and six plant growth regulators obtained from roots of *S. bigelovii*. Seedlings were seed- and soil-inoculated with *Streptomyces tritolerans* (*St*) grown in an evaporative-cooled greenhouse and maintained at 25±2°C (*, P< 0.05, **, P< 0.01 and ***, P< 0.001)

Parameter		*St*			Root							
		Put	Spd	Spm	L	DW	IAA	IPYA	Put	Spd	Spm	ACC
St	Put	1										
	Spd	0.986 ***	1									
	Spm	0.952 ***	0.934 ***	1								
Root	L	0.922 ***	0.905 ***	0.949 ***	1							
	DW	0.926 ***	0.918 ***	0.948 ***	0.848 ***	1						
	IAA	0.886 ***	0.890 ***	0.871 ***	0.840 ***	0.879 ***	1					
	IPYA	0.790 ***	0.843 ***	0.724 **	0.619 *	0.818 ***	0.719 **	1				
	Put	0.977 ***	0.967 ***	0.962 ***	0.929 ***	0.959 ***	0.888 ***	0.787 ***	1			
	Spd	0.962 ***	0.954 ***	0.925 ***	0.935 ***	0.914 ***	0.897 ***	0.778 ***	0.969 ***	1		
	Spm	0.943 ***	0.918 ***	0.915 ***	0.898 ***	0.862 ***	0.900 ***	0.700 **	0.892 ***	0.917 ***	1	
	ACC	0.247	0.209	0.192	0.241	0.095	0.163	0.006	0.210	0.168	0.312	1

Table S8: Pearson correlation coefficient (n= 8) of 13 variables, including the actinobacterial 1-aminocyclopropane-1-carboxylic deaminase, six agronomic traits and six plant growth regulators obtained from shoots of *S. bigelovii*. Seedlings were seed- and soil-inoculated with *Streptomyces rochei* (*Sr*) grown in an evaporative-cooled greenhouse and maintained at 25±2°C (*, P< 0.05, **, P< 0.01 and ***, P< 0.001)

Parameter		*Sr*	Shoot											
		ACCD	L	DW	SWD	Chla	Chlb	Car	IAA	IPYA	Put	Spd	Spm	ACC
Sr	ACCD	1												
Shoot	L	0.889 ***	1											
	DW	0.978 ***	0.893 ***	1										
	SDW	0.959 ***	0.827 ***	0.970 ***	1									
	Chla	0.726 **	0.520 *	0.745 ***	0.724 **	1								
	Chlb	0.964 ***	0.871 ***	0.915 ***	0.880 ***	0.655 **	1							
	Car	0.974 ***	0.845 ***	0.968 ***	0.953 ***	0.729 **	0.949 ***	1						
	IAA	0.943 ***	0.774 ***	0.884 ***	0.908 ***	0.728 **	0.900 ***	0.922 ***	1					
	IPYA	0.863 ***	0.763 ***	0.830 ***	0.830 ***	0.552 *	0.888 ***	0.825 ***	0.753 ***	1				
	Put	0.565 *	0.607 *	0.573 *	0.470	0.445	0.616 *	0.568 *	0.488	0.560 *	1			
	Spd	-0.088	0.158	-0.063	-0.213	-0.171	-0.051	-0.128	-0.178	-0.171	0.222	1		
	Spm	0.179	-0.054	0.186	0.248	0.300	0.199	0.334	0.275	0.192	0.024	-0.213	1	
	ACC	-0.965 ***	-0.820 ***	-0.923 ***	-0.934 ***	-0.753 ***	-0.931 ***	-0.954 ***	-0.956 ***	-0.820 ***	-0.471	0.181	-0.302	1

Table S9: Pearson correlation coefficient (n= 8) of nine variables, including the actinobacterial 1-aminocyclopropane-1-carboxylic deaminase, two agronomic traits and six plant growth regulators obtained from roots of *S. bigelovii*. Seedlings were seed- and soil-inoculated with *Streptomyces rochei* (*Sr*) grown in an evaporative-cooled greenhouse and maintained at 25±2°C (*, P< 0.05, **, P< 0.01 and ***, P< 0.001)

Parameter		*Sr*	Root							
		ACCD	L	DW	IAA	IPYA	Put	Spd	Spm	ACC
Sr	ACCD	1								
Root	L	0.701 **	1							
	DW	0.848 ***	0.766 ***	1						
	IAA	0.710 **	0.651 **	0.714 **	1					
	IPYA	0.930 ***	0.465	0.713 **	0.612 *	1				
	Put	0.238	0.484	0.473	0.221	0.043	1			
	Spd	-0.472	-0.013	-0.387	0.041	-0.538 *	-0.083	1		
	Spm	0.269	0.516 *	0.452	0.743 ***	0.152	0.029	0.349	1	
	ACC	-0.114	-0.132	-0.118	-0.391	-0.066	-0.245	-0.310	-0.323	1

Table S10: Pearson correlation coefficient (*n*= 8) of 18 variables, including actinobacterial auxins, polyamines and 1-aminocyclopropane-1-carboxylic deaminase, six agronomic traits and six plant growth regulators obtained from shoots of *S. bigelovii*. Seedlings were seed- and soil-inoculated with *S. chartreusis*, *S. tritolerans* and *S. rochei* (*Sc*/*St*/*Sr*) grown in an evaporative-cooled greenhouse and maintained at 25±2°C (*, *P*< 0.05, **, *P*< 0.01 and ***, *P*< 0.001)

Parameter		*Sc*/*St*/*Sr*						Shoot											
		IAA	IPYA	Put	Spd	Spm	ACCD	L	DW	SWD	Chla	Chlb	Car	IAA	IPYA	Put	Spd	Spm	ACC
Sc/*St*/*Sr*	IAA	1																	
	IPYA	0.995***	1																
	Put	0.955***	0.962***	1															
	Spd	0.948***	0.950***	0.975***	1														
	Spm	0.907***	0.898***	0.944***	0.907***	1													
	ACCD	0.949***	0.952***	0.998***	0.979***	0.945***	1												
Shoot	L	0.923***	0.934***	0.971***	0.937***	0.951***	0.970***	1											
	DW	0.949***	0.947***	0.978***	0.952***	0.971***	0.978***	0.981***	1										
	SDW	0.957***	0.939***	0.957***	0.942***	0.952***	0.963***	0.940***	0.975***	1									
	Chla	0.891***	0.904***	0.935***	0.928***	0.908***	0.934***	0.912***	0.933***	0.893***	1								
	Chlb	0.964***	0.957***	0.973***	0.970***	0.962***	0.976***	0.959***	0.975***	0.976***	0.916***	1							
	Car	0.920***	0.911***	0.969***	0.944***	0.982***	0.973***	0.953***	0.978***	0.964***	0.917***	0.974***	1						
	IAA	0.857***	0.864***	0.948***	0.944***	0.913***	0.954***	0.912***	0.916***	0.899***	0.930***	0.918***	0.943***	1					
	IPYA	0.607	0.599	0.684**	0.595	0.691**	0.666**	0.636**	0.671**	0.638**	0.555*	0.634**	0.695**	0.615*	1				
	Put	0.946***	0.961***	0.980***	0.975***	0.912***	0.977***	0.958***	0.957***	0.917***	0.950***	0.950***	0.932***	0.934***	0.629**	1			
	Spd	0.925***	0.921***	0.978***	0.960***	0.921***	0.982***	0.958***	0.963***	0.948***	0.897***	0.954***	0.962***	0.935***	0.673**	0.955***	1		
	Spm	0.934***	0.935***	0.943***	0.955***	0.904***	0.939***	0.892***	0.919***	0.890***	0.918***	0.936***	0.936***	0.917***	0.622*	0.956***	0.920***	1	
	ACC	-0.824***	-0.852***	-0.913***	-0.898***	-0.770***	-0.906***	-0.836***	-0.823***	-0.785***	-0.857***	-0.829***	-0.834***	-0.904***	-0.600*	-0.905***	-0.889***	-0.879***	1

Table S11: Pearson correlation coefficient (n= 8) of 14 variables, including actinobacterial auxins, polyamines and 1-aminocyclopropane-1-carboxylic deaminase, two agronomic traits and six plant growth regulators obtained from roots of *S. bigelovii*. Seedlings were seed- and soil-inoculated with *S. chartreusis*, *S. tritolerans* and *S. rochei* (*Sc*/*St*/*Sr*) grown in an evaporative-cooled greenhouse and maintained at 25±2°C (*, P< 0.05, **, P< 0.01 and ***, P< 0.001)

Parameter		*Sc*/*St*/*Sr*						Root							
		IAA	IPYA	Put	Spd	Spm	ACCD	L	DW	IAA	IPYA	Put	Spd	Spm	ACC
Sc/*St*/*Sr*	IAA	1													
	IPYA	0.995 ***	1												
	Put	0.955 ***	0.962 ***	1											
	Spd	0.948 ***	0.950 ***	0.975 ***	1										
	Spm	0.907 ***	0.898 ***	0.944 ***	0.907 ***	1									
	ACCD	0.949 ***	0.952 ***	0.998 ***	0.979 ***	0.945 ***	1								
Root	L	0.929 ***	0.932 ***	0.973 ***	0.962 ***	0.954 ***	0.976 ***	1							
	DW	0.962 ***	0.970 ***	0.979 ***	0.968 ***	0.957 ***	0.975 ***	0.960 ***	1						
	IAA	0.891 ***	0.913 ***	0.943 ***	0.943 ***	0.852 ***	0.943 ***	0.897 ***	0.947 ***	1					
	IPYA	0.779 ***	0.799 ***	0.800 ***	0.837 ***	0.664 **	0.787 ***	0.728 **	0.799 ***	0.781 ***	1				
	Put	0.918 ***	0.927 ***	0.975 ***	0.948 ***	0.959 ***	0.974 ***	0.982 ***	0.968 ***	0.901 ***	0.757 ***	1			
	Spd	0.944 ***	0.957 ***	0.961 ***	0.970 ***	0.915 ***	0.958 ***	0.972 ***	0.968 ***	0.915 ***	0.789 ***	0.962 ***	1		
	Spm	0.917 ***	0.909 ***	0.946 ***	0.908 ***	0.887 ***	0.944 ***	0.895 ***	0.908 ***	0.899 ***	0.713 **	0.873 ***	0.864 ***	1	
	ACC	-0.928 ***	-0.930 ***	-0.967 ***	-0.978 ***	-0.905 ***	-0.974 ***	-0.948 ***	-0.956 ***	-0.939 ***	-0.801 ***	-0.941 ***	-0.950 ***	-0.905 ***	1